WT-1369 (EX)
EXTRACTED VERSION

OPERATION REDWING

Project 1.9a
Direct Water-Wave Measurements

Pacific Proving Grounds
May – July 1956

Headquarters Field Command
Defense Atomic Support Agency
Sandia Base, Albuquerque, New Mexico

May 5, 1961

NOTICE

This is an extract of WT-1369, Operation REDWING, Project 1.9a, which remains classified SECRET/FORMERLY RESTRICTED DATA as of this date.

Extract version prepared for:

Director
DEFENSE NUCLEAR AGENCY
Washington, D.C. 20305

15 May 1981

Approved for public release; distribution unlimited.

UNCLASSIFIED
SECURITY CLASSIFICATION OF THIS PAGE (When Data Entered)

REPORT DOCUMENTATION PAGE	READ INSTRUCTIONS BEFORE COMPLETING FORM
1. REPORT NUMBER: WT-1369 (EX)	2. GOVT ACCESSION NO.: AD-A995150 / 3. RECIPIENT'S CATALOG NUMBER
4. TITLE (and Subtitle): Operation REDWING - Project 1.9a Direct Water-Wave Measurements	5. TYPE OF REPORT & PERIOD COVERED
	6. PERFORMING ORG. REPORT NUMBER: WT-1369 (EX)
7. AUTHOR(s): L. W. Kidd	8. CONTRACT OR GRANT NUMBER(s)
9. PERFORMING ORGANIZATION NAME AND ADDRESS: University of California, Scripps Institution of Oceanography, La Jolla, California	10. PROGRAM ELEMENT, PROJECT, TASK AREA & WORK UNIT NUMBERS
11. CONTROLLING OFFICE NAME AND ADDRESS: Headquarters Field Command, Defense Atomic Support Agency, Sandia Base, Albuquerque, New Mexico	12. REPORT DATE: May 5, 1961
	13. NUMBER OF PAGES
14. MONITORING AGENCY NAME & ADDRESS(if different from Controlling Office)	15. SECURITY CLASS. (of this report): Unclassified
	15a. DECLASSIFICATION/DOWNGRADING SCHEDULE

16. DISTRIBUTION STATEMENT (of this Report)

Approved for public release; unlimited distribution.

17. DISTRIBUTION STATEMENT (of the abstract entered in Block 20, if different from Report)

18. SUPPLEMENTARY NOTES

This report has had the classified information removed and has been republished in unclassified form for public release. This work was performed by Kaman Tempo under contract DNA001-79-C-0455 with the close cooperation of the Classification Management Division of the Defense Nuclear Agency.

19. KEY WORDS (Continue on reverse side if necessary and identify by block number)

Operation REDWING
Water-Wave Data
Nuclear Weapons Effects
Military Effects

20. ABSTRACT (Continue on reverse side if necessary and identify by block number)

The direct-wave group of Project 1.9 had as its objectives the gathering and analyzing of water-wave data from the Bikini and Eniwetok lagoons. The data was required (1) to improve the ability to predict wave effects from operational use of nuclear weapons, and (2) to determine safety criteria for future test operations.

The water-wave time-height history was to be determined at various ranges from ground zero. Where significant, the terminal effects were to be measured as the waves inundated the reefs and islands of the atoll. The data was to be summarized, integrated with data from Operation Castle (higher yields, identical physical topography), and

20. Abstract (Continued)

compared to present theories and concepts of impulsively generated waves.

During Operation Redwing, as in previous test series, principal observations were made by means of bottom-pressure-versus-time recorders of several types adapted to different locations, and by means of technical photography.

Data from this operation, when correlated with all previous pertinent data, has permitted considerable progress in this investigation and in the understanding of all of the various facets of wave systems, but particularly has this been so about the dimensions and the relative importance of the parameters of generation, the separability of observed wave systems, the reflections, and the inundation of shorelines. A scaling law for wave height versus range has been derived, which considers the water depth of generation as well as yield. Possibly, the most significant result at this stage of the continuing investigation has been the demonstration of the limited applicability, for purposes of wave predictions, of wave data collected to date, and from this, recommendations are made for a more conclusive program for further research.

FOREWORD

This report has had classified material removed in order to make the information available on an unclassified, open publication basis, to any interested parties. This effort to declassify this report has been accomplished specifically to support the Department of Defense Nuclear Test Personnel Review (NTPR) Program. The objective is to facilitate studies of the low levels of radiation received by some individuals during the atmospheric nuclear test program by making as much information as possible available to all interested parties.

The material which has been deleted is all currently classified as Restricted Data or Formerly Restricted Data under the provision of the Atomic Energy Act of 1954, (as amended) or is National Security Information.

This report has been reproduced directly from available copies of the original material. The locations from which material has been deleted is generally obvious by the spacings and "holes" in the text. Thus the context of the material deleted is identified to assist the reader in the determination of whether the deleted information is germane to his study.

It is the belief of the individuals who have participated in preparing this report by deleting the classified material and of the Defense Nuclear Agency that the report accurately portrays the contents of the original and that the deleted material is of little or no significance to studies into the amounts or types of radiation received by any individuals during the atmospheric nuclear test program.

ABSTRACT

The direct-wave group of Project 1.9 had as its objectives the gathering and analyzing of water-wave data from the Bikini and Eniwetok lagoons. The data was required (1) to improve the ability to predict wave effects from operational use of nuclear weapons, and (2) to determine safety criteria for future test operations.

The water-wave time-height history was to be determined at various ranges from ground zero. Where significant, the terminal effects were to be measured as the waves inundated the reefs and islands of the atoll. The data was to be summarized, integrated with data from Operation Castle (higher yields, identical physical topography), and compared to present theories and concepts of impulsively generated waves.

During Operation Redwing, as in previous test series, principal observations were made by means of bottom-pressure-versus-time recorders of several types adapted to different locations, and by means of technical photography.

Data from this operation, when correlated with all previous pertinent data, has permitted considerable progress in this investigation and in the understanding of all of the various facets of wave systems, but particularly has this been so about the dimensions and the relative importance of the parameters of generation, the separability of observed wave systems, the reflections, and the inundation of shorelines. A scaling law for wave height versus range has been derived, which considers the water depth of generation as well as yield. Possibly, the most significant result at this stage of the continuing investigation has been the demonstration of the limited applicability, for purposes of wave predictions, of wave data collected to date, and from this, recommendations are made for a more conclusive program for further research.

FOREWORD

This report presents the final results of one of the projects participating in the military-effect programs of Operation Redwing. Overall information about this and the other military-effect projects can be obtained from WT-1344, the "Summary Report of the Commander, Task Unit 3." This technical summary includes: (1) tables listing each detonation with its yield, type, environment, meteorological conditions, etc.; (2) maps showing shot locations; (3) discussions of results by programs; (4) summaries of objectives, procedures, results, etc., for all projects; and (5) a listing of project reports for the military-effect programs.

PREFACE

The work that has resulted in this report commenced in June 1955, and since that time many personnel have made significant contributions toward this presentation. The author acknowledges the contributions of those who are no longer associated with this work and unable to view the results.

Subsurface instrumentation placement and recovery in the field was accomplished by project personnel: J. E. Lasch, R. H. Johnson, and W. W. Beckwith. Each completed more than fifty dives for this purpose, many of them under adverse conditions.

Contributions to the theoretical analysis and manuscript preparation by R. H. Johnson and W. S. Montgomery materially increased the scope and inclusiveness of the results. The technical review and comments of Professor John D. Isaacs were greatly appreciated.

CONTENTS

TABLES

FIGURES

Chapter 1

INTRODUCTION

1.1 OBJECTIVES

The direct-wave group of Project 1.9 had as its objectives the gathering and analyzing of water-wave data from the Bikini and Eniwetok lagoons. The data was required (1) to improve the ability to predict wave effects from operational use of nuclear weapons, and (2) to determine safety criteria for future test operations.

The water-wave time-height history was to be determined at various ranges from ground zero. Where significant, the terminal effects were to be measured as the waves inundated the reefs and islands of the atoll. The data was to be summarized, integrated with data from Operation Castle (higher yields, identical physical topography), and compared to present theories and concepts of impulsively generated waves.

1.2 BACKGROUND AND THEORY

Project Seal was initiated to explore the possibilities of offensive inundation by water waves resulting from high explosives (Reference 1). Comparison and correlation of the small quantity of data from rough exploratory experiments prior to the Seal work with subsequent data and scaling laws was difficult. The experimental phase of Project Seal, completed in New Zealand in early 1945, produced, under controlled conditions, the first data in sufficient quantity to permit development of empirical scaling laws.

During Project Seal, the water waves resulting from above-surface, surface, and subsurface chemical explosions were measured. Charge weights ranged up to 600 pounds, but plans to use larger charges were not carried out. Empirical relationships were developed relating the resultant wave phenomena to charge size, depth of detonation, and water depth. Data was correlated as a function of the energy content of the single wave group as $H_r \propto W^{1/2}$ where H was the maximum trough-to-crest height in the water depth of generation, r was the range (feet) from surface zero at which the wave was observed, and W was the charge weight (pounds). Although the primary intent of Project Seal was to examine waves generated and radiated in deep water, recent reexamination of the data indicates that the characteristics of a significant number of the generated wave systems were influenced by the proximity of the pond bottom to the water crater bottom. From this it appears that some of the waves were generated under shallow water, or very nearly shallow water conditions, and that conclusions from the data are subject to revision upon reexamination of the parameters of generation and their effect upon the recorded waves. For this reexamination, the data from charges supported on rafts was not considered.

During Project Seal, the investigators neglected the scaling effect of atmospheric pressure with charge size, which could partially account for the noted increase in wavemaking efficiency with increased charge size under similar conditions. It was discovered that, adjacent to the water surface, there existed a depth of charge submergence at which the efficiency of energy coupling to water waves was at a maximum. The results of this work were considered in planning Shot Baker of Operation Crossroads, and the Baker waves were within the allowable error for such predictions. In these predictions, the linear dimensions at the source (depth of submergence) were scaled in proportion to the cube root of the charge weight, and the linear dimensions of the wave system (wavelength and height) were scaled in proportion to the fourth root of the charge weight. Although a small percentage of the Seal data was from scaled parameters of generation similar to those of Shot Baker, it is noted that the type of wave system generated by Shot Baker was not referred to in the Seal report, and in the absence of the original traces of the Seal work, it must be assumed that the Shot Baker type of wave system was not found. This seems to indicate that the correlation of the scaled predictions with the results from Shot Baker was coincidental.

The Scripps Institution of Oceanography has participated in Operations Crossroads, Ivy, Castle, Wigwam, and Redwing to study impulsively generated water waves. Shot Baker afforded the first opportunity to measure directly generated water waves from a comparatively large, essentially point source disturbance. Prior to this event, a few isolated and spontaneous natural phenomena (volcanic, seismic, and the like) had obliged to produce high energy water waves, and qualitative observations of results at their termination had been exemplary of the potential wavemaking capacity of large nuclear weapons in the deep ocean. Shot Baker initiated waves which, within the ranges of observation, consisted of a solitary type of wave with constant and relatively high velocity followed by a wave train which behaved as though emanating from a point source in accordance with the Cauchy-Poisson theory (Reference 2).

The first wave, a crest followed by a trough of approximately equal amplitude, was the highest wave of the system at ranges less than 8,000 feet. Its height decreased inversely with distance according to $Hr = 94{,}000$ where H is the height of the wave from crest to the succeeding trough, and r is the range from surface zero. Beyond 8,000 feet the highest wave was not the first wave but a wave in the following group, and its height-range relationship was expressed by $Hr^{0.8} = 42{,}700$. The experimental data and scaled model data for the highest wave was found to fit the empirical relationship $Hr = 4.2W^{1/2}W^{1/12}$ throughout the ranges of observation. It has since been observed that this equation more accurately represents the first wave height as a function of charge size (Reference 3). The discrepancy between the observed W scaling and related theoretical model laws, which assert that $Hr \propto W^{1/4}$, could not be resolved. The Seal data, however, could be interpreted to indicate that, for the much shallower water depth (scaled depth) of Shot Baker, the Hr products would increase more rapidly than $W^{1/2}$. For ranges less than 8,000 feet, more than half the energy in the wave system was contained in the first wave. The behavior of these waves as they entered shallow water and broke upon the nearest beaches and reefs was well documented photographically.

Shot Mike of Operation Ivy failed to produce significant directly generated wave action. It did, however, indicate the presence of a distributive mechanism that permitted energy transfer to initiate deep-water waves of the tsurami (seismic sea wave) type. These have been referred to as indirectly generated waves. As a result, the investigative work for Operations Castle and Redwing was performed by two groups. The distant-island group concentrated on recording waves at distant stations (150 to 1,000 miles) and found

energy levels much higher than could have escaped through lagoon channels and over lagoon reefs. The direct-wave group concentrated on studying the direct-generative processes, the propagation of resultant waves, and the water-wave damage to installations when these waves terminated on reefs and islands.

Although there is only a very small quantity of data on water waves resulting from nuclear devices, this lack in quantity is partially compensated for by the large range of yield values. The ratio of the lowest to the highest yields for which there are data is about 1 to 750. At the start of nuclear testing, the mechanism of wave propagation was reasonably well understood and could be handled independently of source size and location, but the generation phenomenon and potential terminal effects of water waves from these devices require continued study.

From the first high-yield water-wave data collected in quantity during Operation Castle, it was immediately apparent that data reduction and analysis were complicated by the geometry of the test site; i. e., the effects of cratering in the lagoon bottom, refraction, reflection, breaching (where applicable in reef or island shots), and seiche-like oscillations of the lagoon.

Results indicated that the waves from the open lagoon Shots Union and Yankee during Operation Castle differed fundamentally from those of Shot Baker during Operation Crossroads. Only two wave records, one from Shot Union and one from Shot Yankee, were obtained whose ranges from surface zero were small enough to permit conclusions about the type of wave system before it was altered beyond recognition by shore and bottom influences. The Shot Union record (lower yield) indicated that the wave system consisted of a pair of oscillatory waves, not a solitary type followed by a wave group as from Shot Baker. Although the portion of the Shot Yankee close-in record describing the second wave was missing, it could be deduced from records at other, and greater, ranges that the wave system of Shot Yankee was identical to that of Shot Union. This basic difference between the wave system of Shot Yankee and Shot Union and that of Shot Baker was a very discouraging observation, because it restricted generalized conclusions about scaling until all the possible wave-system types and energy distribution within the systems could be identified and categorized. Analysis of wave-height histories was limited to the first wave, because without the categorization data about wave-system types, height-time-range conclusions in simplified algebraic form about waves following the first wave were impossible. The Castle data was fitted to the model law $Hr = KW^{1/2}$ where K was a constant of proportionality, with the addition of factors to account for the degree of breaching on reef shots, and for the effect of the density of the material in the region of crater formation (Reference 3). The value of H used in this instance was the vertical elevation of the first crest above tide stage. All measured wave heights were adjusted by use of Green's law to a water depth of 60 feet for comparison purposes, but no attempt was made to evaluate the increased wave heights from shore and near-reef stations, even though such reflectance-induced effects were apparent. Averaged constants of proportionality relating the product of first-crest heights and range to yield to the one-half power were determined. They ranged from 0.96×10^5 to 1.63×10^5 for the Castle water waves (Reference 3).

While the evaluation of Castle data-procurement techniques and data significance was taking place, Operation Redwing was documented in the spring of 1956. It was anticipated that some of the same complexities encountered in the Castle data would exist for Redwing, but to a lesser degree as a result of the lower yields involved. This assumption was proved correct as the smaller waves did delay in time the previously observed confusion of the radiating wave system. The Redwing data has supplied the information

necessary to isolate some of the peculiarities of water waves within this particular lagoon (Bikini). Successful records from several close-range stations were obtained.

Between Operations Castle and Redwing, the water waves from Operation Wigwam were studied. The waves from this test although not comparable to any previously recorded, because they were generated and propagated in deep water, were unaffected by any of the lagoon influences, and the agreement between observed values and available deep-water theory inspired new vigor in efforts to obtain a clear picture and understanding of the water-wave systems from Operations Castle and Redwing.

While the above-discussed field data on water waves from nuclear tests were being collected, significant advancements were made in the development of mathematical models applicable to these wave systems. The three-dimensional description of wave systems in water of finite depth was investigated (Reference 4). Arbitrary distributions of initial impulse and initial elevation were studied; the successful application of the developed mathematical model is highly dependent upon the functions assigned to represent this distribution.

Two-dimensional laboratory tests were carried out to determine the applicability of available mathematical theory (Reference 5). In these tests, wave generation was by an initial elevation or depression of a volume of water at one end of a wave tank. The results of this work were very informative; they showed that impulsive wave systems can be grouped into various classes or types, and that classification of a wave system is a function of the assigned, or measured, parameters of generation. Wave systems generated ranged from those having two or three solitary waves radiating from the generating area to a single symmetrical wave group in deep water, propagating according to the linear theory of surface waves. This classification of wave systems provided the first comprehensive look at the various height-time-range combinations that generated waves could take and more clearly demonstrated the problems in scaling, for example between Seal, Baker, and Castle results. The criteria of geometric similarity of wave systems has become of primary importance and concern.

Scaled high-explosive tests designed to be applicable to water waves from nuclear charges in the 20-kt range were completed by the Waterways Experiment Station (Reference 6). In this series of tests, Froude's law was considered to be the valid scaling principle, and the experimental data tended to verify this. The results were correlated and summarized as reduced wave heights as a function of reduced distance of observation for an assortment of reduced water depths. Extrapolated curves for determination of wave heights from 1- to 200-kt surface-mounted nuclear charges were prepared. This work was completed and published before the results of the laboratory tests (Reference 5), and the Castle results (Reference 3) indicated the import of geometric similarity of wave systems.

Chapter 2

PROCEDURE

Study of the records from Operation Castle revealed that, in some cases, the records obtained from shore stations where the transducers were in shallow water (30 feet or less), the water level versus time history of the wave trains had been radically and unsystematically altered because of shoaling, reflectance, and absorption by the adjacent lagoon bottom and the island and reef shorelines. This was determined by comparing the records of the inshore stations with the records of other stations on the same radial line from surface zero. From this it was concluded that in any subsequent test, where, because of practical considerations, it was necessary to measure waves at shore stations, the station locations should be chosen with consideration of the altering effects mentioned above, and that the deeper the transducer could be placed the more realistic the records would be.

Because the practical aspects of instrument installation limit the transducers to those depths easily serviced by divers with self-contained underwater breathing apparatus (SCUBA), and easily reached by insulated cable from the beach when such cable is required, and because the Castle data was already adjusted to a standard 60-foot depth, the Redwing stations were planned so that this transducer depth was standard for all stations, both inshore and midlagoon types.

Lagoon pressure-time instrumentation consisted of shore, floating, and bottom (submerged) stations. Their locations are given in Table 2.1, and Figures 2.1 and 2.2.

2.1 SHORE STATIONS

Semipermanent wave-measuring stations were installed on four sites at Bikini. The sites were on Nan, How, Oboe, and William.

Each station consisted of a recorder, timing and energizing circuits, auxiliary power source, and related auxiliary instrumentation (Figure 2.3). The recorder was connected by a heavily armored submarine four-conductor cable to a Statham pressure transducer (Figure 2.4) located in the lagoon at 60-foot water depth. The cable was strongly anchored at the reef area and at its water terminus (Figure 2.5) and was undamaged and unmoved by repeated test-generated wave action.

The transducer was an absolute, temperature-compensated, pressure-measuring device and transmitted the pressure fluctuations as a direct-current millivolt potential. The absolute accuracy of the transducer over its total range of 115 feet of water was within ±1 percent. With the variable-range recording potentiometer used to record these signals, the resolution of the system could be increased to ±0.1 percent of full range, to resolve small relative pressure changes with no sacrifice of linearity or temperature compensation.

This combination of components gave good adaptability for shots of various sizes. These stations participated in all shots and maintained a high degree of accuracy and reliability.

2.2 MIDLAGOON STATIONS

In addition to the shore stations, a number of portable units were used in the open lagoon on various sites selected to be compatible with individual shot size and location. They were of two types, floating and submerged.

2.2.1 Floating Type. Four of these units installed on skiffs, were employed at intermediate ranges from surface zero (3½ to 9 miles) to document wave action in the region of stable, well-developed surface waves. In addition, a spare recording mechanism for one of these units was installed in Coca Tower. Except for minor changes these units were the same as those used during Operation Castle. The circular chart pressure-time recorders (Figure 2.6) were connected by means of a pneumatic pressure transmitting hose to a compliant bladder attached to the skiff's anchor. The recorders were activated by an electric signal initiated by the overpressure response of a salt-water-filled manometer.

2.2.2 Submerged Type. These units, called turtles, were designed to measure pressures very close to those measured during Operation Crossroads and were constructed to withstand high pressure (6,000 psi) and heavy shock. Each unit was a self-contained pressure-time recorder installed on the lagoon floor in a heavy lead fairing as close to ground zero as probable recovery conditions permitted. This was usually in the range of 1 to 2½ miles. The recording mechanism was activated by an electric signal from a thermally initiated device attached to a surface float. The data from these units contributed significant information on the close-in generative processes.

2.3 INUNDATION SURVEYS

For each major event in Bikini Lagoon, the shorelines, structures, and land areas considered likely to receive damage from water waves were documented by: (1) photography (before and after), (2) can-type maximum water-level gages, and (3) postshot sketches. The sketches were useful in interpretation of aerial photographs in later photo analysis.

This data, combined with wave amplitude and period as recorded by lagoon instrumentation, gave a more realistic picture of shore water-wave damage from these events and permitted a better understanding of uprush and bore phenomena.

TABLE 2.1 STATION LOCATION AND DESCRIPTION

Station Number	Coordinates		Instrument Type
	North	East	
190.01	112,400	177,100	Shore station, Nan, Bikini
191.01	104,200	126,100	Shore station, Oboe, Bikini
192.01	110,000	81,300	Shore station, William, Bikini
193.01	144,400	169,000	Shore station, How, Bikini
195.01	50,140	131,000	Shore station, Elmer, Eniwetok
196.01	132,400	168,200	Floating type
196.02	128,200	155,200	Floating type
196.03	134,300	135,500	Floating type
196.04	122,400	106,100	Recording equipment from floating type installed in Coca Tower
196.05	122,000	129,000	Floating type
197.01	114,500	112,500	Submerged
197.02	127,300	119,000	Submerged
197.03	100,800	173,700	Submerged
197.04	166,000	123,700	Submerged
197.05	146,250	115,500	Submerged
197.06	160,200	122,800	Submerged

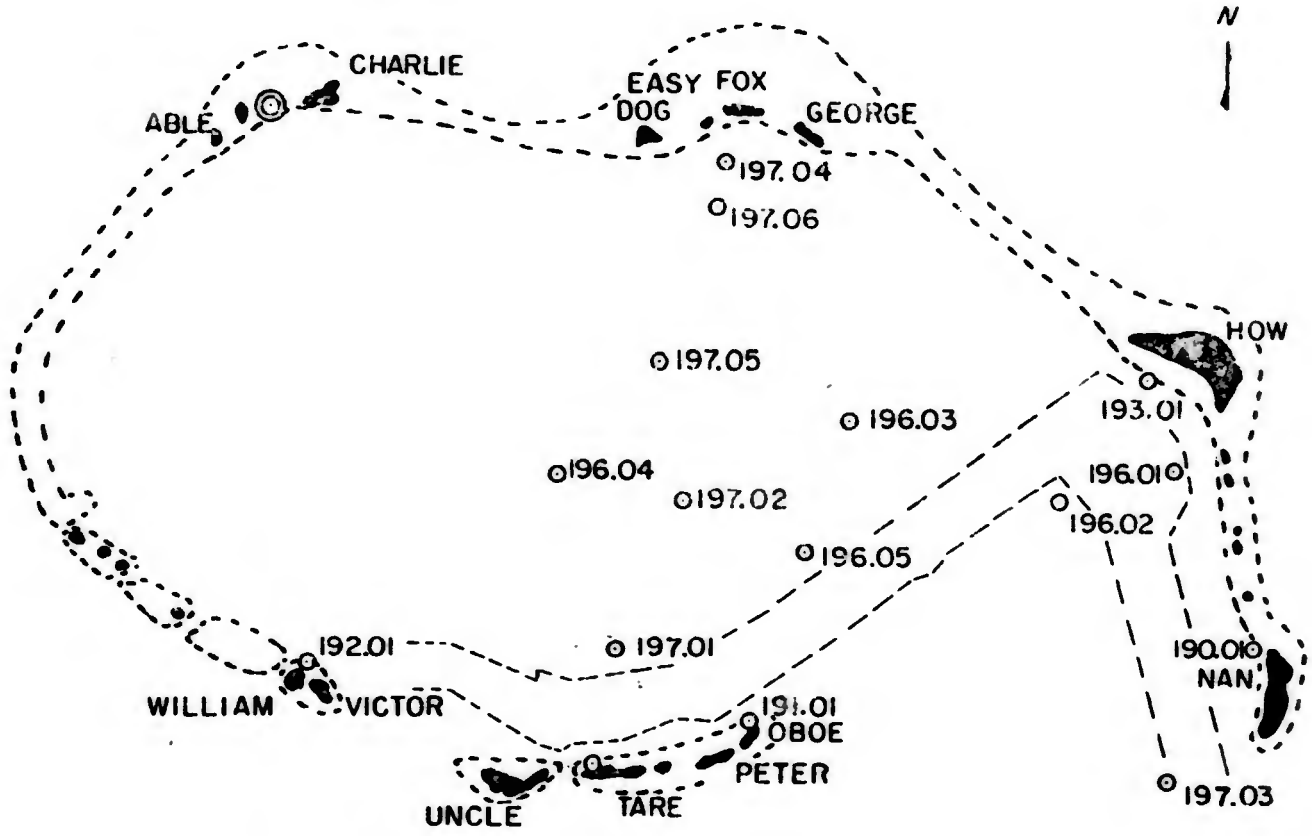

Figure 2.1 Station locations, Bikini lagoon.

Figure 2.2 Station locations, Eniwetok lagoon.

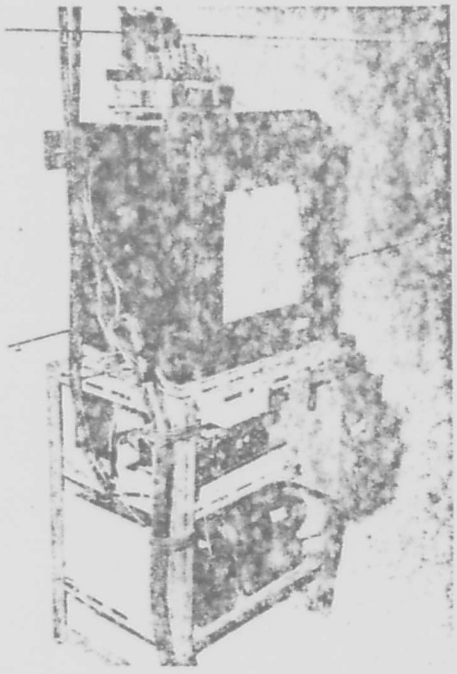

Figure 2.3 Typical shore station recording instrumentation.

Figure 2.4 Modified Mark VIII transducer attached to armored submarine cable. Note: Splice has not been waterproofed.

Figure 2.5 Transducer installed in lead fairing and ready for placement on lagoon bottom.

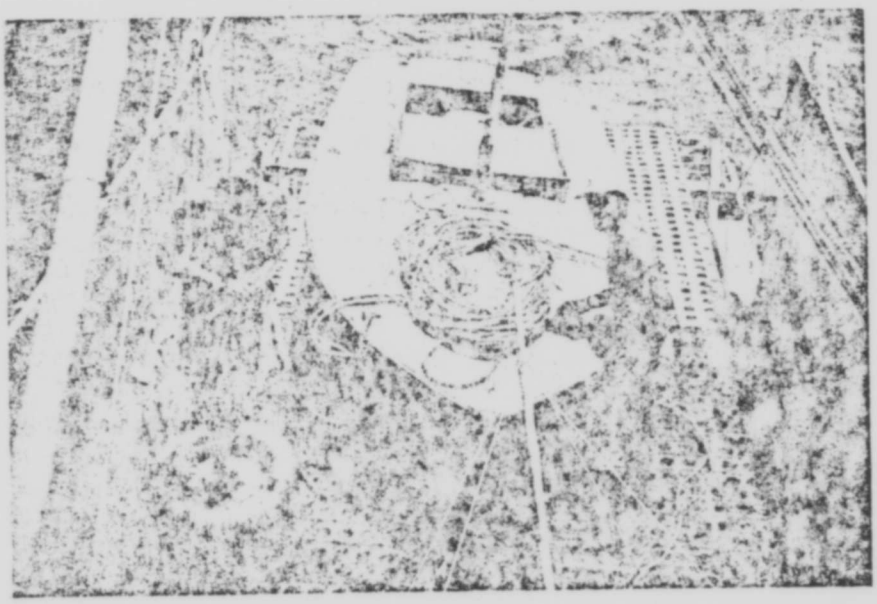

Figure 2.6 Floating station. Pressure-time circular recorder in open hatch. Overpressure starting device mounted at mast. Pressure line and anchor line leading to anchor and compliant bladder.

Chapter 3

RESULTS

3.1 INTRODUCTION

With the exception of Cherokee, all of the shots at Bikini produced lagoon water waves originating from the central region of the explosion. At Eniwetok, Shots Apache, Huron, and Yuma resulted in measurable wave action in the lagoon. The shot participation is listed in Table 3.1.

Appendix A contains traces representing water-surface elevation as a function of time and range at a common water depth of 60 feet during Operation Redwing. The traces in Appendix C give data on close-in water-wave action from Operations Redwing and Castle. Original pressure curves and the interpreted water-surface elevation in 60 feet of water are reproduced.

Although nonlinearity in the shore-based wave recorder system was discovered during field operations, detailed recalibration upon return to the home laboratory permitted correction of the recorded data. The techniques employed to derive surface elevations for presentation and analysis are the same as those used for data from Operation Castle. These techniques are discussed in detail in this chapter along with interpretation of specific records.

Shot Cherokee (with the unexpected ground zero outside the lagoon) created unusual conditions of wave generation and propagation. It was initially suspected that low-amplitude seiching occurred within the lagoon either as a result of overpressure impulse on the northwestern portion of the lagoon, or that a wave originating at surface zero refracted around the atoll and entered the lagoon through the Nan-Oboe channel. Four stations were in operation from H−1 minute through H+1½ hours, and the records do not show the presence of test-induced wave action inside the lagoon through either mechanism. Maximum instrument resolution for the detection and interpretation of seiche or wave motion was 1 inch of water.

3.2 TEST SITE AND WAVE SOURCE GEOMETRY

The wave traces recorded in the Redwing series have characteristic features induced by (1) the individual station (transducer) locations, (2) the ground zero location, i.e., its location relative to the recording station and to deep lagoon water, and (3) the geographic location of ground zero within the lagoon. By way of clarification of item (3) above: If shots of equal wave-generating capability were located in the northern and southern central shoreline areas of Bikini Lagoon, and wave stations were activated in the southern area for the northern shot and vice versa, the recorded waves would probably be significantly different, even though they had traveled identical paths and ranges and the conditions of generation were selected to be identical. Such an anticipated difference could be ascribed to the expected variation of a set of observations from a single

physical phenomenon, the suspected asymmetry of energy release at the source, or an inability to define and select identical conditions of generation.

When the additional variable of yield is injected, the most prominent factors affecting these wave systems become difficult to determine, isolate, and study.

The above factors determining wave-system characteristics are also applicable to the waves during Operation Castle.

Shot Zuni, although, fired adjacent to the lagoon shoreline and to an earlier crater, has to be classed as a reef or island shot which breached to the lagoon water. Of the previous similar test shots, Koon, Bravo, and Romeo of Operation Castle, and Mike of Operation Ivy were the most similar with respect to generation parameters; however, (1) the Koon, yield was too low to generate significant waves, (2) Bravo was fired on a shallow reef and a substantial portion of its energy was spent in coral crater formation before energy was expended in the formation of directly generated water waves, (3) Romeo was fired in the center of the Bravo crater and, because the opening between the crater and the lagoon was comparatively large, was able to generate larger waves than Bravo despite a substantially lower yield, and (4) Mike was an island-reef shot similar to Bravo but unlike Bravo did not generate water waves whose origin can be attributed to the crater formation and collapse. The ground zero of Shot Zuni was on the northeastern edge of the Koon, crater, very near the lagoon shoreline, and the source geometry is a combination of that of Bravo and Romeo and can be treated only in an approximate manner.

Because Shot Zuni was the first on Site Tare to produce measurable water waves, study and analysis of the characteristics of waves generated in and propagated from this lagoon area are not supported by data adequate enough for isolation of the induced characteristics of geographic location. Instrumentation failure at close-range central lagoon stations for this shot prevent early determination of the wave-system characteristics. Waves from this shot recorded by shore stations require interpretation of station location induced characteristics resulting from different directions of approach compared to other shots of this test series.

Shots Flathead, Dakota, and Navajo were in the north-central lagoon area approximately $\frac{1}{2}$ to 1 mile from the nearest reefs or islands. Enough of the close-in instrumentation was operative to adequately document the generated waves in the early phase of propagation. The source geometries of these shots are very similar to and wave data can be compared directly with those from Shots Union and Yankee (Castle) and Baker (Crossroads). With the exception of Baker, the test site geometry of these shots was similar. It was from this group of data that the most significant conclusions were drawn.

Three shore-type wave recorder stations were operative during Shot Tewa. The ground-zero location in shoal lagoon water (approximately 20 feet) adjacent to the Dog-Charlie reef introduced a new source geometry not directly comparable with those from any previous shots, but one that is a compromise between that of the open lagoon shots and Shot Zuni. Similarly, the wave data from Tewa is not directly comparable with data from any previous tests.

Water waves in Eniwetok Lagoon from Shots Apache, Huron, and Yuma were recorded by the shore station on Site Elmer. The characteristic influences of this island upon impinging waves is not as well documented as for similar station sites in Bikini Lagoon. Shots Apache and Huron were tested in the Mike (Ivy) crater, and the geometries of generation compare favorably with each other, and with that of Romeo (Castle). The recorded water wave from Yuma (an island tower shot) was an unexpected bonus resulting from continuous operation of the shore station. The waves from this shot obviously stand

apart in a classification based upon conditions of generation, and with the possible exception of Shots Able (Crossroads) and Cherokee (Redwing) cannot be compared with data from other tests.

The above generalized classification according to source geometry and geographic location is a brief summary of available data on water waves from nuclear tests in the Eniwetok Proving Ground. It points out the assorted generative conditions to be considered in analysis of the Redwing data. The analysis and interpretation of propagation and terminal characteristics are additional items of concern, and it is apparent that data from one test series cannot be properly analyzed and interpreted without reference to, and possible reevaluation of, conclusions from previous experiments. Data from future tests will necessitate a review and reassessment of present interpretations; to facilitate this, the basic data is included in the appendixes.

3.3 CLOSE-RANGE DATA

Shots in open lagoons, shots in old water-filled craters, and shots on shore near lagoon water generate water waves by direct impulsive action upon the water mass near the charge. For barge shots and shots in the range of the tests herein considered, high pressures at zero point (burst point) cause the rapid formation of a water crater which extends to, or into, the lagoon bottom. In the absence of direct observation of the generative process, the water wave train is assumed to be initiated as follows. The rapid crater formation causes an annular elevation of the water adjacent to the expanding crater to some value appreciably above the original mean water level. As the crater approaches its maximum radial expansion, gravitational forces become more and more determinant in the shape and motion of the elevated water mass until, at some time after the maximum expansion, this elevation radiates as a smooth-crested water wave. As this first wave crest moves outward, the water crater collapse commences. This collapse initiates in sequence, (1) the radial movement from surface zero of a wave trough and (2) the radial movement from surface zero of a wave crest. The trough (1) can be imagined to have a depth roughly equal to the crater depth at surface zero, and the crest (2) is the result of a water mount at surface zero due to the inrush of the peripheral water. Subsequent vertical oscillations of water level at surface zero result in additional troughs and crests. For the purpose of analysis, the first trough, the second crest, and all subsequent troughs and crests are considered to be manifestations of the potential energy of the fully expanded water crater. The number of observable oscillations and the relative size of the resultant waves are functional with crater radius and water depth.

Wave data from explosives tests are expressed as the relationship of the three variables: time, water-surface elevation, and radial distance from surface zero. In practice, the radial distance is held constant, and wave height as a function of time is recorded. Because the resultant waves at all ranges outside the zone of generation are dependent upon water motion within the zone of generation as a function of time, it is necessary to examine the parameters of generation [illegible]ociate them with the characteristics of the resulting wave system. Before attempt[illegible]fine, assign values to, or discuss these parameters of generation, it is necessary to examine the wave data available and note some of the general characteristics of the generation phenomenon. This is done for barge shots in open lagoon waters in this section and in the two following sections. Discussion of wave data from shots having more complex generation geometries are discussed in Section 3.18.

For yield values and water depths in the range of the Redwing tests, the generated wave systems observed have a few characteristics in common. The first wave is always a crest followed by a trough. Following this trough is a series of waves occurring as a discrete group, or groups, of waves. For near ranges, the highest wave is the first wave, but as range increases, the first wave progressively diminishes in amplitude relative to the amplitudes of following waves. Almost invariably one or more of these later waves are reinforced or otherwise altered by reflectance effects from other parts of the lagoon. The closer the reefs and islands are to the generating area or to the instrument station, the earlier in the wave system history this can occur. These alterations to the traces complicate their interpretation.

All test records presented in Appendix C are from barge shots with the device mounted on the barge. It is understood that it has been customary to ballast such barges with 200-plus tons of silica sand, and consideration was given to the fact that this additional interface between the burst and the water acts as an additional surface for reflecting energy from the water crater; however, considering the yields involved (0.375 Mt and up), it is felt that for the purpose of water-wave generation in these depths of water, burst point is at the water surface and the sand in the barge has very little influence upon the wave pattern or wave size. It is felt that the principal factors in determining the wave size and system type from these larger yield tests is the average lagoon water depth within the radius of the water crater and the magnitude of this radius.

The wave profiles given in Appendix C show the surface-water elevation as a function of time for the Castle and Redwing turtle stations. The wave heights referred to are those the waves should have had if they had been traveling in water 60 feet deep. For purposes of study and analysis, all waves were transferred to this common water depth. The reason for selection of this depth and the techniques employed to transfer the measured waves to this depth are discussed in a later section.

The data given in Appendix C has been grouped in order of increasing yield, with Flathead (Redwing) first and Yankee (Castle) last. The time scales (abscissa) have been expanded from that of the same data given in Appendix A (Redwing only) to give a more symmetrical and balanced picture. This time scale gives an abscissa-ordinate proportion approximately the same as the original recorded traces.

Figure C.1 represents the surface-water elevation as a function of time at Station 197.04 for Shot Flathead. The instrument was in 73.1 feet of water at shot time, and at a range of 7,190 feet (straight line) from surface zero. The average water depth surrounding the instrument was 73 feet. The recorded waves traveled 7,500 feet from their generation area approximately parallel to the Dog-Easy reef (Figure 2.1) over a gradually shoaling bottom to reach the instrument. One coral head was in this path, approximately 2,500 feet from the instrument, that protruded 28 feet from the bottom, but was negligible in extent (estimated at 200 feet) compared to the wavelength of the earlier waves. Conversion of the recorded subsurface-pressure information to surface-water elevation in 60 feet of water involved minor amplitude increases in all waves except for the shorter period, low-amplitude waves in the latter part of the system, which were increased a maximum of approximately 50 percent. Interesting features of this record are: the first crest is followed by a trough whose amplitude is substantially greater than that of the first crest, the second crest is essentially the same amplitude as the first, and this crest with the following two crests and their following troughs form a three-wave group of decreasing amplitude whose nodal point occurs at about 190 seconds. For times greater than 190 seconds, the amplitudes appear to first increase and then decrease to form a second group with a second nodal point around 240 seconds, at which time the

amplitudes of the waves decrease to background and beyond the resolution of the instrumentation. It is noted that the recorded waves between 190 and 240 seconds seem to be varying about a changing mean water level (a long-period trough), and the influence of first crest and trough reflections from the nearby Dog-Easy reef is indicated. There is no indication of a comparatively small sustained water-level rise prior to the arrival of the first crest as had been noted in the Castle close-in records and discussed in Reference 3. The indicated slope on the front face of the first trough is steeper than the back face of the first crest; i. e., the time of maximum trough depth is asymmetric to the first- and second-phase zeros.

Figure C.2 is the reduced data from the identical station of Figure C.1 but for Shot Dakota. The operating water depth of the instrument was 70.1 feet at shot time. The range was again 7,190 feet (straight line) from surface zero. The first-crest height is approximately equal to the following trough depth. The crests and troughs following the first trough have amplitudes less than the first crest or trough, and, as above, waves passing between 195 and 230 seconds appear to be superimposed upon a longer-period trough. The first trough is again asymmetric about the adjacent phase zeros.

Figure C.3 is the data from Station 197.06 for Shot Dakota at a nearly identical range (7,540 feet) as that of Figure C.2 but in a direction from surface zero more removed from the Dog-Easy reef (Figure 2.1). The wave path from surface zero to this station was over essentially constant water depth. One coral head was north of this path about 600 feet, at a range of 1,870 feet from the station. It protruded 36 feet from the bottom and its extent (estimated at 200 feet) was negligible when compared to the wavelengths of early waves. The instrument was operating at a depth of 62.2 feet of water (on a coral head) at shot time. The average water depth surrounding the instrument site was 168 feet.

The record shows the first wave to be a crest followed by a trough of approximately twice the crest amplitude. The second crest is greater in amplitude than the first and is followed by crests and troughs of regularly decreasing amplitude till the threshold of instrument resolution is approached at about 240 seconds. Again, the first trough is asymmetric about the adjacent phase zeros, and the waves following the first trough appear to be moving upon a longer period undulation of the lagoon water level. Comparison of Figures C.2 and C.3 shows the wave system as measured at these two stations to have different characteristics such as surface profile, relative amplitudes, and energy distribution. This difference could have been induced at the station location, along the wave path to surface zero, or at the periphery of the zone of generation. The group characteristic (beat phenomenon) noted in the Flathead record (Figure C.1) is not indicated in the Dakota record (Figure C.3). The record in Figure C.2 might be interpreted to contain this node at around 172 seconds when it is considered that the traces of Figures C.1 and C.2 are not at the same scaled range (different yields).

The records from close-in stations for Shot Navajo are given in Figures C.4 through C.6. Figure C.4 shows the record from the same station as Figures C.1 and C.2. The instrument range from the shot barge was 8,300 feet. The operating depth of the recorder and the average depth of the surrounding water was 73 feet at shot time. The comparatively small, gradual pressure rise preceding arrival of the first crest is noted. The forward face of the second crest is very steep compared to the back face of the first crest. The first crest is slightly greater in amplitude than the first trough. The waves following the first trough first increase in amplitude and then decrease with increasing wave number until 230 seconds, at which time a nodal point, or phase shift, appears to exist. The wave group following the first trough passed the station between 170 and 230 seconds. After 230 seconds, there is weak evidence of the passage of a second group.

Crests or troughs at 285, 302, and 350 seconds mark the passage of reflected waves.

Figure C.6 shows the surface elevation as a function of time for Station 197.05. This instrument was located due south of surface zero at a range of 14,380 feet. Its operational depth was 73.4 feet, and the average water depth surrounding the installation was 156 feet at shot time. The wave path from the area of generation to this station was in water 150 to 168 feet deep. Three to four comparatively small (compared to the wavelengths under consideration) coral heads exist adjacent to this path. The ground and/or water shock caused the recording disk to back up in time and parts of the earlier portion of the record could not be resolved. The maximum height of the first crest could not be determined, but the record becomes readable during the passage of the first trough. As zero time could not be read from this record (thermal start) it was necessary to fix the time scale to within ±5 seconds, for this trace by other techniques (Section 3.14). Comparison of this record with Figure C.4 shows the development with increased range of the waves following the first trough into groups, and shows this wave system to contain nodal points, or the beat phenomenon. The first nodal point was at approximately 325 seconds and the second at approximately 435 seconds.

Because of adverse field conditions, the wave record (Figure C.5) from Station 197.06 for Shot Navajo could not be recovered until the spring of 1958. Its location at range 6,500 feet from surface zero gave the wave height-time picture at the closest scaled range for nuclear tests to date, and permits a more conclusive discussion of the generation phenomenon. Figure C.5 shows the first resolvable pressure information at this range to be negative. This pressure is associated with the negative phase of overpressure, the positive phase having passed in the first second. This conclusion is supported by examining and comparing the early portions of these records with records from other more distant stations, and it is found that the first resolvable negative pressure moves at a velocity substantially greater than any conceivable water-surface elevation. Stations 190.01, 191.01, 192.01, and 193.01 at Sites Nan, Oboe, William, and How had sufficient sensitivity to record this negative pressure at extended ranges and show this portion of the subsurface pressure-time record to be associated with air overpressure. Figure C.5 indicates a return to ambient water pressure at 23 seconds. After the first negative phase, the record shows that a comparatively gradual increase in the mean water-surface level preceded the major elevation of the first crest. The magnitude of this advance water level rise was of the order of 2 feet. This phenomenon was first noted in Reference 3 wherein the possibility that this could be the result of impulse from close-in debris fallout was discussed. Comparison of the records given in Figures C.4, C.5, C.7, and C.8 indicates that this portion of the first crest is associated with the first crest only, because it stays a proportionate distance ahead of the first crest at all ranges, and that it was originated by the formation of the first crest from the rapid expansion of the water crater. As pointed out by earlier investigators (Reference 2), the first disturbance theoretically travels with acoustic velocity, and should be accompanied by a minute change in water surface slope. The conclusion of Reference 7 that the measured first rise represents a sudden increase in an already existing slope of the water surface, and is associated with the rate of travel of the first crest, appears to be confirmed. It is only when the energy release is sufficient to produce this phenomenon above background that it is observed.

In Figure C.5, the first crest, which is not as great in amplitude as the first trough, passed at 62 seconds. There is an inflection point on the forward face of the first trough, and again, the first trough maximum is asymmetric with its phase zeros. It is noted that a similar inflection point was indicated in a slightly different location in Figure C.6.

Following the first trough (Figure C.6) a series of crests and troughs with first increasing and then decreasing amplitudes were recorded. In Figure C.5, the first nodal point is indicated at approximately 207 seconds with the second following at around 231 seconds. In Figure C.6, a reflected crest passes at 432 seconds, probably from a nearby reef or island.

Figure C.7 is a wave height-time history for Shot Union of Operation Castle (Reference 3). The instrument was located on a coral head 3,900 feet from shoaling water (60 feet or less) adjacent to the George-How reef, the average water depth around the station was 138 feet, and the straight line range to surface zero was 21,400 feet. The bottom depth on a line to the surface zero ranged from 138 feet to 168 feet. There were several coral heads of negligible size (compared to the wavelengths involved) along the wave path from surface zero. This record shows the wave system from this test to consist of a gradual rise preceding the first crest, the first crest, a first trough, and second crest. After passage of the second crest, the wave action immediately drops to comparatively low levels. A reflected trough passes at 460 seconds. There is evidence of an inflection point in the first trough at 318 to 328 seconds. This record was so unlike any of those from Operations Crossroads (Shot Baker) and Redwing, and the records for this same shot at more distant ranges, that the influence of the George-How reef was considered the probable cause. When the laboratory experiments of Reference 5, were completed, and the various forms that wave systems could take had been indicated, it was realized that the Union wave system at its origin probably did consist of two solitary-type waves connected by a trough. Integration of the Redwing data with the Castle data permitted reevaluation of the more distant records from Shot Union and showed these records to contain identifiable locally induced reflectance, or shoaling, effects. These effects had restricted projection of the Union waves to nearer ranges for confirmation of the indicated wave-system type observed by this turtle station. This reevaluation of Castle waves confirms the conclusion that the wave system of Shot Union was the two-solitary type and unlike any other wave systems generated by nuclear tests to date.

Figure C.8 is a wave height-time history for Shot Yankee of Operation Castle. The recording instrument was placed in the same location as for Shot Union (Figure C.7). The record was discontinuous during a portion of the first trough and second crest (317 to 370 seconds). The arrival of the first crest was again preceded by a sustained pressure rise of approximately 2.8 feet of water (75 to 240 seconds). Between 240 and 308 seconds, the first crest passed with a maximum height of 25 feet. Again an inflection point exists on the following face of the first crest. Such inflections were observed in the experimental work of Reference 6 and were associated with very early stages of propagation. The first crest was followed by a trough whose shape and depth were not recorded. The passage of a longer period trough between 438 and 600 seconds corresponds almost exactly in timing with a similar trough in Figure C.7. Such a trough undoubtedly results from earlier crests that pumped water over reefs and islands and left a negative sump to propagate within the lagoon. In Figure C.8, a trough at 550 seconds could correspond to the trough at 560 seconds in Figure C.7. A comparison of the more distant range wave traces from Union and Yankee shows the wave systems to be identical in character. Wave size is larger for Yankee because of the higher yield and increased water depth in the zone of generation. Wave system was of the same type for both shots, because increased water depth in the generation zone for Yankee was in the correct scaled relationship to the larger yield.

A comparison of the subsurface-pressure record with the surface-elevation curves of Figures C.1 through C.8 shows that the above wave system characteristics are not the

result of the technique of interpretation of a subsurface pressure versus time trace. The general characteristics discussed above are verified by both sets of data.

3.4 INTERMEDIATE-RANGE DATA

It was noted in Section 3.3 that the wave systems at close ranges had identifiable characteristics with respect to water level rise ahead of the first crest, ratio of energy in the first crest to first trough, asymmetry of the first trough, and group pattern and beat phenomenon of waves following the first trough. In this section the records from floating-type instrumentation (Section 2.2.1) are examined to ascertain, in a general way, if the characteristics observed in Section 3.3 are present at more distant ranges. The basic data for this and the following section is included in Appendix A.

For Shot Dakota, Station 196.02 showed identically the same system characteristic (Figure A.3) as the close-range record (Figure C.3). The first trough was deeper than the first crest was high. The amplitudes of the second, third, and fourth crests and troughs decreased regularly from a second crest amplitude that was approximately equal to the first crest. The first trough was still asymmetric about its phase zeros, and the waves following the first trough appeared to be superimposed upon longer period changes in lagoon water level. Waves after the fourth trough exhibited nonsystematic variations in period and amplitude until they diminished to the amplitudes of the disturbed background at approximately 16⅓ minutes. The reflected wave that passed this station at 23½ minutes was a relatively large trough followed by a smaller crest. The trough is estimated to contain energy equivalent to that in the first crest.

For Shot Dakota, the record from Station 196.01 shows the wave system to have almost the same characteristics as indicated at Stations 196.02 and 197.06 (Figures A.3 and C.3). The exceptions are: (1) the first three waves immediately following the first trough do not measurably decrease in amplitude, and (2) the change in lagoon water level for waves following the first trough appears to be more prominent and of a longer duration. A discontinuity in regularity of wave period occurred at 16¼ minutes, after which the wave action reduced to background. As will become apparent when the shore station records are summarized, items 1 and 2 above result from the proximity of the atoll reef line and shoaling water. At 26¾ minutes, a large reflected crest passed this station. This was followed by a trough and three smaller crests and troughs that were almost identical in period to waves which passed earlier.

The intermediate-range wave system characteristics from Shot Navajo at Stations 196.01 and 196.02 records are shown in Figure A.5. Figure A.4 for Station 196.04 is also intermediate-range data, but the recording instrument was unpredictably temperature sensitive, and only the time of arrival of the first crest is reliable data. This trace does not accurately represent wave profiles.

The close-range records, examined in Section 3.3, indicated the Navajo wave system consisted of a first crest followed by a trough and two groups of waves. The record at Station 196.02 (Figure A.5) shows this very clearly. The first crest height was equal to the first trough depth, and the first trough was still asymmetric about its phase zeros at this range. The first node was at 14 minutes, and the second at about 16¼ minutes. The maximum amplitude of the waves in the first group was proportionately larger, compared to the first crest, than at the close-range stations. A reflected trough followed by a crest passed this station between 22¾ and 23½ minutes, and in shape and timing they were identical to those observed at this station after Shot Dakota.

The Station 196.01 record for Shot Navajo (Figure A.5) tends to verify the characteristics exhibited by the Station 196.02 trace, but again, the wave character was altered by the nearby shoal water and reef. The manner in which the open lagoon wave system was altered at this station is very similar for Shots Dakota and Navajo. The regular manner in which the waves decrease and increase in the following groups was not preserved. There was a longer period change in lagoon water level than that observed at Station 196.02, about which the shot-generated waves appeared to oscillate, and the regularity of the wave system was altered. A reflected trough and crest passed Station 196.01 between 24 and 25¼ minutes. This reflected crest was higher than the first crest as was the case for Shot Dakota; however, the similarity between the waves following this reflected crest and the earlier waves of the system is not as obvious as it was in the Dakota record. The trough preceding this crest was not apparent in the Dakota record, but this is probably due to the ratio of size to background of the Dakota waves.

The central lagoon records show that, once the wave system characteristics have been determined in the zone of generation, they are preserved throughout their propagation across the lagoon, and only when these waves approach shoal water, reefs, or island areas do alterations in the time-height history occur, which tend to mask the original wave characteristics. Prominent reflectors of wave energy are indicated; these require consideration when shore station records are inspected, and island-inundation potential is examined.

Reference 3 contains three wave records from Operation Castle—two from Shot Union and one from Shot Yankee. Their characteristics are discussed here, because the magnitudes of the later waves (probably reflections) noted for Navajo and Dakota become quite large in comparison, and permit conclusions about their source and the mechanism of their formation. These three records were taken at two stations: the closer of these, Station 163.04, was 1½ miles from Jig-King reef, and the other, Station 163.05, was 0.25 mile from the Nan-Mike reef and near a reflecting boundary. Records were obtained from both stations for Shot Union.

At Station 163.04, Shot Union, the characteristics of the record in Figure C.7 were preserved in the first two crests and connecting trough with the addition of 3 to 4 waves following the second crest. The second trough was deeper than the first, and it appears that the energy in earlier waves is moving back in the system to form waves after the second crest. Four and one-quarter minutes after passage of the first crest, the effects of the nearby reef were manifested as longer period changes in lagoon water level (of the same character noted in the Station 196.01 records of Navajo and Dakota). Eight and one-quarter minutes after the first crest arrival, a reflected crest passed, possibly coming from the nearby reef, and 12¼ minutes after first crest arrival, a large reflected crest passed from the same reflective boundary as the reflections noted in the Redwing stations above, and similarly it was preceded by a trough. The record at Station 163.05, Shot Union, was from a range approximately 3¼ miles greater than that of Station 163.04. The characteristics were similar to those shown in Figure C.7—the first two crests with a comparatively long and shallow connecting trough. The record from Station 163.05 shows the second trough to be equal in depth to the first trough. The amplitudes of the waves following the second trough are near background (approximately 1½ feet) until the arrival of a reflected trough whose depth is 1.6 times that of the first trough, and about 0.8 times the first crest height. This trough is followed immediately by a crest of equal amplitude. Subsequent waves decrease in amplitude until the arrival of three crests approximately 2½ minutes later. This wave record is almost identical in character to that at Station 196.01, Shot Navajo, except that the second, third, and fourth

waves of Navajo are proportionally larger than those of Union.

For Shot Yankee, the record at Station 163.05 is identical in character to that for Shot Union discussed above. Wave size has increased in proportion to the higher yield.

The location of reflecting boundaries and phasing of reflected waves is discussed in Section 3.7.

3.5 DATA FROM SHORE STATIONS

Shore stations located at Sites How, Nan, Oboe, and William, were operated for all tests in Bikini Lagoon except for the How station during Shot Tewa.

For the three open-lagoon shots, the wave records reflect the open-lagoon characteristics noted in Sections 3.3 and 3.4, plus characteristics induced by the lagoon, island, and reef topography. The wave systems from Shots Zuni and Tewa were unlike the other wave systems and, because an analysis of these waves will have to be made from the shore station records alone, it is necessary to analyze the location-induced changes at the shore stations for those tests in which the open-lagoon system is well defined, and apply, if possible, these conclusions to the data obtained for Zuni and Tewa.

For the three open-lagoon shots — Flathead, Dakota, and Navajo — Station 191.01 was the closest in range (on the basis of refracted not direct paths), and the waves in reaching it traveled along the short axis of the lagoon. The station transducer was in 60 feet of water approximately 375 feet from shore. Another 100 feet from shore the bottom depth was about 130 feet, and this slope continued to the average lagoon depth in the area.

This slope is typical of the Oboe-Tare lagoon bathymetry with the consequence that the waves approached very close to the shoreline before being altered by bottom influences.

For Shot Flathead, the record from Station 191.01 (Figure A.2) can be compared with the open-lagoon wave system as recorded by the close-range Stations 196.03 (Figure A.2) and 197.04 (Figure C.1). The first trough was greater in amplitude than the first crest and the second, third, and fourth crests were superimposed upon a very pronounced long-period change in water level. The nodal point in Figure C.1 at 190 seconds coincides with the start of an extended trough (Station 191.01) at 16 minutes in Figure A.2. The two waves following this discontinuity were of an amplitude similar to the first crest and trough. Following these, the wave pattern was erratic and inconsistent.

For Shot Dakota, the record from Station 191.01 can be compared with the open-lagoon wave system records of Stations 196.01 and 196.02 (Figure A.3)and Station 197.06 (Figure C.3). Again, at Station 191.01 the first trough was deeper than the first crest was high, and was symmetrical with respect to its phase zeros. The five waves following the first trough were much smaller in amplitude than the first crest or trough, and were again superimposed upon a long-period water level fluctuation. The third wave following the first trough appears to have the greatest amplitude of these later waves, but the variation of amplitude with wave number for these waves does not indicate any clear-cut trend as do those at Stations 197.06 and 196.02. This same tendency to random variation of wave amplitude for waves following the first trough was detected in the record of Station 196.01 and was attributed to the proximity of a reflecting boundary.

For Shot Navajo, the waves recorded by Station 191.01 (Figure A.5) had the following prominent features. The first crest and trough were more than twice greater in amplitude than any other wave. The wave-group phenomenon for waves following the first trough observed at Stations 197.05 (Figure C.6) and 196.02 (Figure A.5) was preserved,

and nodal points are indicated at 16¼ and 18¼ minutes. The waves following the first trough were superimposed upon a fluctuating lagoon water level, but the regularity of increasing and decreasing amplitudes with wave number observed at Station 196.02 (Figure A.5) was not preserved. There is also evidence of a third wave group between 18¼ and 20¼ minutes.

The arrival at later times of waves with energies equal to that of the first wave, similar to those observed at the skiff Stations 196.01 and 196.02 (Figure A.5) was not observed in any records for Station 191.01. Characteristic changes in the open-lagoon wave system recorded by the station are summarized as follows: (1) The crest heights of all waves following the first trough are substantially reduced relative to the first crest height. This is a function of wave size and tide stage, and is most prominent for Navajo waves and least prominent for Flathead waves. (2) Waves following the first trough are superimposed upon locally induced long-period changes in water level. (3) Arrivals of prominent reflected waves are not detectable.

The records from Station 190.01 show locally induced characteristics that are unlike those of Station 191.01. For Shot Flathead, the record for Station 190.01 (Figure A.2) shows: (1) the first eight waves were symmetrical about the mean water level, (2) like the open-lagoon record in Figure C.1, the first trough was greater in amplitude than the first crest, and (3) the second crest was the highest crest. The first nodal point of the Figure C.1 was not detected at Station 190.01. A trough whose amplitude was approximately the same as that of the first trough arrived at 23¾ minutes, and was followed by a crest of equal amplitude. This was very nearly the highest crest at this station. Other waves of equal amplitude arrived at later times but could not be identified with the more significant features of the open-lagoon wave system.

For Shot Dakota, the record from Station 190.01 (Figure A.3) has features very similar to those of Stations 197.06 (Figure C.3) and 196.02 (Figure A.3). Again the first eight waves were symmetrical about the mean tide stage, the first trough was deeper than the first crest was high, and the second crest was slightly higher than the first crest. A trough arrived at 23¾ minutes, followed by the highest crest on the record. The relative times of these features are almost identical with those recorded for the Flathead waves. Similarity of periods and grouping between the first waves recorded and those after 25½ minutes indicate these later waves are reflections from some other part of the lagoon.

For Shot Navajo, the record at Station 190.01 (Figure A.5) can be compared with those of Stations 197.06 (Figure C.5), 197.05 (Figure C.6), and 196.02 (Figure A.5). The first crest and trough are of approximately the same amplitude, the second, third, and fourth waves are symmetrical about the mean water level, and decrease regularly in amplitude similar to the record for Station 196.02. The first nodal point was at 20½ minutes and marks the beginning of a long-period trough which reached its maximum depth at 22¾ minutes. The second group of waves, as also observed at Station 196.02, is superimposed upon this long-period trough and could possibly extend into the following crest. This trough and crest were equivalent in amplitude to the first crest and trough and the periods of the waves which arrived between 25¼ and 26¾ minutes are identical with the periods of the second through third waves. It becomes apparent that the large waves on this record, which arrived after 25¼ minutes, are reflected waves from another part of the lagoon.

The records for Station 190.01 show: (1) as the wave size increases, the first four waves increasingly maintain their open-lagoon configurations; (2) the early waves tend to be symmetrical about the original mean water level; (3) later in the record a prominent

trough and crest indicate the arrival of waves that are identifiable by their periods as being reflections of the first waves of the system from another part of the lagoon; (4) the time from the first crest arrival to the arrival of the reflected crest is the same on all records, indicating that the reflector is the same for all shots; and (5) either the reflected-wave velocity is independent of wave size, or the reflector is physically close enough to the recorder to prevent detection of velocity differences due to the relatively small differences in wave height.

The records for Station 193.01 are the most complex of all, because waves arriving at this station traveled a refracted path adjacent to the How-George reef. As a consequence, the open-lagoon wave systems were superimposed upon much longer period and greater amplitude changes in water level, which made the characteristics of the wave system very difficult to detect. The confusion of waves at this location appears to be a function of wave size and wave number, and the system characteristics can only be identified by their periods.

For Shot Flathead, the record for Station 193.01 (Figure A.2) does not compare with any of the other records for this shot. The amplitude of the generated waves was very small, the first crest is approximately equal in amplitude to the first trough, and the discontinuity between the fourth and fifth crests at 16½ minutes has been identified in records for Stations 191.01 (Figure A.2) and 197.04 (Figure C.1). Either the second or third crest was missing at Station 193.01.

With an increase in wave size from Shot Dakota, the site-induced features of the wave system at Station 193.01 became more discernible (Figure A.3) and is very similar to the record of Station 196.01 (Figure A.3). The first trough was greater in amplitude than the first crest, the regularity of decrease in amplitude for the second, third, and fourth waves, as was shown at Station 196.02 (Figure A.3), was changed in a manner similar to that at Station 196.01 (Figure A.3), and the second through ninth waves were superimposed upon a longer period change in water level. Wave action reduced to background at 19 minutes, and the first reflected trough and crest arrived at 28¾ and 29½ minutes. Other reflected waves are apparent at even later times.

The waves from Shot Navajo were of sufficient size to amplify the location-induced characteristics at Station 193.01 so that they become quite apparent. In Figure A.5, the first crest was preceded by a small comparatively long period trough, and as in the record at Station 196.01, the first trough was shallower than the first crest was high. The first trough was asymmetric about its phase zeros, and the second through eighth waves were superimposed upon a long-period water-level change whose maximum occurred at approximately 17¾ minutes and whose amplitude was about 1.5 times that of the first trough. These long-period water-level oscillations, between 15 and 25 minutes, are the result of wave activity along the George-How reef and are characteristic of the station for shots located in the northwestern part of the lagoon. These long-period water-level changes are associated with the selectivity of a shallow reef parallel to wave path. By refraction of the waves, the reef traps and absorbs wave-crest energy, but reflects wave-trough energy to the deeper lagoon waters. The net effect is that of a negative half-wave rectifier. This is best observed at Station 193.01 shortly after the arrival of the first trough. A reflected first crest and trough, typically the same reflected wave observed at proportionately later times at Station 190.01, arrived from a more remote part of the lagoon at 27¾ and 28⅓ minutes.

In summary, the principal location-induced characteristic at Station 193.01 is a long-period reference water-level oscillation induced by the George-How reef, with relative amplitudes great enough to drastically alter the absolute wave height versus time picture of the open-lagoon system.

Station 192.01 had locally induced effects upon the open-lagoon wave system that were different from those of the other shore stations. The records are given in Figures A.2, A.3, and A.5 for Shots Flathead, Dakota, and Navajo. The record for Flathead shows the first crest and trough and the second crest to be equal in amplitude. The second trough and third crest, have the greatest amplitudes in the recorded system, and only after 17 minutes do the waves assume a regular pattern similar to what would be expected in open-lagoon waters. The wave record does not compare in characteristics with those from the other shore stations, or with the one turtle record.

Because of increased wave size, the Dakota waves recorded by this station (Figure A.3), show the same characteristics as for Flathead but more prominently. The first crest height was equal to the first trough depth, and, as before, the second trough and third crest were the greatest in amplitude. The top of the second crest was at the original lagoon water level and was apparently influenced by a large-amplitude, long-period lowering of the mean water level. The small fourth crest at $16\frac{2}{3}$ minutes, coincided with the inflection point at 17 minutes at Station 196.02, and the fifth through ninth waves were again approximately equal in amplitude to the first wave. A comparison with those for Stations 196.02 and 196.01 shows that the most prominent feature of the record at Station 192.01 is the alteration of the second, third, and fourth wave heights and periods. The ninth crest was the highest with respect to the mean water level but it is observed to be so because of a longer period rise in lagoon water level and is not considered representative of the open-lagoon wave system.

The Navajo waves at Station 192.01 (Figure A.5) amplify these characteristics even more. The first trough was slightly greater in amplitude than the first crest. The inflection point at 14 minutes on the back face of the first crest was noted before in the records for Stations 196.02 (Figure A.5) and 197.06 (Figure C.5). As in the Dakota record, the second crest maximum was about equivalent to the mean lagoon water level. The third crest was considerably higher than the second, and the fourth crest represents a nodal point in amplitude as was indicated by the Station 196.02 record. The fourth through tenth waves form a second group; the sixth and ninth crests are the highest. As was detected in the record at Station 191.01 for this shot, there is evidence of a third, much smaller group starting with the eleventh crest. Wave action returns to background at 22 minutes, and at this time a long-period reflected trough arrives from another part of the lagoon. The prominent reflected crests at later times, recorded at Stations 196.02 and 196.01, are not observed at this station.

In summary, wave systems recorded at Station 192.01 are altered as follows: (1) the degree of alteration is dependent upon wave size and energy content, and (2) any regularity in absolute and relative values of wave heights observed in the open lagoon are changed, and this change appears to be most prominent for the second wave and decreases in proportion to increasing wave number. Nodal points and inflection points of the open-lagoon system appear to be preserved.

3.6 WAVE ACTION AT NORTH NAN SHORELINE

A camera station was established, maintained, and operated by Edgerton, Germeshausen, and Grier (EG&G) on the wooden tower located at the north end of Site Nan. The cameras were mounted adjacent to the Station 190.01 recording equipment at about the 20-foot level, and timed photographs were obtained of the wave action along the shoreline from this tower south to approximately the Nan camp area.

These films have been studied, and the information on wave heights and times of arrival at a point on the shoreline are presented in Appendix B, along with the waves

measured by the project Station 190.01 tran ducer, which was 2,500 feet distant on a bearing of 286 degrees true. The vertical scale for these photo records was determined from known vertical dimensions on the LCU wreck located in the foreground between the tower and the Task Group 7.3 recreation area in Figure 3.1. The exposure and grain size of these films (16 mm) do not permit detailed photogrammetric analysis or enlargement for detailed examination; therefore, the continuous curves shown in Appendix B represent a substantial amount of smoothing of data points, which would otherwise appear more accurately as saw-toothed, vertical-fronted, breaking waves.

All major waves at the shoreline entered the camera field of view from the right as breaking waves. The condition of the smaller waves as they enter the field of view is uncertain. The field of view of the lenses for the first 200 yards down the beach is quite narrow, and beyond this range, the film resolution does not permit conclusions about how far from the shoreline the waves started to break. Consequently, the curves of Appendix B are applicable only to the shoreline between the north Nan tower and the Task Group 7.3 recreation area. The times of arrival of peak values of the major waves are very accurate, the relative heights are within the experimental error of the other wave data, and the absolute heights are estimated to be accurate within 2 feet. The data shows several interesting features of these waves as they move onto a shoreline.

One of the more apparent features of the Navajo wave record (Figure B.3) is that the first wave arrived at the shoreline $1\frac{1}{3}$ minutes after passing the project transducer. Based on the direction of wave propagation and the relative location of the two points of observation, the distance traveled is approximately 2,500 feet. At a velocity of 44 ft/sec, $\sqrt{gh}$ in 60 feet of water, the indicated travel time is 1 minute and in 30 feet of water, the travel time would be $1\frac{1}{3}$ minutes. The bottom in this area shoals from 120 feet to the shoreline in the direction of wave propagation in a horizontal distance of 3,200 feet. Hence, waves of this long wavelength (greater than 5,000 feet) respond to the comparatively rapid shoaling of the bottom. Another characteristic of these waves is the increased height due to shoaling, or reflectance. The first crest of Navajo increased from 4.5 to 6.8 feet in moving from 60-foot water depth to the shoreline. The trough depth changed from 3.8 to 3.7 feet. The shoreline trough depth is defined as the minimum elevation of water recession prior to an advancing crest. The lagoon bottom is bare inshore of this area.

The second, third, and fourth Navajo waves measured at Station 190.01, arrived at the shoreline as one continuous front of water with the same travel time from the transducer as the first wave. Although the individual crests could be detected as breaking waves superimposed upon a water-level rise as they entered the field of view and were observed to move up on the beach, the distinct troughs accompanying the crests in deeper water were not observed.

The next major Navajo wave action to pass the Station 190.01 transducer was a large trough between 21 and $23\frac{1}{3}$ minutes, which was followed by a crest equal in height to the first crest. This large trough was not apparent at the shoreline, but the following crest was the major inundating wave and was much larger than the first crest at the shoreline. Scientific personnel occupying Station 70 on south Nan, who watched the waves arrive at Nan, reported that the third wave was the one that did the damage. It is apparent that, from the standpoint of a water-level change at the shoreline, the third wave was the largest. Observations indicate that waves at the shoreline are not always representative of the wave system in deeper water. The travel time of this major inundating crest from the Station 190.01 transducer to the beach was approximately $\frac{2}{3}$ minute and was significantly less than the corresponding time for the first crest. Also, the increase in height

was approximately 180 percent compared to an increase of 50 percent for the first crest. The trough passing the Station 190.01 transducer at 25.1 minutes was also observed at the shoreline, $\frac{2}{3}$ minute later. The three prominent crests that followed this trough at the Station 190.01 transducer between $25\frac{1}{2}$ and $26\frac{2}{3}$ minutes are observed to behave as did the second, third, and fourth waves in that they joined together at the shoreline to present a continuous head of water. At $27\frac{2}{3}$ minutes, a trough was indicated at the shore, which on a relative basis, is much larger than the trough that was at the shore at $25\frac{2}{3}$ minutes. While the Station 190.01 record shows the first of these two troughs, it does not indicate the presence of the second and larger trough. The induced changes in an open-lagoon wave system as it moves onto a shoreline are obviously very complex.

Because the water waves from Shot Dakota were much smaller, the changes in height and arrangement were less prominent than those for Shot Navajo. The data is summarized in Figure B.2. The first crest and trough arrivals at the shoreline were so imperceptible that this section was accidently cut in the film editing and is no longer available. The grouping of the second, third, and fourth waves at the shoreline did not occur as it did for the Navajo waves. The travel time for these waves between the transducer and the shoreline was, as for the Navajo waves, approximately $1\frac{1}{3}$ minutes. In general, the wave sequence recorded at the shoreline followed that at the transducer very closely. For example, the general lowering of the waves about a mean amplitude line at $22\frac{1}{2}$ minutes for the 60-foot depth was apparent at the shoreline at 23 minutes. The longer period undulations of the mean water level between 22 and $24\frac{1}{4}$ minutes were reproduced at the shoreline between $22\frac{1}{2}$ and $24\frac{3}{4}$ minutes. The second prominent crest which passed the 60-foot depth at $24\frac{1}{2}$ minutes was seen to arrive at the shoreline approximately $\frac{2}{3}$ of a minute later, which duplicates the trend in arrival time for this crest noted in the Navajo records. For Shot Dakota, the highest wave at the shoreline was this later crest, but its increase in height compared to the increase in the height of the first waves to arrive is not indicated to be as great as was the corresponding increase for the Navajo system.

The Flathead waves (Figure B.1) recorded at the shoreline continue the trend, detected in Navajo and Dakota waves, to alter the character of the wave system recorded at the transducer less and less as the wave size decreases. The second crest produced more of an inundation threat than the first, and, as for Dakota and Navajo, there was a later wave which was also prominent in this respect. The travel time of the second crest from the transducer to the shoreline was approximately $1\frac{1}{3}$ minutes as anticipated, but the first crest travel time appears to be only about $\frac{1}{2}$ minute and so is ahead of schedule. This value of $\frac{1}{2}$ minute may very well be due to inability to resolve the first crest maximum for this small height, because the film is badly underexposed. It should be remembered that, between 18 and 22 minutes, there is a great difference in light intensity, because all of these shots were fired just before daylight and the attendant problems in photography and film development were numerous.

One characteristic of the Flathead waves in Figure B.1, which differs from those of Dakota and Navajo, is that the difference in arrival times at the transducer and at the shoreline of the second prominent crest was of the order of $1\frac{1}{3}$ plus minutes and not the $\frac{2}{3}$ minute of the corresponding Dakota and Navajo crests. This is interpreted to indicate that this crest arrived from a different direction for Flathead than for Dakota and Navajo. This feature is reviewed in detail in Section 3.7.

In summary, the changes that occur to waves in traveling from deep lagoon water to an island shoreline appear to be directly proportional to wave size and energy content. For the smaller waves observed, the deep-lagoon pattern is fairly well preserved at the

shoreline but for waves the size of those from Navajo the alterations of the deep-lagoon water elevation versus time curves at the shoreline are quite extensive. This same conclusion was indicated in the discussion of the shore-station records of Section 3.5 and was most vividly exemplified by the records obtained from Station 191.01.

3.7 REFLECTED WAVES

At most station locations, there were recordings of waves that did not travel directly from surface zero, and in some instances the waves passed over the instrument at the same time as waves generated and radiating from surface zero. Sometimes these reflected waves were traveling in the same direction as those from surface zero, and at other times they were not. Except for the study of inundation from these tests, the reflected waves could be ignored, and analysis restricted to reflectance effects upon wave heights of the original system near a reflecting boundary.

The damaging inundation at Site Nan was the result of a reflected wave. Approximate water level as a function of time curves at the north Nan shoreline were developed from EG&G timed photography for Shots Zuni, Flathead, Dakota, and Navajo, as has been noted earlier in Section 3.6. The significance and size of the reflections increased rapidly with shot size, and as a result, the reflectance phenomenon being discussed was barely detectable for Flathead and became quite noticeable for Navajo. A review of the wave data for Shots Union and Yankee during Operation Castle shows this identical reflection at Nan and confirms the conclusions derived and presented in this report. The identification of this reflection in the Castle data, which has become possible only since this analysis of the Redwing data, also confirmed earlier conclusions about the type of wave system generated by Shots Union and Yankee, where previously the small quantity of data from these shots had not permitted the exclusion of these prominent reflected waves from the original open-lagoon system.

The analysis of these reflections has been difficult with the amount of data available; all the facets of the phenomenon cannot be explained. The conclusion drawn stems in part from a negative approach: a number of possibilities are examined and one conclusion is arrived at by exclusion.

The majority of wave instrumentation was located in the eastern half of the lagoon, to minimize problems of placement and recovery due to radiation. Station 192.01 was in the southwestern end of the lagoon and recorded all significant wave action in the western half of the lagoon. The prominent reflections under discussion were not apparent at this station, and it was concluded that significant reflections were directional and peculiar to the eastern half of the lagoon. The reflector was the lagoon shoreline of Sites Oboe and Peter. The mechanism of reflection is discussed below. The Navajo wave system (Figures A.4 and A.5) is used as an example.

The wave systems from barge shots in the north-central area of the lagoon approached the Oboe-Peter shoreline at an angle of incidence approximately 25 degrees from perpendicular. The approaching wave system is as shown by the Station 196.02 record in Figure A.5. The first crest ran up the shoreline and spilled onto and flowed across the island. The amount of flooding was dependent upon wave height, tide stage, and first-crest half wavelength. A significant volume of water was momentarily removed from the lagoon and resulted in a general lowering of the mean water level adjacent to the shoreline. In exact phasing with this level change, the first trough was totally reflected from the shoreline and moved off to other parts of the lagoon. The water that was upon the island had only partially returned to the lagoon at the time the second crest arrived

at the shoreline. Because the mean water level near the shoreline was sufficiently lowered by the water remaining upon the island, and also by the presence of the later portion of the reflected trough, the second and third crests did not exceed the shoreline elevation and were totally reflected (minus the energy losses of turbulence, and so forth) and moved off behind the reflected first trough. The second trough lost its identity at the reflector, and the energy of the second crest and trough and the third crest were reflected as a single crest.

This is shown by the Station 191.01 record (Figure A.5) whose transducer was located at the eastern edge of the reflecting boundary. The second crest, second trough, and third crest arrived at this station at 14.2, 14.4, and 14.6 minutes respectively and are only faintly detectable in the pressure-time record. The representativeness of a subsurface pressure record in this zone might be doubted, but if this reflected crest is examined out in the open lagoon, well removed from the reflecting boundary, the second trough seems to have been absorbed by this wave and no longer exists. By the time this crest has left the area, the mean water level is back to normal and subsequent waves are too small in amplitude to repeat the process. There is slight evidence that a trough much smaller than the first is reflected next, which would imply that the fourth crest flowed upon the island. It can be imagined that the whole process is dependent upon delicate phasing and the effects of many variables. By this mechanism, a wave consisting of a trough followed by a crest is radiated from the reflecting boundary.

This reflected wave (a trough followed by a crest) traveled toward Sites How and Nan, and is observed to pass Stations 196.02, 196.01, and 193.01 at the times given in Table 3.8. The celerity of this reflected crest is 74.3 ft/sec, the same as that of the first crest. The reflected wave (trough and crest) does not appear to be dispersive over these ranges, because it maintains its identity and integrity. Its amplitude is, on an average, everywhere equivalent to that of the first wave of the direct wave system.

The reflected wave (trough and crest) from Oboe-Peter traveled in a northerly refracted path over slightly shallower lagoon water to Station 190.01 and arrived at this location at 25 minutes (trough) and 25.5 minutes (crest). Prior to this, however, a comparatively long-period trough followed by a crest was observed to arrive and cause the maximum inundation of Nan. The first disturbance of this trough arrived at approximately 21 minutes. The maximum depth of the trough arrived around 22.5 minutes, and the following crest was at 23¾ minutes. By comparing the travel times between the Station 190.01 transducer and the north Nan shoreline, the first crest from surface zero, and these reflected crests, it can be determined that these reflected waves are approaching from the direction of Oboe (Section 3.6). The reflected wave arrival at 23¾ minutes dictates that this crest traveled from Oboe to Nan at an average celerity of 88.5 ft/sec, or 10 ft/sec faster than the first disturbance traveled across the deepest parts of the lagoon. If allowance is made for the reduced celerity into the shoal areas of the transducers and reflection time at Oboe, a maximum celerity of 100 ft/sec is more realistic. This celerity value indicates that it must have been traveling part of the time in water deeper than can be found in the lagoon, and the conclusion must be that it followed a path that at some time during its travel placed it over the much deeper, and rapidly increasing, depth along the southern face of the Enyu Channel (Figure 2.1).

Examination of the hydrographic chart of Enyu Channel shows a subsurface ridge extending from Oboe to Nan and if the wave angle of incidence to this ridge were sufficiently small, by refraction the wave could track along this ridge, and follow it to Nan. In addition, because the reflected wave originates inside the lagoon and is refracted onto this ridge, and then by refraction is forced to follow it, the reflected wave moving along

the ridge can receive reinforcement and increase its energy content as it moves toward Nan. This is apparently what happened as the comparative size and accompanying inundation of the two reflections at Nan indicates that the first arrival contained considerably more energy. This greater energy is manifested as increased period and wavelength. Even though a wave path out into deeper water of the ocean and back into Nan would be a considerably greater distance than directly across the Enyu Channel, increased velocity in the deeper water could more than compensate for this. The full wave period of the inundating reflection at Nan is of the order of 3½ minutes. Assume a celerity of 70 ft/sec, which gives a full wavelength of approximately 1.47×10^4 feet. The velocity C, of a wave in any depth h is expressed by

$$C = \sqrt{\frac{g\lambda}{2\pi} \tanh \frac{2\pi h}{2}} \tag{3.1}$$

If the water depth (408 fathoms) is one-sixth the wavelength

$$C = \sqrt{0.78\ g\ \frac{\lambda}{2\pi}} = 242 \text{ ft/sec} \tag{3.2}$$

and a wave moving into this water depth could make up lost time due to a longer path.

It is concluded, therefore, that the inundation at Nan after Shot Navajo resulted from a reflected wave originating at Oboe-Peter and that this wave moved along the deep-water side of the Oboe-Nan ridge in the Enyu Channel. This reflected wave reentered the shallows of the lagoon in the vicinity of Nan and, at this point and time, acted as the source for another reflected wave. Indeed, it can be tracked as it moved north past Stations 196.02 and 196.01 at an average celerity of 74.3 ft/sec. This reflection moved on north to the Station 193.01 transducer and was recorded. With three significant waves (the original first wave, the reflected wave from Oboe-Peter, and the second reflected wave from Oboe-Peter reentering at Nan) moving about in the eastern half of the lagoon, the attendant confusion in preliminary analysis with a comparatively small quantity of data is apparent.

The wave data from Shot Dakota confirms the above conclusions. Smaller waves and a lower tide stage (Navajo was shot at a high tide) tended to reduce the magnitude of the phenomenon. With this reduction a relative change is noted in the wave trace recorded by Station 191.01; in Figure A.3, the second trough has been eliminated as it was for the Navajo waves at this station.

For Flathead waves at this station (Figure A.2), the second trough was identifiable and arrived at 14.8 minutes, and in general the waves recorded at this station began to resemble that of the open-lagoon system. The time difference between passage of the reflected wave past the Station 190.01 transducer and its arrival at the Site Nan shoreline for Shot Flathead (Figure B.1) indicates that this reflection phenomenon has reduced with wave size to the point that the Oboe-Nan ridge path is not a significant factor and that the primary reflected path for Shot Flathead is the lagoon refracted path (Section 3.6).

3.8 INUNDATION DATA

To complete the study of these waves from their generation to their termination, a portion of the project effort was directed to gathering data about the extent a wave traveled upon or across an island, the order of intensity of its flow, and what erosion, structure damage, and miscellaneous phenomena were caused by the wave. Experience and information gained from a similar effort during Operation Castle suggested specific areas

for given shot locations in which the inundation effects would be a maximum, and the project attention was focused upon these areas.

It has developed that one of the most efficient ways to gather this type of information is by low-altitude aerial photography of the island shorelines from a helicopter, and project personnel carried out flights around the atoli on a scheduled basis for both pre- and postshot photographic mapping of the island shorelines using both black and white, and color film. Five cameras were used: two Rolleiflex (2¼ by 2¼ inches), one for black and white, and one for color transparencies; one Hasselblad (2¼ by 2¼ inches color) with interchangeable lenses for standoff shots of highly contaminated shorelines; and two handheld semiautomatic K-25 aerial-mapping types (black and white). The aerial cameras were particularly well adapted for this application, because the 50-exposure roles permitted maximum coverage before reloading. It is noted, however, that black-and-white photography alone is not sufficient for these purposes. Color photography is required as an adjunct, because the wet and dry areas and eroded areas show much more prominently in these pictures. Reliance upon the black-and-white photographs primarily for continuity of coverage and upon the color for assessment of relative effects resulted in the best coverage.

As it turned out, the full-atoll sweeps were not necessary except as confirmation of negative inundation, in that the waves did not exceed the high-tide elevations at most of the islands. The possibility that the predicted yield for a particular test might be low rather than high and that anything less than a full-atoll survey prior to a shot would exclude the possibility of accurately comparing before and after effects at a location of special interest justified the expenditure of the additional time and effort that resulted in a full-atoll photographic survey immediately prior to each shot day. Approximately 1,600 black-and-white pictures and 500 color transparencies were exposed and processed. Of this quantity, approximately 10 percent contain positive information about inundation.

Another technique used for studying water levels from wave action upon an island was by the placement of can-type gages on structures or palm trees at various levels to retain water should they be submerged. Empty beer cans were readily available, and these were tacked up at an assortment of locations and elevations. The placement of these gages was time consuming, compared to aerial photography; therefore, the effort in gage placement was reduced during the operation, for all except the readily accessible locations, in favor of aerial surveys. Because the waves from the early shots did not result in major inundation, very little data was obtained from these can gages.

During the planning stage, it was conjectured that, should Shot Zuni (at Tare) breach the ocean reef and communicate significant energy to the deep ocean water, the inundation at south Nan around Station 70 could be very severe. Refraction diagrams showed that wave energy from both the lagoon waves and deep ocean waves could be funneled onto and trapped upon the subsurface ridge running from Oboe to Nan. The cumulative effect was prophesied as a very large wave at south Nan. Project effort was directed to mount inundation gages along the Tare-Oboe complex, Uncle-William sites, and around Station 70 at south Nan. Shot Zuni did not breach through to deep water, and the particular phenomenon that was expected did not occur. The blast effects removed all gages and the objects to which they were attached within the range where a water wave did cover a section of island, and at more distant ranges where everything was not carried away, the water wave inundation was of a minor extent.

The detailed examination of inundation as related to the approaching waves is discussed in Section 3.9. In summary, the inundation attributable to the direct waves from the Redwing series was comparatively minor except for special areas. The two principal

areas—Oboe-Tare and Dog-George complexes—were diametrically opposed from the Flathead, Dakota, and Navajo barge sites. The two other shots in Bikini Lagoon that generated measurable waves in relatively protected locations, and consequently, the resultant inundation was negligible. For the Oboe-Tare areas, the amount of inundation and the flow across the islands was dependent upon tide stage and wave size. These islands and shorelines were more susceptible to inundation than others in the southern portion of the lagoon, because the wave direction of approach was sufficiently near perpendicular to the shoreline, and the lagoon bottom shoaled more abruptly in this area making this shoreline a more efficient reflector of wave energy. As a consequence, the maximum wave height upon reflection was greater. Shorelines west of Tare are relatively well protected by extensive lagoon reef areas except for those islands bordering deep channels to the ocean, in which case the channel constitutes a leak of energy to the deep ocean, which tends to protect the adjacent islands. Nan was reasonably well protected from direct wave action, and except for an unusual phenomenon discussed in Section 3.7 would have been undisturbed throughout the whole operation.

The island and causeway areas from Dog to George were quite heavily inundated by waves from Shots Flathead, Dakota, and Navajo. Waves from Dakota and Navajo did extensive damage to the three manmade structures used on the Dog-Charlie reef for Shot Cherokee test. Although the project was not prepared to instrument inundation effects in this area, the aerial photography gives a very vivid picture of the severity of this wave action. After Shot Flathead, the blast and the waves cleaned off the loose coral sand cover on these island areas; the Dakota and Navajo waves then tore away the more permanently cemented coral foundations. This effect was especially heavy along the lagoon shorelines. In the postshot aerial photographs of the lagoon area, a progressive deterioration of the below-tide-stage shoreline is apparent, as is the deposition of large blocks of coral on the outer, ocean fringe reefs. Erosion and water-level marks on mounded structures in this area indicate that 20 to 30 feet of water passed over the islands.

Selected photographs related to the discussion of inundation and inundation effects in Section 3.9 are included as Appendix D.

3.9 DISCUSSION OF INUNDATION EFFECTS

The sequence of events attendant to the flooding of an island are visualized as follows. As a wave surmounts the island edge elevation, the velocity of its breaking front, a bore, increases as the water height above the edge elevation increases. Shortly after the maximum water level is reached at the shoreline, the impetus for increasing the volume of water upon the island diminishes. This decrease in head near the shoreline is not immediately reflected as a decrease in the velocity of propagation at the bore front, which is inland an appreciable distance by this time. Eventually the loss of inundating head at the shoreline is communicated through the volume of water upon the island, and this volume returns to the lagoon or ocean by the paths of least resistance at a rate dependent upon the ratio of the volume of water to the area inundated. If the height-time factors of a crest at the shoreline persist long enough, the bore will travel across the island and continue across the ocean reef to the ocean. Because the sequence of these events and the flow from the first crest onto the island occur at a slower rate than the energy is being brought to the shoreline by succeeding crests, the initial head of water at the shoreline can be replenished by the second and succeeding crests before the water already on the island has completely receded. Under these conditions the first three or four waves of the system can pump an increasing quantity of water onto the island, and consequently

inundation effects in some cases may be the result of a considerably greater quantity of energy than can be accredited to the first crest. An example of this type of phenomenon was noted for the second, third, and fourth crests at the Nan shoreline (Section 3.6). A rigorous treatment of the problem is beyond the scope of the data and present theory, and it is only feasible to correlate the on-shore and shoreline effects with the recorded waves on a crude and approximate basis, which considers only the first crest of the systems.

The one exception in which the maximum inundation did not occur with the first waves was at Site Nan where reflected wave energy from Shot Navajo arrived over an unusual path from the Oboe complex (Section 3.7). Had Navajo shot time been at a low instead of a high tide, it is probable that the inundation at Nan would have been of minor degree.

It has been shown that first-crest heights increase as they move from the deeper lagoon waters to the 60-foot depths of the shore stations and that the amount of increase is sensitive to the surrounding lagoon topography (Section 3.17). It has also been shown that these crests continue to increase in height as they progress from the 60-foot depth to the island shoreline. The data available to give an idea of the magnitude of this increase in height from the deep lagoon to the shoreline is assembled in Table 3.2 and indicates that the first-crest heights were from 2.4 to 2.6 times greater at the Nan shoreline than in the open lagoon at the 60-foot depth. The average increase in first-crest height from deep-lagoon water to the shore-station transducers (excluding the Site How data because of the wave energy absorptivity of this area of the lagoon) was about 1.6, 1.4, and 1.1 for Shots Navajo, Dakota, and Flathead.

As in the case of wave height, the extent and intensity of flow upon an island is dependent upon the time interval for which the water level exceeds an average island elevation near the shoreline. This time interval is in turn related to the wave period and the tide stage. The intensity of flow is visualized as being dependent upon a height dimension, and the quantity, or volume of flow, upon a time dimension. It is impossible to say exactly what changes occurred in the wavelengths between deep water and the shoreline, but the data of Appendix B indicates that the proportionality of the first-wave period, and first-crest and first-trough height dimensions were reasonably well preserved from the Site Nan transducer to the Nan shoreline. As a result, the extrapolation of a first-crest effective time (from the first disturbance to the first phase zero) in the open-lagoon system to the shoreline is considered to be an acceptable approximating assumption. The data required for a comparative estimate of the first-crest effective time at various ranges from surface zero for the barge shots is given in Table 3.3 and Figure 3.2.

For this discussion to accommodate changes in the tide stage from shot to shot and the various island area elevations, an approximating wave shape is required. In Section 3.16 it is shown that the front half of the first crest is approximated by a solitary wave and the back half by a sine wave; this composite wave shape is reproduced in Figure 3.3. This profile graphically indicates the relative protection from inundation to be gained for low lying islands by firing at a low tide stage. For example, a reduction of the effective wave height of 0.1 at the shore level of an island, due to a lower tide, is indicated to reduce the crest length and its effective time interval from 1 to 0.6. As indicated in Figure 3.3, the vertical and horizontal scales are not in correct proportion, but on a percentage basis, the above numbers are representative.

The velocity of propagation of a steep fronted bore is given by $\sqrt{gh_b}$, where h_b is the height of the bore face. This is a variable across an island and is a function of time and range. In order to have a vertical dimension applicable to h_b for purposes of discussion of the extent and intensity of inundation from these first crests, the average velocity of

flow is approximated by taking two-thirds of the crest height on the island rim, as determined from first-crest height at the shoreline minus the difference between the island elevation and the tide stage.

To facilitate the discussion of inundation effects, some of the data on first-crest heights in 60 feet of water presented in Figure 3.22 has been transcribed to Figure 3.4. As indicated in the figure, it is necessary to estimate the Flathead height.

The manner in which the above information is utilized to study the photographic evidence of inundation is as follows. The shoreline of Site Dog was an average of 4,500 feet from the surface zero of Flathead. The first-crest height in the open lagoon at this range is estimated from Figure 3.4 at 5.5 feet, and with the average shoaling and reflectance factor of 2.6, from Table 3.2, this indicates a first-crest height of 14.3 feet above tide stage at the Dog shoreline. From Figure 3.2, the first-crest effective time at this range is 29 seconds. The road elevation along the lagoon shoreline of Dog was 10 feet above mean low low water level (MLLW) or about 4.3 feet above the 5.7-foot tide stage at Flathead time zero. The first crest has to top this elevation before it can proceed inland. From Figure 3.3, it can be estimated (1.0 − [4.3/13.7] = 0.69) that approximately the upper 70 percent of the crest height, and 47 percent of the first-crest effective time (0.92 − 0.45 = .47) is active, or 14 seconds. Two-thirds of the upper 9.4 (13.7 − 4.3) feet of the first crest across the road indicates a velocity of 14 feet per second, and if this is applicable over a time interval of 14 seconds, the first wave is indicated to have penetrated inland from the road approximately 200 feet. However, in Figures D.2 and D.6 it can be seen that Site Dog was completely covered by the Flathead waves which indicates that the penetration was 1,500 feet through one mechanism or another. It is impossible to assess the variation of maximum water elevation with distance inland from the roadway, but the severity of erosion at the lagoon shoreline compared to inland areas is apparent in the photographs. The Station 197.04 record of the Flathead wave shows that the second and third crests were as high as the first, but their contribution to the inundation effects at Site Dog cannot be estimated.

If the above calculations are repeated for Site Dog with the first crests from Shots Dakota and Navajo, their heights above the shoreline road are indicated at 25.5 and 53.4 feet, their effective times at 20.5 and 20.3 seconds, and the first-crest penetrations at 470 and 690 feet respectively.

Preshot and postshot photographs of Site Dog for the Flathead, Dakota, and Navajo events are included as Figures D.1 through D.9. The first four are of the large bunker, Station 1320, at the west end of Site Dog, and show the progressive deterioration of the mounding and the surrounding island area. The destruction and removal of the coral lagoon-fringing reef directly in front of this station is also apparent in these photographs. Although some of this must be attributed to airblast and shock effects, a very large percentage of it is a direct consequence of the water-wave action. The mounding behind the left wing of this station was partly removed by the Flathead wave, and an additional amount was removed by the Dakota wave. The joint between the wing and the structure was fractured during Shot Dakota. After Shot Navajo, the mounding behind this wing was completely removed while that behind the right wing remained. This is interpreted to indicate that the direction of water-wave approach was perpendicular to the lagoon shoreline. Inasmuch as the collimator tubes of this station were aimed at surface zero, the water waves were very definitely refracted in this short distance to enable them to approach the shoreline so directly.

Figures D.5 through D.9 give coverage of the Site Dog area adjacent to, and east of, this bunker. The concrete block adjacent to the unmounded bunker, Station 75.01, in the

left center foreground of Figure D.5 was moved onto the road, and the berm around the ocean side of the manmade Structure 3 (center background) was completely removed by the Flathead water wave. There is also evidence of water erosion around the foundations of the structure, and the mounding on Station 312.04, just to the right of this, was partially removed by the same water action. The concrete slab just inland of the borrow pit (left center in Figure D.5) remained in position through all three shots.

Figure D.7 shows that Shot Dakota caused further erosion around Station 75.01 (left foreground), the concrete block located on the road prior to Dakota was broken up and the reinforced base moved about 500 feet farther inland, and the mounding around Station 312.04 was completely removed.

The effects of Shot Navajo in this area are shown in Figures D.8 and D.9. The loose coral rubble around the foundation of Station 75.01 (Figure D.8) has been completely removed, and the station rests upon the exposed coral slab of the reef. Another shot similar to Navajo would probably have moved this station. All evidence of the road has been removed. Figure D.9 shows Station 312.04 to be even more exposed than in Figure D.7. The heavy cutting and erosion around the front and corners of this bunker indicates severe and sustained water flow. The whole area has been generally cleaned off by wave action, and the ocean reef to the north is littered with transient coral blocks and debris.

Figures D.10 through D.13 show the progressive inundation effect, from the three barge shots, at Station 1320 on the southeast tip of Site George. A calculation as outlined above, for the inundating first crests at this location indicates the following: the heights were 2.7, 7.5, and 30.4 feet, effective times were 14, 20, and 27 seconds, and the penetration distances were 106, 254, and 685 feet for Flathead, Dakota, and Navajo respectively. The average shoaling and reflectance factor of 2.5 was used as before, and the average island elevation in front of these structures was taken at 8 feet.

The width of the island at this point is about 350 feet. In the figures, the near sides of these bunkers face surface zero and the approaching waves. The right extremity of the waterline from the Flathead wave (Figure D.11) can be seen to extend directly from the front of the large bunker, while the other extremity of the wetted area is approximately 200 feet to the left. The water drained past both sides of the smaller bunker onto the ocean reef in the background. This indicates that the Flathead wave action barely surmounted the island elevation in this area, and that the flow was negligible. The calculated first-crest effective height of 2.7 feet and the corresponding time and penetration values appear to be of the right order of magnitude.

Figure D.12 shows that the Dakota waves swept the whole area. The marks on the mounded bunker in front of, and slightly to the right of, the largest unmounded bunker give some idea of the intensity and maximum water level in this area. The bulldozer-blade marks and cuts have been smoothed out to the top of this mounding, and the erosion and cutting action of the water on the left front face indicates that the more severe wave action in this area reached approximately 6 feet above grade. Some idea of relative dimensions in this photograph can be obtained from the height of the man standing to the left of the unmounded bunkers, and from the helicopters parked near the ocean shoreline. The 7.5-foot first-crest height calculated for Dakota and the dimensions derived from this photograph are in acceptable agreement.

The Navajo waves completely topped the two mounded structures directly in front of the DUKW in Figure D.13 and removed an appreciable volume of the mounding that remained after the Dakota wave. The general cutting back and erosion around the foundation slabs of the unmounded structures is quite apparent. The maximum water-level rise is not indicated in the post-Navajo pictures of this area, but other records show that the

water wave was to the top of the mounded structure 500 feet northwest of the small craft landing channel. This bunker was on the ocean shoreline and was mounded to 12 feet above grade.

At Site How, water waves were low in height because of the range from surface zero, and because this lagoon area is a good absorber of wave energy. The How shoreline was not surmounted except by the Navajo waves, and this occurred only in random areas and was of a very minor nature. A calculation, as described above, of the wave inundation potential at the center How helicopter landing pad shows the following for Shot Navajo. The wave height in the open lagoon at this range was 3.7 feet. The data of Table 3.2 shows that in this area the wave height was reduced by an average factor of 0.78, or to 2.9 feet in 60 feet of water. An increase in ratio of 1.5 to 2.4 or a factor of 1.6 is indicated as the Navajo wave moves from the Site Nan transducer to the Nan shoreline, and if this figure is applied from the Site How transducer to shoreline the 2.9-foot crest height becomes 4.7 feet. The tide stage was 5.9 feet, and the maximum water level rise at the shoreline is indicated as approximately 11 feet which is within a foot of the elevation of the copter pad. The copter pad was about half flooded with lagoon water.

The progressive inundation effects at Site Oboe are shown in Figures D.14 through D.17 for Shots Flathead, Dakota, and Navajo. The recording instrumentation for Station 191.01 was housed inside Station 1515 shown in this sequence. The waves from Flathead penetrated the area around this station, to the same extent as those from Shot Zuni. Calculations of the inundation expected for this site, in the manner above, give the following: Maximum crest heights were 0,1, and 7.9 feet using an average grade elevation of 7.5 feet. The effective inundating times were 0, 19, and 45 seconds, and the associated penetration distances were 0, 87, and 600 feet for Flathead, Dakota, and Navajo respectively. The Flathead wave penetrated about 200 feet as shown in Figure D.15 in which the high-water mark encompasses the concrete slab. The Dakota waves reached farther inland as shown by the debris line in Figure D.16. The elevated fill directly in front of the bunker mounding, as outlined by the debris line in Figure D.15, was removed by the Dakota wave as is shown by Figure D.16. The penetration for the Dakota wave was approximately 290 feet.

Figure D.17 shows that the Navajo wave penetrated 550 feet to a point across the Oboe-Peter landing strip, that the heavy drag chain attached to the aircraft-arresting barrier on the airstrip was moved, and that the mounding on the front of the bunker has been heavily cut by water action. The maximum water-level rise around this bunker is estimated at 10 feet above grade. The generator and sandbags atop this bunker are at an elevation of 20 feet.

As was discussed in Section 3.7, this shoreline area is a prominent reflector of wave energy, and the reflectivity has been indicated to be a function of wave size. As a consequence, the wave height on this shoreline, and the attendant inundation, would be expected to vary in a nonsystematic manner. A comparison of the calculated inundation above with the photographic evidence indicates that the calculated waves for Flathead and Dakota where low in height and extent, but that they were in better agreement for Shot Navajo. The post-Navajo cut on the mounding at the Site Oboe bunker is in general agreement with the calculated 7.9-foot water elevation.

Figures D.18 through D.21 show a before-and-after sequence for the three shots at Station 2300 on Site Peter. The range of this station was only 800 yards more than that of Site Oboe already examined, so the same calculated inundation values are applicable. These photographs indicate that the wave action and flow at this point was much less severe than at Site Oboe. From other photographs of the lagoon shoreline between the

beaching DUKW and Station 2300 in Figure D.19, it can be determined that the Flathead wave barely topped the island grade in this area, and that the Dakota wave moved inland only slightly more. The Navajo wave crossed the airstrip, but the deposited derelict jeep in the center of the runway indicates that the wave, or waves, had lost most of their force at this position. This is in agreement with the penetration indicated by the photographs of Site Oboe. However, the mounding and fill on the west face (right front in Figure D.21) of Station 2300 was comparatively undisturbed by the Navajo waves, and it has been concluded that the intensity of flow was much less at this point, and that this station is in a location protected from water waves because of the more gradually shoaling lagoon bottom directly to the north. Aerial photographs and fathometer soundings in this area show the existence of a bench of shallow water extending from this location west to Site Sugar, and although post-Navajo photographs of the road and causeway connecting Sites Peter and Tare show through-cuts and severe washouts, the degree of destruction of the roadway does not appear to verify the calculated 7.9 feet of water over the road.

The Navajo wave which caused the maximum inundation at Site Nan was determined to have originated at Site Oboe as a reflected wave (Section 3.7). The maximum water-level rise, determined from the EG&G photographs of the north Nan shoreline, was of the order of 11 feet above tide stage (Section 3.6). The camp area at Site Nan is shown in Figure D.22. The maximum elevation reached inland in the Site Nan Camp Area was 12.5 to 13.5 feet. The tide stage for the Navajo wave arrival was 5.9 feet, and if the 11-foot dimension at north Nan approximates the shoreline wave at center Nan, the maximum potential head of water adjacent to the baseball field would be 16.9 feet above the zero-tide reference. Holmes and Narver (H&N) charts show the grade level from the baseball field past the beer hall to the shoreline to be 11 feet. The maximum water-level rise above this elevation at the shoreline is then estimated at (16.9 – 11) 5.9 feet. Figure D.23 shows that the debris line in the wire mesh of the baseball backstop approximately 320 feet from the shoreline was $4\frac{1}{2}$ feet above grade.

At a point 400 feet from the shoreline on the main street in front of the H&N accounting office, a can gage showed the maximum water depth to have been 3 feet above grade. The maximum grade elevation reached on this street is 13 feet in front of the post office, 680 feet from the shoreline. As estimated from Figure B.3, the effective time for which this inundating wave was indicated to exceed the grade level at the shoreline was 48 seconds, i.e., the time duration of the upper 5.9 feet of the inundating crest shown at $24\frac{1}{2}$ minutes. If this time, 43 seconds, is functional with the extent of water flow, the 680 feet traveled inland indicates an average velocity of 14.2 ft/sec. Following the same line of reasoning as in earlier calculations of inundation, 14.2 ft/sec indicates an effective $\frac{2}{3}$ height of $6\frac{1}{4}$ feet or a total of 9.4 feet potential height at the shoreline. The maximum was estimated as 5.9 feet from the north Nan data.

It does not appear likely that such approximate methods as these will ever give much reliability, but a more rigorous and exact approach cannot be suggested at the present. (Work is presently in progress on more complete inundation data acquired during Operation Hardtack.)

3.10 WAVE GENERATION, ENERGY BALANCE, AND WATER-CRATER SIZE

The records of Operation Redwing together with those of the two open-lagoon tests of Operation Castle and Shot Baker of Operation Crossroads comprise the totality of data from nuclearly generated waves for the less complex shallow-water generation parameters.

To obtain an accurate value of the energy content of generated waves, the records under study must not contain reflected components or be from locations near a reflecting or absorbing boundary. Therefore, only those wave records taken in open-lagoon waters as close to surface zero as possible are of primary interest. The above reference records are from wave stations at ranges of from 3,000 to 21,000 feet, and for yields from

Of the theoretical works concerning the characteristics of wave trains generated by local disturbances, only Reference 4 considers the three-dimensional case in limited water depths. Because the tests under consideration produced water craters which reached the lagoon bottom and represent unusually shallow water conditions of generation, this theoretical work was looked to as the one most likely to give agreement with recorded results.

Reference 4 gives two basic approaches to the problem, that of an initial impulse applied to the water surface, and that of an initial displacement of the water surface. As all lagoon records showed the leading part of the wave train to be a crest, it was at first considered that analysis from the standpoint of initial impulse would most closely agree with the records. By contrast, an initial downward displacement (water depression) that is suddenly released would yield a leading trough.

However, the analysis from the standpoint of initial impulse was incompatible with the data in that the calculated wave envelopes for shallow water at close ranges do not admit of both a crest and a trough of nearly equal energies. Therefore the wave records (including the first crests and troughs) cannot be fitted to any calculated wave envelope, even by a simple translation in time of the envelope curve to make the theoretical and measured initial disturbances coincide. Reference 4 does not allow for any wave arriving earlier than at that time determined from $\frac{r}{\sqrt{gh}}$ as is the case with the entire first crest in all of the close-in records to date. (In the previous sentence, r is the range, feet, from surface zero.) This early arrival of the first crest is traceable to two causes: a higher velocity, because this first crest is seen to be the outward moving lip of the water crater whose higher rate of travel coincides with that of a solitary wave, and a head start; unlike the remainder of the wave train it is not emitted from the origin but is already beyond the water-crater radius at the time taken as zero for wave propagation (see next paragraph). For purposes of theoretical analysis, the wave train is considered to be the result of two separate mechanisms: the lip formation and the crater collapse.

It was, therefore, necessary to modify the approach to the problem as follows. (1) The initial condition is considered to be that of a cylindrical water crater extending to the bottom, with a raised lip representing the first crest. (2) The energy in the first crest is considered to be equal to the energy in the crater lip, and to have not materially decreased in energy over its travel to the recording station, because the records were taken at close ranges. The energy in the remainder of the train is considered to be equal to that contained in the depression of the water crater. (3) Zero time is considered to be that time at which the water crater has reached its greatest radius. At this time, the energy of the crater is entirely potential, although the lip has both potential and kinetic energies (which are assumed to be equal).

The geometry represented is an extreme extension of that considered by Reference 4, due to the high ratios of crater radius and depth to water depth, and the proximity of the recording stations. This must be kept in mind when judging the extent of agreement and applicability of results.

The problem was attacked in the following manner utilizing the basic data given in Appendix C, and the close-in wave records of Shot Baker during Operation Crossroads (Reference 7).

1. In order to "fix" zero time and the range of wave origin, it is necessary to estimate a time of maximum water-crater radius. Calculations indicating the approximate crater radius expected, and a review of available motion pictures of surface-plume phenomena for similar shallow-water shots suggested a maximum water crater at a time on the order of 1 second. The periods of bubble oscillation observed in Operation Wigwam were also influential in the estimate of this time.

2. The wave paths and associated water depths from each shot to the recording stations were plotted, and $\frac{r}{\sqrt{gh}}$ travel times were computed. For Station 197.04 (Figures C.1 and C.2) this was a refracted, not a straight, path.

3. The $\frac{r}{\sqrt{gh}}$ travel times plus the 1-second crater-formation time invariably predicted the passage of the first-phase zero point at the wave stations. In absolute values, the maximum divergence was of the order of 14 seconds in 70 seconds, but as is noted below, the more important consideration is that this $\frac{r}{\sqrt{gh}}$ travel time was close enough to the measured first-phase zero time that the majority of the first-trough energy travels at $\sqrt{gh}$ celerity, i.e., for the maximum divergence value above, 85 percent of the trough energy passed after 84 seconds. Although the theory of Reference 4 is formulated upon the proposition that the first disturbance propagates at $\sqrt{gh}$, and in this application, where the source for theoretical analysis is an initial depression, the consistency of the coincidence of $\frac{r}{\sqrt{gh}}$ times and the first-phase zero times (the first disturbance after the separately considered first crest in this case) is remarkable. This is not considered significant, however, because the theory is intended to apply only for $r >> R$, and for the ranges and yields under consideration this is not the case. (In the previous sentence, R is the water crater radius in feet.)

4. The energy in each recorded wave train was measured in total, for that part following the $\frac{r}{\sqrt{gh}}$ arrival times, and for that part following the first crest. The latter two energy values were the same for all practical purposes. A choice of techniques for determining wave-system energy were available and are discussed in detail in Section 3.16. The long-period water-level-change characteristic of Station 197.04 was eliminated by plotting the midpoint of each face of each wave and using a smoothed curve through these points as a base line for replotting the record. The wave shape for waves passing over these stations was assumed to be sinusoidal, and wave velocity was taken as the $\sqrt{gh}$, for even though the average first-crest velocity from the crater lip to these stations was noted to be greater than this, it is close enough for use in these calculations.

5. Before this energy can be interpreted dimensionally at the water crater, it is necessary to determine a representative water depth at the crater. This depth can be arrived at by two techniques. Measurements of water depth prior to some shots are available, but occasionally a second shot was located in the same place as a previous one without a crater survey in between. In this situation it is necessary to estimate a bottom depth for the second shot. The second technique available is less direct and involves application of wave equation theory as outlined below. The results obtained when measured and estimated water depths are utilized are examined later. The theory of Reference 4 gives the wave period T as a function,

$$T = \frac{2\pi}{\sqrt{\frac{g\sigma}{h}\tanh\sigma}} \qquad (3.3)$$

Where: $\sigma = \frac{2\pi h}{\lambda}$, a parameter

$$\varphi(\sigma) = \frac{r}{\sqrt{gh}\, t}$$

h = water depth
λ = wavelength for period T
t = time (wave zero time)
r = range (feet) from surface zero

This, in effect, relates t to T at a constant r for a given depth of water. Whereas Reference 4 assumed the water depth to be finite and constant, it was necessary to calculate an effective equivalent constant depth over the wave path and use an average $\sqrt{gh}$ in evaluating T as a function of t for corresponding values of σ. (The basic procedure for determining T as a function of t is given on Page 6 in Reference 4.) The wave periods were plotted as a function of time for the records of Appendix C, and these curves compared very well with those calculated from the above theory.

6. The theory of collapse of a cylindrical crater (Reference 4) requires nodal points in the wave train. Where these nodal points were not obvious in the records, they could be detected by departures of the observed T values below the theoretical T versus t curves. Theoretically a nodal point represents a 180-degree phase shift, at which time the observed wave period is significantly reduced.

7. The nodal points thus determined represent times at which the amplitude factor of the wave equation (Reference 4) is zero. For nodal points the zero order Hankel transform is zero which gives a finite value of the variable $\frac{\sigma}{hR}\sqrt{\frac{2Q}{\pi\rho g}}$ (η_o = h, i.e., the crater extends to the bottom). This can be solved for h, a theoretical water depth in the zone of generation. The theory considers cases in which the waves are generated and propagated in water constant depth and in which $\eta_o \neq h$. As a result, it was permissible for the symbol h to represent water depths at the zone of generation and over the paths of wave propagation. In this application it has been necessary to distinguish between the various h's to establish an average h for wave propagation (see 5 above), and to calculate another h for the water depth of generation. The possible implications of this distinction in the theoretical derivations of Reference 4 cannot be evaluated at the present, but it is believed that the h's in the amplitude term are all depths of generation and these have been interpreted as such.

8. The water depths of generation were calculated for each nodal point of a given wave record, and an average of these was taken as a compromise value for a particular record. These nodal depths fell within a very narrow range, and were usually very near that of the measured or estimated water depths at zero point prior to the shot. The one exception was the Station 197.04 record which consistently indicated shallower generation depths, but the waves passing this station were also consistently low in relative energy compared to the other records. Examples of the scatter of these calculated depths for Shot Navajo are as follows. At Station 197.06, the calculated water depth at generation was 213 feet for the first node, 223 feet for the second, and 216 feet for the third; the average was 219 feet. The calculated average water depth at generation was 163 feet at Station 197.04 and 219 feet at Stations 197.06 and 197.05. The measured average water depth at surface zero prior to Shot Navajo was 230 feet.

9. From the water depth thus derived and the energy calculated to be contained in the water crater for a given station record, a crater radius in the direction of the station was obtained.

Because the first trough portion of the Yankee record (Figure C.8) was not obtained, it was necessary to approximate the energy value of the waves following the first-phase zero for this shot. Also, to maintain geometric similarity for the calculation of

these crater radii, it was necessary to move the Union and Yankee waves and energies of Figures C.7 and C.8 to a scaled range that was in better agreement with those of the close-in stations of the Redwing series. To determine this range, $\frac{r}{W^{1/3}}$ was assumed to be the valid scaling relationship for geometrically similar ranges. Range scaling for the close-in stations of the Redwing series was not considered necessary because of their much closer proximity to the zone of generation.

The Union and Yankee data was interpreted as follows. The energy content of the Yankee waves following the first crest was measured at a more distant open-lagoon station (Station 163.05, Reference 3). The results of Reference 3 show that the wave systems from Union and Yankee were identical except for an increase in size due to higher yield and increased water depth of generation. The energy content of Union and Navajo waves following the first crest were plotted as a function of range. The slopes of these curves were in good agreement. The measured energy of the Yankee waves (after the first crest) from the more distant station and the energy of corresponding Union waves were projected to the scaled range of the Navajo Station 197.06 at the experimentally determined decay rate of the measured Union and Navajo wave systems. This energy value was then used to calculate a corresponding water-crater radius for Union and Yankee. These results are tabulated in Table 3.4 and are plotted as a function of shot size in Figure 3.5, which indicates this theoretical crater radius to vary as the fourth root of charge size. The radius for Baker is indicated to be disproportionately large; a possible explanation is that the Baker burst point was below the water surface.

10. In the projection of the first-crest position as a function of time back toward the origin, its height was varied inversely as the range and the fourth root of water depth, and its velocity was assumed to be that of a solitary wave. These calculated positions of the first crest at zero time are in good agreement with the crater radii derived from crater-energy considerations in that they indicate the same order of magnitude and a slope similar to the theoretical results derived above. The central-area dimensions for Baker were again indicated to be disproportionately large. The results of these projections are also plotted in Figure 3.4.

11. The derived water depth and crater radius for Navajo waves recorded by a specific station were applied to the wave equation of Reference 4. The crater dimensions in the form of an initial cylindrical depression extending to the lagoon bottom were inserted, and the wave amplitude envelope at the range of the station plotted. This theoretical envelope was compared with the recorded waves at the three close-in stations, and they were not in good agreement. Generally speaking, the cylindrical depression gave nodal points in the correct time relationship, but the amplitudes of the observed waves were not regular and symmetrical within the groups. Where wave amplitude was symmetrical within a group, the maximum wave height in some groups was considerably less than in the theoretical envelope, while in others it was greater. The results were not consistent. A calculation using an energy equivalent to the cylindrical depression but with this energy in the form of an initial impulse with parabolic distribution gave wave envelopes where the maxima decreased at a faster rate with increasing group number, and which more nearly resembled the trends indicated by experimental wave amplitudes. The first wave amplitude was of the same magnitude as the first trough. The nodal points did not fit the experimental data, however. Another calculation in which the measured energy was used in the form of an exponential distribution of impulse gave a single-amplitude envelope that resembled the observed wave amplitudes but did not permit the nodes and beat phenomena observed. It is to be noted that the above applications of impulse exclude the first-crest energy, and in practice it is difficult to attach any real meaning to this. The

problem of applying theoretical equations to describe these observed wave systems resolves upon the ability to mathematically describe the initial energy distribution. These exploratory calculations indicate that, for the Redwing waves, this shape probably lies somewhere between a cylinder and paraboloid.

If, in Step 4 above, the wave energy following the first-phase zero instead of that following the $\sqrt{gh}$ travel time is used, and all succeeding steps are as outlined, the derived theoretical crater radii are as given in Table 3.5.

If the wave energy following the first-phase zero is utilized as above, but, as noted in Step 5, the water depth at surface zero is that measured or estimated rather than that calculated from the theory of nodal points, the derived crater radii are those of Table 3.6.

If (a) the wave shape is not assumed sinusoidal but the energy is determined by graphic integration of the wave traces (Section 3.16), (b) the energy following the first-phase zero is utilized, and (c) the measured or estimated (where necessary) water depths are applied, the derived crater radii are as given in Table 3.7.

All derived crater radii for a given shot are averaged and plotted in Figure 3.6. As in Figure 3.5, with the exception of Shot Baker, this theoretical crater radius is indicated to vary as the fourth root of charge weight for yields from

In summary, it should be noted that the energy losses of the wave systems from their formation to these nearest stations have not been considered, and that, because of turbulence, these losses may be quite large during the early stages. Methods of evaluating these losses are not apparent.

The primary contributions of the above analysis are as follows. It indicates source dimensions and their variation as a function of charge size, and the separability of the generation processes of the first crest and the rest of the wave system. Implied variations of energy proportion indicate the uncertainties of scaling the first-wave height (first crest to following trough) as a function of yield, and also the quantity of water lost to the lagoon with subsequent changes in the first-crest height with increasing yield becomes a primary source of uncertainty. This is graphically illustrated in Figure 3.7 in which the dimensions of generation are given in approximate scale. The first crest is depicted just outside the maximum crater radius at zero time. The data from Navajo Station 197.06 was utilized to construct this figure, and the energy content of the crater approximates the energy of waves following the first crest. The volume of water necessary to represent the estimated first-crest energy is as indicated and suggests that a substantial volume of water which might otherwise appear in the first crest was removed from the lagoon in the first 2 seconds.

3.11 FIRST-WAVE CELERITY IN THE LAGOON.

The celerities of generated first waves in their travel across the lagoon are examined, utilizing the data given in Appendixes A and C, for the three open-lagoon barge shots and Shot Tewa. Three variables—finite wave height, water depth of propagation, and the refracted range—are significant in determining the arrival times of waves at the various stations. The degree to which arrival times were affected by these variables was dependent upon the station location, shot location, and shot size.

Stations near reefs and islands were the most sensitive to these location effects, except for Stations 191.01 and 192.01 which were on straight lines from surface zero over the average lagoon water depth. Any delays in arrival times induced by the rapidly shoaling lagoon bottom very close to these transducers were of such small magnitude, when

compared to the total travel time, that the values based upon these times are essentially the open-lagoon celerities.

All shore stations were initiated by EG&G hard-wire timing, and the recording rate was marked by chronometric clock to give time resolution within 1 second over a 1-hour run time.

Waves arriving at Station 190.01 were delayed in time primarily because of the shoaling water near the transducer; refraction over this path was negligible. Waves arrived at Station 193.01 relatively much later in time because of a refracted path over gradually shoaling water.

In the open lagoon, arrival times at Station 196.01 were affected by refraction, but the arrival times at Station 196.02 were unaffected by either refraction or shoaling. Unfortunately the zero times for some records from these stations (196 series) are uncertain. Some of this uncertainty in the data was due to problems inherent with these instruments which were first designed for and used in Operation Castle.

The close-in stations received such rough treatment at zero time that there could be no question about their starting, and,provided the record disk was not loosened on its spindle, zero and arrival times were accurately determinable. From Shots Flathead and Dakota, the waves traveling to Station 197.04 were slow in arriving because of a refracted path and shoaling water. From Shot Navajo, the wave arrived late at this station because of shoaling water only. Waves arrived at all other close-in stations over straight-line paths and through water of depth equal to the average in the central lagoon areas.

The arrival times of the first wave and second crest at all stations for Shot Navajo are given in Table 3.3. The celerities for this data, without regard for refracted paths or shoaling water, are plotted in Figure 3.8, and the lines, representing the open-lagoon constant-depth celerities, have been placed according to the data from Stations 191.01, 192.01, 196.02, 197.04, and 197.06. If the first crest and trough can be considered to be sufficiently related to represent a first wave (Section 3.17), then the increase in time interval, with increasing range, between the lines connecting the data points represents an increase in first-wave length. The celerities of the first portion of the wave system are as indicated, and the second crest is observed to move at nearly the same rate as the first trough. The degree to which the wave-arrival times at the remaining stations have been altered by the variables of refraction and water depth are apparent. It is noted that the asymmetry of the first trough (Sections 3.3 through 3.5) is apparent and maintained throughout the range of observation.

A study of data from stations where the arrival time of the first crest is delayed indicates that, for locations where refraction is the principal deterrent, a shift in time to place the first-crest arrival time on the open-lagoon curve brings the arrival times of the other points into agreement with the open-lagoon curves. For station locations where shoaling water is a significant deterrent, arrival times of waves after the first crest are progressively later in time, and the shifting of the first-crest arrival time to the lagoon curve does not bring the other arrival times into correct relationship. The first disturbance (the first measurable rise in water level associated with the first crest) arrival times as observed are a function of instrument resolution, and it is believed that, if the sensitivity of the more distant station instrumentation had been great enough, the advance increase in water level detected at the close-in stations would be observed at the more distant ranges (Section 3.3), and that the celerity of the first disturbance would be much higher than is indicated.

It has been shown experimentally that the velocity of solitary waves in very shallow water can be greater or less than $\sqrt{gh}$ and that this difference is a function of the finite wave height $\pm \eta_1$ or H_C and H_T (a single crest or trough) (Reference 5). The first-crest celerity in Figure 3.8 is 74.3 ft/sec. For this celerity, the water depth based upon $\sqrt{gh}$ is 171 feet. If, however, the ratio of $\frac{\eta}{h} \geq 0.10$, a 5-percent or greater error can be induced by the use of $C = \sqrt{gh}$ instead of $C = \sqrt{g(h \pm \eta)}$. For example, at the depth of 171 feet, a wave height of 17.1 feet would be reflected as a velocity increase of 3.8 ft/sec, and such a change in slope in Figure 3.8 would be detectable over the ranges involved, i. e., 1 to 13 miles. At 13 miles, this small increase in celerity would show as a 42-second difference in arrival time. If the celerity effect of finite wave height is a variable to be considered in the data, this should be reflected in the time of arrival versus range curve for Shot Flathead, where the first-crest height at 1 mile was of the order of 5½ feet, when compared to those for Shots Union or Yankee, where the first-crest heights were 19 and 30 feet respectively at a range of 3½ miles. First-crest arrival times for waves from all barge shots of Operations Castle and Redwing in Bikini Lagoon were compared, and it was observed that all times for open-lagoon stations are contained between lines representing celerities of 74.6 and 72.4 ft/sec. This small difference seems to indicate that the celerity of the waves under consideration is independent of finite wave height over ranges of 1.5 to 13 miles, because the observed difference between Flathead and Yankee waves over the same path is less than the theoretical difference indicated by the two formulas.

However, there are two other sources of evidence which contradict this. First, the questionable time resolution of the Castle data, combined with the fact that the Castle stations most affecting these celerity values were located in the western section of the lagoon, and the Redwing data from similar station locations have shown the measurable time delay due to shoaling water to be critical and not sufficiently determinate for these small changes in celerity. For example, the time of arrival of the first crest at Stations 191.01 and 192.01 more accurately show variations in celerity from shot to shot than times from Stations 190.01 and 190.01, which were very near the Castle stations being considered. Second, the gradual increase of first-crest celerities for Shots Navajo, Dakota, and Flathead (Figures 3.8 through 3.10) shows the effect of increasing height. The discussion in Section 3.10 proved conclusively that the first crest has to move faster than $\sqrt{gh}$ from the crater lip to the nearest instrument locations, i. e., at $\sqrt{g(h + \eta)}$. It was also determined that the first crest is a smooth crested wave very close to the crater, and as such can respond to the celerity formula $\sqrt{g(h + \eta)}$. The continuity of these waves implies that the formula applies also at greater ranges. There is also evidence that the first trough moves slower than $\sqrt{gh}$ over these ranges, and this appears to be more than just a function of its wavelength. It is pointed out in Section 3.16 that the first crest has the form of a solitary wave on the front side and the form of an oscillatory wave on the back side. The celerity of the first crest is a function of its height.

The linearity of first-crest celerities in Figures 3.8 through 3.10 indicate that the refracted path and water depth are the remaining variables to be considered. Reference to a refraction diagram for waves from the Shot Navajo location (Reference 3) and hydrographic charts of Bikini Lagoon have yielded the data in Table 3.11 on the difference between the measured and open-lagoon first crest arrival times in Figure 3.8, and the difference between the measured and calculated first-crest arrival times with refraction and shoaling effects included. Data from Stations 193.01, 196.01, and 197.04 are compared for Shot Navajo, because they best show the effects under investigation. The method of estimating the shoaling time increment for Station 197.04 is very much simplified because

of lack of data on wave motion at this range, but the calculated arrival time (1.75 minutes) and the measured arrival time (1.83 minutes) are in acceptable agreement. The data shows that the arrival times and celerities of the first crest of the systems can be calculated by standard methods for refracted wave paths over shoaling water.

First-wave celerities in the open lagoon for Shots Dakota and Flathead are given in Tables 3.9 and 3.10 and are plotted in Figures 3.9 and 3.10. Late arrival times due to refraction and shoaling are again apparent for certain station locations, and these can be brought into proper open-lagoon perspective by consideration of refraction diagrams and the lagoon hydrography as outlined above for Shot Navajo. The asymmetry of the first trough about its phase zeros is not apparent in Figures 3.9 and 3.10; however, an examination of the individual records for these two shots shows that this asymmetry did exist at ranges of 1 to 3 miles, but that by the time the first troughs were at ranges of 6 to 8 miles they had become symmetrical.

3.12 CLASSIFICATION OF WAVE SYSTEMS

Types of wave systems that result from explosions can be discussed only in a general way, because to date there is no experimental data that explores in three dimensions the variation of wave systems from point-source disturbances over the full ranges of the parameters of generation. The two-dimensional wave channel tests of Reference 5 are very informative, and denote the range over which these wave systems can vary. The data from high-explosive and nuclear tests have given spot checks on the theoretical systems and have confirmed a few of the various combinations and forms that generated waves can take. The problem of predicting water waves from nuclear explosions has become considerably more difficult, but it has also become more accurately definable.

The following discussion of waves from explosions is based on certain assumptions and conditions outlined below. In a series of test shots, all variables of generation are held constant except the water depth. To eliminate questions about the effect of depth of submergence with changing depth of water, the center of the generating charge is fixed at the water surface. The water depth in all directions is constant and equal to that at surface zero. The bottom at zero point is flat and level for each shot, and the material density and compaction are constant. The wave heights, as a function of time, from these tests are observed as they pass a fixed and constant range. This range is sufficiently distant, in excess of 20 crater radii, from the zone of generation that the wave pattern is well formed and stable. The water depth (the only variable involved) is decreased in suitable increments from about 4 times the maximum water-crater depth to approximately 0.1 of the initial depth. All experimental evidence indicates that the generated wave systems will undergo extensive changes in energy content and distribution as the water depth is progressively decreased. It appears that these wave systems can be grouped or typed, and that they can be related as a continuous function of the parameters of generation. Some of the indicated changes in wave arrangement, as the water depth in the above model is progressively decreased from the deep-water end of the spectrum to the shallow-water end, are discussed below.

Waves from explosions in deep water, where the maximum water crater depth $<<\frac{1}{2}$ water depth, are dispersive waves. This dispersion results from the fact that the velocity of the individual waves (phase velocity) is greater than the velocity at which the wave energy propagates (group velocity). For these conditions of generation, the wave energy, when observed at a point very near the water crater, is in the form of one or possibly two waves. As these move out radially, they increase in number and decrease

in size. A vertical section passing through the origin will show these waves to be symmetrical in amplitude about a center point which is moving at the group velocity; the height of the wave occupying this position at any instant is the group height (the height of the envelope curve) of the waves. The phase velocity of this center wave is twice the group velocity. The wavelengths and periods of the system decrease from the front to the back of the group, and because the leading waves are decreasing in amplitude with increasing time and range, the first disturbance (crest or trough) to be detected with an instrument of a fixed resolution depends upon its range from the origin. If the generated waves travel far enough before diminishing to obscurity, the wavelength will increase to the point where the phase velocity is no longer dependent upon wavelength but upon water depth. When this point is reached, the individual waves are traditionally described as shallow-water waves. In view of this, waves originating from the central zone where the parameters are defined as deep-water parameters of generation can become shallow-water waves if their range of travel is great enough even when the water depth is constant. In general, the generation process for these low ratios of water-crater depth to water depth are typified by an initial cavity with a comparatively small (if any) lip. This cavity collapses with one major mount at surface zero and the subsequent oscillations are very small. The waves from Operation Wigwam were of this single group type, and in the absence of direct measurements of the phenomena at surface zero, it was necessary to assume the generation phase to be a simple cavity and collapse type. The comparison of theoretical to measured waves tended to validify this assumption (Reference 8).

An examination of the basic data of Reference 1 has indicated that, as the water depth in the above-assumed test series is decreased, the wave energy begins to decrease when the water depth is less than twice the maximum water crater depth. Further decreases in depth result in substantial decreases in wave energy until the crater begins to expose the bottom; beyond this point the decrease in wave energy continues but at a much slower rate. The only experimental data available which suggests what changes in form might accompany this decrease in energy, and the continuity of these changes, is the two-dimensional wave-channel study of Reference 5. These results suggest that the first detectable change in wave system type as the generation parameters quit the deep-water conditions is the shift of the maximum wave height from the center of a symmetrical single group toward the front of the group, i. e., the wave-group envelope assumes a teardrop shape, and this renders questionable the applicability of the conventional technique of using the product of the highest wave and the range as a measure of the wave-group energy. The data of Reference 5 indicates that certain ratios of generation parameters can result in not one but two or three wave groups, either symmetrical or asymmetrical about their group nodal points without any evidence of a prominent leading wave with solitary-wave characteristics, and no evidence can be found to indicate that these patterns could not be duplicated with explosives in three dimensions. It is possible to speculate that the two or three group patterns should occur somewhere in the spectrum after the water crater reaches the bottom, but there is no evidence that multigroup systems have been detected. After projection to this range of generation parameters from those of the Redwing tests in which close-in wave data shows a number of oscillations of crater and mount at surface zero, it is possible to visualize that the number of oscillations at surface zero are increasing proportionally to the decrease in water depth, and that the crater collapse, mount, and rapid subsidence associated with the deep-water condition is changing. It is conceivable that each remount at surface zero is responsible for a wave group, and that a horizontal radial dimension of each oscillation governs the wavelengths in the dependent group and indirectly the relationship of the phase velocities to the group velocity.

A further decrease in water depth results in the increasing dominance of a leading wave (a crest followed by an equal trough) whose crest assumes features similar to those of a solitary wave, and as such it is distinguishable from the following oscillatory waves. It is shown in Section 3.10 that the crest portion of this wave is formed as the water-crater lip, and that the trough portion is formed by the crater collapse. The waves following the first crest are the result of the vertical oscillation of the water level at surface zero as a consequence of the crater collapse. In other words, the minor crater lip in the deep-water generation condition has increased in size to become of major concern. The wavelength of the first wave is sufficiently great that its velocity, or celerity, is determined entirely by the water depth. Waves following the first may be dispersive and develop into a wave group. The work of Reference 5 shows this type of wave system, and has classified it as a system with solitary wave characteristics, first crest followed by trough. The wave system of Shot Baker during Operation Crossroads was of this type. The first wave was distinct, and, within the range of observation, was followed by a single group of waves which appeared to be dispersive, similar to the single group of a deep-water wave system.

A further decrease in the water depth results in the type of wave system observed from the Redwing barge shots. The most obvious differences in the types of wave systems of Redwing, compared to those of Shot Baker, are the increased energy content of the first wave compared to following waves, and the development of additional groups of waves following the first wave. Waves following the first trough for Shots Flathead, Dakota, and Navajo, tended to group themselves according to increasing and decreasing amplitude, and the presence of a beat phenomenon has been detected. The prominence of this is a function of shot size, i.e., the ratio of water depth to water-crater depth had the bottom not restricted this dimension, and it became quite apparent in the waves from Navajo. This beat phenomenon was observed in the experiments of Reference 5 and is predicted by the theoretical work of Reference 4 for water of finite depth. Undoubtedly, a large percentage of the irregularity of amplitudes in the waves exhibiting the beat phenomenon in the Redwing tests is accreditable to the complex geometry of Bikini Lagoon, but it also noted that the smooth and regular data of laboratory tests are seldom duplicated in the ocean or lagoons.

As the water depth of the hypothetical model is decreased even further, the parameters of generation give the types of wave system observed in Shots Union and Yankee during Operation Castle. Even though the Yankee yield was considerably greater than that of Union, the types of wave system from the two were identical. The increase in water depth at the Yankee surface zero, caused by Shot Union, was in the correct proportion to maintain the proper combination of water depth and crater radius for Shot Yankee to produce a Union-type wave system. This type of wave system was observed in the laboratory (Reference 5) and was also generated by the three-dimensional high-explosive (HE) tests of Reference 6. The wave systems from Union and Yankee are characterized by a very prominent leading first crest followed by a second crest of approximately half the size. These two crests are connected by a comparatively shallow and long trough. At close-in ranges, these two crests and connecting trough are the only waves, but at more extended ranges there is evidence that other waves are beginning to form following the second crest. A review of the original traces for the 200-foot scaled depth tests of Reference 6 shows the wave systems of this series to be identically described by the above. These types were described as the single solitary and the complex solitary by Reference 5, and if the trend and pattern change already detected is continuous, a further decrease in water depth of the model would result in additional reduction in depth and the

lengthening of the trough connecting the first two crests, and the wave system would very closely approximate two solitary wave crests. Such a wave system would be identical to the complex solitary waves of Reference 5. A further decrease in the model water depth might possibly result in three solitary crests.

At approximately the combination of generation parameters where the wave systems of Union and Yankee can be duplicated by high explosives, the wave traces of Reference 6 begin to show a distortion in the first trough shape due to the restriction by the bottom crater lip of water flow back into the crater. This feature is very pronounced for very shallow water and is detectable only in the closest records, because at extended ranges the first trough has become symmetrical about its phase zeros. The characteristic of increased time (and distance) separation of the first two crests is, however, preserved at all ranges. It is noted that this feature was not detected in the close-in wave data from nuclear tests, and there is no evidence of a significant bottom crater lip from postshot fathometer surveys. The asymmetries of the first troughs observed at the turtle stations for the Redwing shots are of a minor nature compared to those seen on the records of HE-generated waves at comparable scaled ranges. A possible conclusion is that there are distinct differences in the crater-collapse phase of nuclear explosions, at least insofar as the generation of water waves is concerned.

The above simplified model with its associated wave systems is intended to present a more comprehensive picture of the overall problem of describing waves from nuclear devices. It should be remembered also that for simplicity one of the variables, the depth of charge submergence, has been assumed a constant even though the data of Reference 1 shows that relative wave energy is very sensitive to this parameter. There is very little data that gives any real quantitative indication of the effect of the variation of the depth of charge submergence on the type of wave system produced by an otherwise constant set of parameters. There is some indication, however, in the data (Reference 1) that pertains to systems with single-group characteristics, that this parameter has very little effect upon this particular type of system, at least to the point where the lower portion of the gas globe has intersected the bottom. The data of Reference 6 indicates that, for the other extreme of water depth to crater size, the type of system is unaffected by charge submergence. Conclusions about the variation of wave-system energy content cannot be readily drawn from the data of Reference 6; between the extremes of these tests, there is no systematic data relative to the effect of depth of submergence on the energy content or the type of wave system.

The data collected in Operation Redwing applies to only a small portion of the wave-system spectrum, the Operation Castle data another portion. The waves from Shot Baker during Operation Crossroads were very nearly the same type as those from Shot Flathead during Operation Redwing. The problem of predicting waves from nuclear explosions hinges upon the ability to specify the arrangement and energy distribution of the waves that will radiate from the central zone, and this, in turn, is dependent upon the parameters of generation. The use of general terms such as "deep water shot" and "shallow water shot" to describe water waves is not adequate; it is more accurate to speak about the parameters of generation and their relative magnitude. These parametric relationships will determine whether an energy release of the magnitude of Shot Yankee over coastal shelf water would give a single-group wave system or a wave system in which the lead wave had solitary-wave characteristics, or whether a weapon the size of Shot Baker over the deeper channel waters of a harbor would result in a single-group system of the Wigwam type.

It is apparent that the indiscriminate use of the product of a wave height (H) and its range (r) from surface zero without consideration of the possible energy distribution and arrangement of the waves is not permissible in scaling for various yields. At present, the only portion of the wave trains generated in the Redwing series that can be scaled as an Hr product is the first crest, and even this scaling is subject to question, because the loss of water from the lagoon on the first expansion as a function of yield is indeterminate. First-wave heights (crest to trough dimension) are not considered valid, because the first trough is shown to be associated with waves following the first trough (Section 3.10). When the various types of wave systems that can be generated are considered, the development of a mathematical model applicable over the full spectrum appears to be very difficult.

3.13 FIRST-CREST HEIGHT AS A FUNCTION OF RANGE

In Section 3.12, it was pointed out that the arrangement and relative magnitude of the component waves of a system of waves propagating from a zone of generation over constant-depth water can assume many forms depending upon the parameters of generation.

In Section 3.3, examples of a very few of these forms in their early stage of propagation were given, and Section 3.16 discusses data and information about first-crest energy and total wave energy as a function of range and yield A relationship between energy dispersion and characteristic wavelength was indicated, which is a determinate factor in the representativeness of energy measurements at increasing range because it controls the leak of energy from the higher energy section of the systems to the smaller following waves. Dispersion and propagation losses were also indicated to be significant factors influencing first-crest energy as a function of yield and range.

In Section 3.10, it was shown that the first crest is formed at the crater lip by the rapid expansion of the water crater, and that all subsequent wave action is the result of the crater collapse and remount. In that section, examination of the most advanced theoretical work showed that the theory could not describe the whole wave system and that description of waves following the first crest was delicately sensitive to assignment of shape to the initial disturbance. Thus the possibility of examining the highest wave as a function of range on a wave-system basis is postponed. The separability of the first crest and the following waves in their generation phase and the possibility that an increasing amount (per unit of yield) of water is lost from the lagoon with increasing yield, i.e., water which would otherwise be in the first crest at the crater lip, suggests that the most consistent and scalable part of the wave system to study as a function of yield would be the first trough. Indeed, as is discussed in Section 3.16, the shape and proportion of the first trough is a sensitive indicator of the conditions of generation. But the most important dimension as far as overtopping, inundation, and structure damage at various ranges is the wave with the greatest energy content, i.e., the wave with the greatest height and wavelength.

In the wave systems measured during Operations Castle and Redwing, the first crest was equal to, or higher than, any other wave over the ranges of observation (up to 13 miles) and contained the greatest energy of any other crest except the reflected crest from Site Peter-Oboe (Section 3.7). As noted in Section 3.16, the dispersiveness of a wave system and its propagation losses are determinates governing the ranges over which the first is the highest crest. For the Redwing data, the size of Bikini lagoon limited the ranges of observation to those at which the first wave was the highest. Therefore, the data restricts discussion of the first crest as the most significant crest over these ranges

only, with the realization that at more distant points of observation (constant water depth assumed) the highest crest will be found with waves after the first. For example, the relative dispersion of the waves from Shot Yankee during Operation Castle and Shot Flathead during Operation Redwing would predict that at a distance of, say, 50 miles the highest crest in the Yankee system would shift to the second wave, and at perhaps 13 to 15 miles the Flathead highest crest would shift. For Shot Baker during Operation Crossroads, this shift took place at around 8,000 feet, and it is interesting to note that, although the scaled range at which this shift occurred can be visualized as being in some acceptable agreement with those of the Yankee and Flathead wave systems, the energy content of the Baker waves was equivalent to that of the Flathead waves (Section 3.16). A possible implication that the scaled range at which the highest wave moves to later waves is not influenced by the depth of submergence can only be a conjecture at the present.

With the final objective being the scaling of the most prominent crest (height and energy content) with shot size, the measured first-crest heights as a function of range for Shots Flathead, Dakota, and Navajo are examined.

As noted earlier in this report, the desirability of standardizing on a common water depth for wave height comparison of the Castle and Redwing data has resulted in wave heights adjusted to the 60-foot depth. Although this was an improvement over the earlier shallow-water concepts as discussed in Reference 3, it is in contest with the depth of generation as a standard, and in cases where the depth of generation, depth of propagation, and depth of measurement are the same, the desirability of using this latter depth is obvious.

The basic data is presented in Table 3.12, which includes the first-crest heights H_c, the first-wave heights H (crest to following trough) in 60 feet of water, and first-crest heights H_{cg} in the water depths of generation. The data for Shots Navajo, Zuni, Dakota, and Flathead is plotted in Figures 3.11 through 3.13. The Navajo curves in all three figures have been positioned by the data from Stations 196.01, 196.02, and 197.06.

The reflectance effects upon wave heights in shoaling water as measured at the shore stations are quite apparent. The wave heights at Station 193.01 are consistently low, while the heights at all other shore stations are consistently high. These consistencies demonstrate the selective absorption of crest energy along the George-How reef (Section 3.5) and the reflectance effects at all of the other stations that have more direct angles of approach. Station 191.01 consistently records the highest waves, which indicates the proximity of the best reflecting boundary. The slopes of the first-crest height versus range curves are the same for the 60-foot water depth and the depth of generation. The first-wave height curve is slightly steeper, which implies that the first-trough amplitude decreases with increasing range at a rate greater than does that of the crest.

The curves for Shot Dakota show the same trend in slope as do those for Navajo. For Dakota, the first-crest height measured at the Station 197.04 is disproportionately large compared to the height at Station 197.06, and it is believed the Flathead bottom crater is responsible as discussed in Section 3.16. When the first-wave height at Station 197.04 is considered (Figure 3.12), the close-in data for Dakota is in a more proper perspective for influence upon the curve slope. As was the case for Shot Navajo, the Dakota crest height at Station 191.01 is high due to reflectance.

Although there is an insufficient amount of close-in and central lagoon data to determine a wave height versus range exponent for Shot Flathead, the shore station data appears to cluster about the indicated height versus range curve (Figure 3.11) in a pattern similar to the same station data for Shot Dakota.

The first-wave height is the only dimension for the Zuni wave that tends to exhibit a consistent slope over the full range of data. These data are approximated by the Flathead curve in Figure 3.11.

Interpretation of the available data for the Tewa first wave requires an assessment of the reflectance effects at the shore stations at Sites William, Oboe, and Nan. An estimate of this effect could probably be arrived at by averaging the indicated increased wave heights at these stations for Shots Dakota and Navajo, to give an open-lagoon wave height at a range for Tewa. The wave systems from Shots Zuni and Tewa are not comparable to those from the barge shots, so it appears that such an estimate would lack reliability in this particular instance. The waves from these events are discussed further in Section 3.13.

The first-crest heights in 60-feet of water for Shots Union and Yankee were found to vary inversely with range to the first power (Reference 3). This information is included with the data in Figure 3.13. The average exponent of the curves of Figure 3.11 is 0.95 or

$$H_c \propto r^{-0.95} \tag{3.4}$$

The exponent 0.95 is sufficiently close to those indicated for the curves in Figure 3.13 that it is permissible to say that

$$H_{cg} \propto r^{-0.95} \quad \text{for Dakota and Navajo} \tag{3.5}$$

3.14 GROUP VELOCITIES IN THE OPEN LAGOON

In the examination of close-range data (Section 3.3), the tendency for the waves following the first crest to form into groups separated by nodal points is not always apparent from visual inspection of the wave traces. The nodal points are readily detected, however, from curves of wave period versus time. These nodal points represent a phase shift of 180 degrees in the wave amplitude versus time curves. In some records, a trend for the waves to be arranged with regularly increasing and decreasing amplitudes within the groups is detected, but this feature is not consistent.

The trend of wave energy to fall back with increasing range to later waves within a given wave system (Sections 3.12 and 3.17) indicates that, for ranges of observation greater than those in Bikini Lagoon, the zone of interest in which to locate the highest wave and predict its height will be in the wave groups following the first wave. In this reference it is desirable to examine the data and see if it will support conclusions about the behavior of later waves.

The observed nodal-point times as a function of range are presented in Table 3.13 and plotted in Figures 3.14 through 3.16. In addition, the curves from Figures 3.8 through 3.10 defining second-phase zero ranges as a function of time for these wave systems are presented in order to give a more complete picture of where the groups are relative to the first trough.

Figure 3.14 indicates the existence of three divisions in the Navajo wave system. The term "division" is used, because it cannot be concluded that the three waves following the first trough and leading the second nodal point constitute a group in the implied sense of the term. Indeed, the mean velocity of this division is 70 ft/sec, which is essentially the same as that of the first trough. The data from the turtle stations shows the existence of a nodal point very soon after the passage of the first trough, and also shows four crests ahead of the second nodal point, but by the time these waves pass the 14,000-foot range

the first nodal point is lost to the system, and the original second and third crest have been replaced by a single larger crest to give a three-crest group ahead of the second nodal point. These three crests maintain their identity to the limits of the lagoon.

Similar data for the Dakota waves (Figure 3.15) indicates a single group after the first trough. The turtle record of Station 197.06 shows the presence of a second group, but this feature cannot be confirmed at the more distant ranges.

The Flathead data (Figure 3.16) also shows the waves to form into one major group following the first trough. As was found in Shot Dakota, the close-in Flathead turtle record indicates the presence of a second group, but there is insufficient data to examine this feature at greater ranges. The wave size at these greater ranges is near background level, and the second nodal point for both Dakota and Flathead may be obscured by this at the shore stations. In examination of the records of Station 192.01 it was noted that the later nodal point arrivals at this location coincided with the times at which the reflection from Oboe-Peter was due, and that the wave patterns around these times were not consistent with the indicated characteristics of the approaching system.

It is concluded, with one exception, that the wave groups following the first wave of these systems were dispersive, because the distance and time between the nodal points increased with range. The one exception was in the three waves following the Navajo first wave, which appeared to be moving in a distinct manner. This conclusion implies that at ranges much greater than those observable in Bikini Lagoon, constant-depth water assumed, the largest waves will not be found in the front of the system.

3.15 FIRST WAVELENGTHS AS A FUNCTION OF RANGE AND YIELD

At the very close ranges of the turtle stations in these tests, a large percentage of wave energy is moving with the first crest and trough, and the rate at which this energy can move back to later waves is indicated to be a function of some wavelength in this portion of the system and of the water depth of propagation (Section 3.17). The period and wavelength increase from the back to the front of the system, and, practically as well as theoretically, the wavelength approaches infinity as the point of observation moves out to the first measurable disturbance, time being fixed.

It is desirable to select a horizontal dimension in the wave system—a dimension that is common to all systems, is accurately measurable, is functionally representative of and sensitive to the magnitude of the parameters of generation, and is usable as a measure of the dispersiveness in a system. The first reference point in the system, which can be measured with sufficient accuracy, is the first-crest maximum. Following this, the points of reference are in succession, the first-phase zero, the first-trough maximum, the second-phase zero, the second-crest maximum, and so forth. The choice of a representative horizontal dimension of sufficient magnitude is between the combination of the the first-crest maximum, with the first-trough maximum, the second-phase zero, or the second-crest maximum. With the sequence of events that constitute the generation process as described in Section 3.10, the following conclusions can be reached: (1) the distance between the first- and second-phase zeros would appear to be the best indicator of the magnitude of the water-crater radius; (2) the distance between the first-crest maximum and the second-phase zero would also be a dimension indicative of the crater radius but would include a factor of measure of the first-crest position and size at zero wave time; and (3) the distance between the first-crest maximum and second-crest maximum would be an indicative dimension including the first-crest position and size, the water-crater radius, and the remount at zero point, which should be functional with the residual energy

in the zone of generation after the first crest and trough have moved away from surface zero. Consequently, it is concluded that from a generation viewpoint, the first crest to second crest is the most inclusive horizontal dimension of the generated wave system.

In the examination of wave records at these close ranges (Section 3.3), the asymmetry of the first trough about its phase zeros has been noted. The variability of this feature indicates that a horizontal dimension with this trough maximum as one extreme would not be sufficiently definitive as a reference dimension.

A characteristic wavelength that could be used as an indicator of the dispersiveness of a wave system, and the measurable dimension most representative of the majority of energy (the first crest and trough at these ranges) is the first crest to second crest wavelength. An alternate dimension, the first-crest maximum to second-phase zero, would tend to further restrict attention to the first crest and trough, but the indicated variability of phase-zero positions with asymmetry of the first crest and trough about the mean water level and the inability of theory to accommodate half or quarter wavelengths suggest that the first crest to second crest is the better dimension.

The basic data for determining the first crest to second crest wavelengths were examined in Section 3.11, and these results are summarized in Table 3.14 and Figure 3.17. Figure 3.17 shows that this wavelength for Navajo increases at a faster rate than for Dakota and Flathead, which are equal in rate of change with range. With the range of observation fixed and the wavelength expressed as a function of yield, Figure 3.18 shows that the wavelength is proportional to $W^{0.21}$ over the range of the data. It is noted that this is reasonably close to the exponential proportionality of water-crater radius $R \propto W^{1/4}$ as derived in Section 3.10.

The above does not, however, give a clue to the correct range scaling for comparison of wave heights. Wave heights are decreasing with increasing time and range and the comparison of wave heights from different-size shots in an assortment of water depths involves the question: At what relative ranges are the wave heights directly comparable to variations in yield and other parameters of generation? This range and its ratio with some exponential value of yield is usually specified as the range criterion for geometric similarity of wave systems, and at this range the wave height is generally conceded to be more simply related to the remaining significant variables. Available information indicates that the types of wave systems that can be generated with respect to wave size and arrangement are more numerous than previously suspected (Section 3.12), and as a consequence, an additional and more important criterion for geometrically similar ranges is that the wave systems be identical in type. If this condition is met and the waves are propagating in water depths of the correct scale ratio for identical dispersiveness, then it would appear that there would be a common scalable range at which wave heights are directly comparable as a function of the other variables. As a result of the study of the Redwing results, the only dimension that can be visualized as indicating the correct range scaling for comparision of wave heights, when two wave systems of identical type are propagating in the correct scaled water depths, would be the range at which the highest wave changes from the first wave to a following wave. Such questions are beyond the scope of this data, and, as far as is known, beyond the scope of any three-dimensional wave data to date.

3.16 ENERGY CONTENT OF WAVE SYSTEMS — REFLECTANCE AND SHOALING EFFECTS

All data collected about wave height and shape in the Redwing tests was in the form of

surface water elevations as a function of time for a fixed range interpreted from subsurface measurements of pressure versus time.

A number of the stations were located in shoaling water near reflecting boundaries (Sections 3.4 and 3.5), and as a consequence the height-time pictures of arriving waves were altered. The more important alterations were changes in absolute and relative heights. The degree to which these changes were noted at susceptible station locations varied greatly from location to location. To correctly interpret the energy content of wave height-time records, it is required that a velocity be determined for the time period in which the wave passes over the point at which its height (pressure effect) is being measured. While the wave is in the central lagoon area where the depth of water is reasonably constant for over a wavelength, average velocities can be utilized to give surface wave profile. When water elevation versus time measurements are recorded in shoaling water, the true surface profile is uncertain, because the wave is decreasing in velocity and increasing in amplitude proportionally to the decreasing water depth. Because large changes in water depth occur near shorelines in distances less than one wavelength, it is difficult to assign with confidence a representative velocity applicable to a whole or even half wavelength for determinations of wavelength, shape, and energy. It has also been observed that alterations in open-lagoon wave heights occur at stations located very near, but not in, shoaling areas. A comparision of the records from Station 196.01 with those of Station 196.02 are examples of this type of alteration (Sections 3.4 and 3.7). The alterations in the Station 196.01 waves are more prominent for later waves in the train, and it is concluded that these are the result of reflected waves from the nearest reef line (approximately 5,700 feet). If these reflectance effects reach to stations outside of the more rapidly shoaling areas, they are also a consideration in the interpretation of wave energy from records closer to the reef and/or in a shoaling zone. The representatives of energy calculations from shore and near-shore records are affected not only by the shoaling water but also by the reflections from nearby islands and reefs. (Station 191.01 records discussed in Section 3.7 are an extreme example of these effects.)

Theoretically, the total energy content per unit of arc of an approaching wave minus losses in scaling is transformed to potential energy as runup or flooding. Such losses as friction from orbital particle motion, turbulence in shoaling and breaking, reflected energy, and energy that might disperse to following waves are significant factors. Thus from a conservation of energy viewpoint, it might be expected that if spot measurements of energy having sufficient accuracy over the range from central lagoon to shoreline could be obtained, an energy balance could be completed, and a link established between waves in deep lagoon water and inundation at a shoreline. In Bikini lagoon: (1) the shoaling rate is not constant, (2) the shorelines are a complex and random shape, (3) the shoaling waters are dotted with coral heads of various sizes and shapes, and (4) waves vary in height, period, and wavelength from wave to wave within a given system as well as from system to system; therefore, the theory and data on shoaling waves and the reflectance of sloping bottoms and shorelines do not permit direct energy analysis, and the desirable energy balance above cannot be obtained. Another factor for consideration is indicated by the laboratory data of Reference 9, which shows that for angles of incidence less than 60 degrees the reflected wave height (the reflectivity of the reflector) decreases, and under the conditions under investigation, changes in direction of approach by refraction could conceivably have as profound an effect upon energy determinations as a shoaling bottom.

The Redwing underwater pressure versus time records were translated to surface elevation versus time by the application of formulas that consider the attenuation of

pressure fluctuations as a function of wavelength and water depth (Reference 10). The technique of this transfer was developed from the theory of trochoidal waves and was not intended to permit reproduction of wave profile. For example, a given pressure change with time at some depth, between a crest maximum and a trough minimum in a series of waves, is representative of a related change in surface-water elevation. The data of Reference 10 gives this relationship, and the results have been shown by laboratory experiments to be accurate within from 1 to 10 percent. The faithful reproduction in time of these maxima, or of any portion of a wavelength, in absolute or relative time is not guaranteed. For an accurate determination of the surface wave profile by a subsurface pressure-time record, wave amplitude corrections would have to be linearly proportional to subsurface-pressure amplitudes and follow in exact time sequence for all wave heights and periods and in all depths of water greater than the breaker zone. Experimental data to assist in resolving this question is not available, and it has been necessary to assume the above to arrive at a surface-wave profile for a fixed range. Examination and study of the pressure records from the comparatively shallow waters of these lagoons have tended, in a negative way, to improve the plausibility of such interpretations. Peculiarities of a wave system such as inflection points, asymmetry of a wave about its phase zeros, and nodal points are faithfully reproduced at various ranges from pressure records at an assortment of water depths, and for waves moving in various depths of water. As yet, any inconsistencies or irregularities induced by these interpretations of subsurface pressure-time records have not been detected.

The potential-energy content Q_P per unit width of a surface elevation as a function of time record is expressed as

$$Q_P = \frac{1}{2} \rho g C \int_0^\infty \eta^2 \, dt \qquad (3.6)$$

where ρ is the density of seawater, C is the celerity in ft/sec, η is the amplitude in feet, and t is the time in seconds. If a wave is moving in water of constant depth and its shape and particle motion are those normally associated with free-gravity waves in the particular depth of water, its total energy is equally divided between potential and kinetic. This equality has been derived theoretically in Reference 11 for deep-water waves and in Reference 12 for shallow-water waves. As long as the particle motion remains of the same form, theoretical considerations show that this equal division of potential and kinetic energy is maintained for both oscillatory and solitary waves in shoaling water. Experimental evidence to confirm this division in shoaling water for oscillatory waves is unavailable and presumably has not been attempted because of the complexity of devising a satisfactory experiment. Experimental measurements of wave heights at times when solitary waves are considered to contain zero kinetic energy and all energy is in the form of potential, do not give confirming values of the energy distribution in the free-moving state. The instability to partition the energy into potential and kinetic is usually a result of the change in form at the instant the wave can be considered to contain zero kinetic energy. This change in form invalidates the application of the energy formula based upon a solitary wave. The two tests referred to are: (1) two solitary waves directly approaching each other and crossing, and (2) a solitary wave reflected from a vertical wall with a 90-degree angle of incidence. Although pure solitary waves are not being dealt with in this data, positive results from such tests would improve the confidence of an equal-energy division in this instance.

After establishment of a central-lagoon wave celerity, the open-lagoon wave profile can be determined and the potential energy about the mean water level calculated. The

total wave energy Q_t in the central lagoon areas is evaluated as twice the potential energy (Equation 3.6).

Although a mathematical expression for surface elevation as a function of time is not available, the total wave energy can be determined in two ways. The first and most obvious approach is to perform graphic integration upon the record. The second is to approximate the wave trace with a simple curve for which the integral can be evaluated. The sine, trochoidal, and solitary waveforms are the traditional approximating forms.

The feasibility of graphic integration is based on the assumption that the shape of the curve has been faithfully preserved through several reproductions such as the transfer from curvalinear to rectangular coordinates (the read out of the original traces) and the interpretation of subsurface pressures as wave heights. For records that were highly compressed along the time axis in their original state, this assumption is optimistic.

Another factor which must be borne in mind in the choice of methods of evaluating Equation 5 is that the preponderance of energy as well as the major irregularities of waveform occur during the first cycle. This is quite apparent for stations close to the origin of the disturbance. Although the waves following the first wave, at all ranges, are more regular in their oscillations, the accuracy of determination of their energy content is of less consequence to the overall picture. In reference to the selection of an approximating waveform, the disparity between the energies calculated for sine and trochoidal waves is well below the experimental accuracy for the flat waves measured. As a result, a simple sine-wave formula, which requires only that the wave height and length be specified, serves very well to approximate the energy in the more regular end of the wave train, i. e., the waves following the first wave, and is affected but little by the attendant waveform distortions due to the techniques of data reduction.

The slopes of the first wave are less steep than those of the other waves succeeding it and give it a more spreadout appearance on the record. It can therefore be more faithfully reproduced, and graphic integration for the determination of its energy content is more accurate.

The effect of hysteresis (friction) in the recording system is to materially reduce the measurable energy. This is due to the fact that surface elevation enters as the second power in the energy equation. A record which shows a flat cutoff on its crests and troughs must therefore be viewed with suspicion for purposes of energy analysis.

A plot of profiles for several different mathematical wave shapes of equal amplitudes and containing equal energies are given in Figure 3.19. Curve 1 of this figure is a half-sine wave about the abscissa, and Curve 2 is a full-sine wave about $\eta = 0.37$ (effective $\eta = 0.37$). At the crest, these curves show a very narrow band of possible surfaces, although there may be marked divergence at the low potential level (stillwater level or trough depending upon the plane of reference). This indicates that minor variations in wave shape near the stillwater level may be neglected and the energy calculation based upon an estimated equivalent-sine wavelength. In any particular open-lagoon record, the majority of waves (approximately 90 percent) are reasonably symmetrical about the stillwater level, and the recorded wavelength quite accurately determines the energy content. For portions of the record where the trace is highly asymmetric about the stillwater level, experience shows that an estimate of the equivalent-sine wavelength, and therefore of the energy of the wave under consideration, is within 10 percent.

The first crest of an impulsively generated wave train in these shallow waters appears to be of two basic components: a half solitary wave on the fore slope followed by an oscillatory form on the back slope. As the first wave is the most prominent over the ranges during Operation Redwing, a pertinent question is: How does the wave height

change as the wave moves into shoaling waters? In the past it has been patent to assume that Green's law applied, the wave height varying inversely as the fourth root of the water depth. This follows directly from the conservation of energy of a sine wave traveling at the limiting celerity for shallow water ($\sqrt{gh}$). This may also be applied to a flat trochoidal wave to the extent that it approximates a sine wave. However, for steep trochoidal waves and solitary waves, the foregoing relationships do not apply.

The energy Q for the theoretical solitary wave (Reference 13) is expressed as

$$Q = \frac{8}{3} \rho g \sqrt{\frac{h^3 \eta^3}{3}} \tag{3.7}$$

With the conservation of energy, wave height is seen to vary inversely as the first power of water depth, which is a significant departure from Green's law. Moreover, Reference 14 suggests that, for purposes of evaluating energy dissipation, the ordinary pattern of the shallow-water oscillatory waves be replaced by a succession of solitary waves. In other words, the shallower the water becomes the more nearly does the trochoidal wave-form approach that of a solitary wave, and if the baseline is lowered so that it is tangent to the trough bottoms (constant amplitude waves), the wave train can be closely approximated by a series of solitary crests, without connecting troughs. Reference 1 suggests the inapplicability of Green's law to waves of finite height and submits supporting data from laboratory tests. However the data is inconclusive, because the test apparatus does not represent the conditions of gradual shoaling encountered in these lagoons. There is an apparent need for experimental work in this area, to establish a relationship for finite wave height to water depth applicable to a system of waves of varying amplitude and period such as those observed during nuclear tests.

Observation of the shallow-water records (30-foot depth) from the Redwing series shows that the steeper waves were of the order $\frac{\eta}{\lambda} = \frac{1}{70}$. This is one-tenth of the steepness of breaking waves; therefore, the waves were somewhat flat. These steepest waves occur at the middle of the wave groups following the first wave, where the oscillations are usually regular. A careful examination of the original traces fails to show any asymmetry between crest and trough curvature that would be indicative of a trochoidal wave-form. Indeed, at this degree of flatness, it is not expected that the difference between sine and trochoidal forms would be detectable.

It would then seem that Green's law is applicable over the oscillatory portion of the wave train. However, its applicability to the first crest, which has the velocity and fore slope of a solitary wave, is still a matter of conjecture. In the absence of experimental evidence, Green's law has been applied throughout in this report.

Attempts to analyze the energy content of waves in shoaling water were unsuccessful because of the inability to determine wave lengths, i.e., velocity, and to evaluate the variability of the reflectance-induced changes in wave height as noted earlier in this section. There is data, however, which permits the study of open-lagoon wave energy, and its change as a function of range and shot size is investigated below. In previous studies of impulsively generated waves (References 1 and 2), it has been customary to approximate the wave shapes with a sine wave and to calculate wave energy from a measurement of wave height and wavelength at a given range. Because the waves being studied in these references varied regularly in amplitude and were symmetrical about their phase zeros and stillwater level, this technique resulted in the desirable accuracy. It has been concluded above that a more applicable method, in certain instances, of figuring the wave energy is by graphic integration of the first wave and by approximation of the remaining waves as sine waves. In all instances, induced errors are not greater

than the cumulative error between the basic measurements and the final wave traces of Appendixes A and C.

When the wave records from Operation Castle (Reference 3) were obtained, the non-systematic and irregular wave traces and the inability to assign velocities to waves following the first wave restricted energy calculations to the first wave and dictated a more cautious approach than a sinusoidal wave approximation. Energy values in Reference 3 were determined by graphic integration of the surface elevation-time curves to calculate potential wave energy. The desirability of this method has been further confirmed by the Redwing results above. This value was doubled to give the total first-wave energy.

The energies of the wave systems generated by Shots Flathead, Dakota, and Navajo as measured at selected stations are presented in Table 3.15. In addition wave energies from Shot Baker during Operation Crossroads, as determined from Reference 7, and the total wave energies of Shots Union and Yankee during Operation Castle are included. As the generation phenomenon discussed in Section 3.10 shows the wave system to be logically separable into two sections by the first-phase zero, so have the energy values of Table 3.15 been divided.

The energy values of the shore stations have not been considered for the reasons outlined above. The one exception is the Navajo data from Station 190.01 wherein the first four waves are symmetrical about the mean water level, and the energy content is the highest of the three Redwing shots being considered. The wave celerity was assumed to be $\sqrt{gh}$ for the 60-foot transducer depth. The energy value is seen to be higher than that measured at Stations 196.01 and 196.02 for this shot, and if the shoaling effects upon wave height and lengths are sufficiently approximated by Green's law, the increased energy content can be accredited to reflected energy from the Site Nan island and reef areas. The Station 190.01 value includes the first five waves and the sixth crest. The fifth crest is at a nodal point at $20\frac{1}{3}$ minutes (Figure A.5) and is not readily identifiable from this record alone. This value does not include the energy of the seventh, eighth, ninth, tenth, and eleventh waves, because they are superimposed upon a reflected trough which arrived from Site Oboe between 21 and $23\frac{1}{4}$ minutes. Inasmuch as the derived wave energy at Station 190.01 is low by an indeterminate amount due to the exclusion of the later waves, the indicated reflectance effect by comparison with energy from the open-lagoon system is conservative. If wave energy is proportional to wave height squared, it can be expected that wave heights observed near these reflectors will vary radically from location to location. It has been previously detected and noted that profound changes occur in wave-system composition and arrangement for stations near reefs and shorelines (Sections 3.4 and 3.5). Changes in wave height are examined further in Section 3.17.

The data available for consideration of total wave-energy decay with increasing range is plotted in Figure 3.20. There is a discouragingly small quantity of data for examination, and the scatter and variation of these do not permit positive conclusions regarding wave-energy decay with range. The lines shown in Figure 3.20 have been positioned as a consequence of some highly selective reasoning, not acceptable as, or representative of, standard techniques of statistical analysis. The Baker data is from stations located in a straight line from surface zero and indicate a definite trend of energy with range. One additional record in these ranges from surface zero is available (Station 24 at 4,000-foot range), but it is in a different direction from those shown. The energy and wave heights at this station are appreciably lower than at the others, and it was noted in Reference 2 that waves from this test had directional characteristics attributable to the generation process.

The Redwing data of Figure 3.20 also shows these directional characteristics, but the trend is not consistent. For example, compare the wave energy at Station 197.04 (located in a northerly direction from surface zero and in shoaling water) to that from Station 197.06 (located east and in deeper water) for Dakota and Navajo; the energy at Station 197.04 was less than that at Station 197.06 for Navajo and greater for Dakota. Had the information from Station 197.04 been consistent, it might be possible to extrapolate this trend to arrive at some estimated value for Flathead wave energy in the direction and range of Station 197.06. Dakota was fired in the Flathead crater, but Navajo was moved farther out into the deeper lagoon water, and a logical conclusion would be that on a per unit of yield basis, the energy of the Dakota waves was greater in a northerly direction than the energy from Flathead waves because of the presence of the Flathead lagoon-bottom crater.

Regardless of the relationship of measured energy at Station 197.04 to the north with wave energy to the east or southeast, the energy content of the waves from Flathead compared to Baker show the increased energy content (wave-making efficiency) of water waves due to the Baker depth of submergence. This is in contradiction to the results implied by a constant first-wave height for constant charge size as the charge position varies near the surface in Reference 6 but is in agreement with the trend established in the experimental work of Reference 1. It is noted, however, that the type of wave system of Reference 6 for the 200-foot scaled depth (Section 3.12) was that of Shots Union and Yankee, and as such the constant first-wave heights and implied energy content of waves for varying charge submergence near the surface may be a unique feature associated only with this range of parameters of generation. If wave energy on a scaled-range basis is compared for geometric similarity of wave systems, the results are even more striking. The scaled ranges for this are given in Table 3.16, and the spread of these values is indicated in Figure 3.20. Any range scaling within acceptable limits indicates the Baker wave energy to be equal to that of Flathead. The conclusion is that had the burst point of Flathead been below the water surface, as was that of Baker, the wave energy would have been very appreciably greater.

The energy values from Station 196.01 are questionable, because it has been concluded that waves at this location are within the zone of influence of the shoaling water and reflective boundary east of the station. The remaining data about energy versus range that can be used with any degree of confidence is shown in Figure 3.20, and through these points the Union, Navajo, and Dakota curves have been drawn. The lines indicate $Q_t \propto r^{-0.58}$ as compared to $Q_t \propto r^{-0.32}$ for Baker waves. This difference in slope can be interpreted as evidence that the rate of wave energy decay with increasing range is a function of energy, i.e., wavelength and height. For larger waves, the energy decreases more rapidly with increasing range. Such an interpretation also implies that for a given wave system the energy content versus range cannot be described by a constant exponent.

For an assumed radially symmetrical radiating wave system in three dimensions from a point source, the measured wave energy passing one zone of observation should be accountable at a more distant zone of observation as wave energy plus propagation losses. With instrumentation of a given resolution and a fixed background for wave measurements, such an idealized energy balance would be impossible to obtain. With increasing range, wave heights decrease primarily because: (1) the wave energy is diffracted over an increasingly larger area, and (2) the wave energy does not move as fast as the individual waves (dispersion). The accuracy of energy measurements also decreases with decreasing wave height. As a result of dispersion, energy can move to

later waves in a system and be lost to observation as small waves near background level. For waves from the Castle and Redwing barge shots, energy diffraction occurs under the same geometry for each shot, and if changes in energy absorption and reflection with wave size along reef lines such as the George-How reef can be minimized, the wave heights and measurable energy content should change at the same rate due to diffraction for all of these wave systems.

The rate at which wave energy advances with a wave (dispersiveness) is a function of the ratio of water depth to wavelength and is determined initially in the zone of generation. The percentage η of energy that propagates with a wave is

$$\eta = \frac{1}{2}\left(1 + \frac{4\pi h}{\lambda}\right) \Big/ \sinh \frac{4\pi h}{\lambda} \qquad (3.8)$$

This equation indicates that, for deep-water waves, half the wave energy moves with the wave, and for extremely shallow water, compared to the wavelength, all the wave energy moves with the wave. Thus, it would be expected that the measurable energy content of a wave system as a function of range would be functional with wavelength, wave energy, and consequently shot size. If depth of water is constant and dispersion is the only effect considered, the larger the waves the greater the percentage of wave energy that is retained in the first and larger waves with increasing range. For smaller waves, the energy begins to drop back earlier and, because the wavelengths within the system decrease from front to back, the process is accelerative. By this process, a wave system continually loses measurable energy out the trailing end or, in other words, increases the proportional energy content of later wave groups.

For the wave systems being investigated, the waves having the greatest wavelengths arrive first. If dispersion is a determinate factor controlling wave energy decay versus range as a function of wave size, this might be detectable by comparing the percentage of wave system energy in the first wave at various ranges from shot to shot. The percent energy in the first crest is shown in Table 3.15. For the Baker system, the data indicates that the first-crest energy, as well as the percentage of total energy in the first crest, increases with range. This is not understandable, and it is necessary to include this feature along with the comparatively high energy content noted above as evidence that Shot Baker was an anomaly from the standpoint of water waves. In a comparison of the percentage energy transported in the first crest for Shots Dakota, Navajo, and Union at Stations 163.02, 163.05, 196.02, and 197.06, it is observed that: (1) the percentage of the wave system energy in the first crest increases with shot size, and (2) the first crest tends to retain its proportional amount of wave energy with increasing range for increasing shot size. This comparison on a percentage basis obviates the question of appropriate scaled ranges for geometrically similar wave systems. It has been pointed out in Section 3.12 that the wave systems of Redwing and Castle are very different, and as a consequence, the problem of scaling range becomes complex and indeterminate. Observation (2) above indicates that dispersion is a significant factor in the first-crest energy (wave height squared) as a function of range, while Observation (1) could easily be explained away on a scaled-range basis. If dispersion were the only factor in determining measurable wave energy with increasing yield (diffraction assumed equal for this data), it would be expected that the larger wave systems would lose less energy with increasing range, but the comparison of energy decay for Baker with the others (Figure 3.20) indicates the opposite. This is interpreted to mean that increased propagation losses with increasing wave size is also an important factor. Observation (2) combined with the above implies that range scaling for different shot sizes is a more sensitive parameter

when dealing with total wave energy from larger shots than when dealing with first-crest energy from smaller shots.

The experimental trends in exaggerated form are summarized on a schematic basis in Figure 3.21. Absolute or relative values cannot be estimated, except to say that the higher yield slope approximates those of Figure 3.20. There is an insufficient amount of data to pursue the subject further.

3.17 SCALING OF FIRST-CREST HEIGHT AS A FUNCTION OF RANGE, WATER DEPTH, AND YIELD

Examination of scaling relationships as applied to the first crests of Shots Union and Yankee during Operation Castle have shown that wave size per unit of yield is very sensitive to the water depth in the zone of generation (Reference 3). For the Redwing tests wherein the water depth of generation as well as the yield varied with each shot, it is necessary to arrive at some understanding of wavemaking efficiency as a function of water depth before a generated wave height versus range can be related directly to a yield value. The variables to be considered are a representative water depth in the zone of generation h_g, the first-crest energy Q_c and total wave-system energy Q_t taken at as close a range to the generation zone as possible, and the yield value W.

In Section 3.10, it is concluded that the first crest is separable from the following waves in any consideration of wave generation and energy. In this section, water depths in the zone of generation are determined from preshot hydrographic surveys, and by the nodal-point theory of Reference 4 applicable to the waves following the first crest. If a value is assigned to the water depth in the zone of generation applicable to analysis of the energy content of the first crest or of the whole wave system, there is a possibility that two different water depths will be involved. The first such depth would determine the amount of water available for the first-crest formation (and consequently its energy), and the second, and greater, depth can be visualized as a parameter of the energy found in the waves following the first crest. This implies that the water depth prior to shot time, averaged over the water-crater radius, is applicable to the energy content of the first crest, and that the nodal-point depth, or a postshot measure of the average depth of the true bottom crater, is applicable to the energy content of all waves after the first crest. The higher percentage of energy in the Navajo first crest compared to that of the Dakota first crest, both measured at Station 197.04, could be construed to be the result of the 2-year-old Union-Yankee bottom crater, the center of which was between Station 197.04 and Navajo surface zero. In the same vein, the percentage of energy in the first crest for Dakota at Station 197.04 might have been greater had the Dakota yield been less than that of Flathead which had the same surface zero.

At the present, there is neither data nor a technique for handling data that would permit the determination of a representative water depth that would be functional with the volume of water going into the first crest over an irregular bottom. Neither is it possible to guess what part of the water originally occupying the crater is lost to the system at zero time, nor what the distribution of this lost volume might be before zero time. The data indicates that the crater maximum is reached quite rapidly in from 1 to 2 seconds.

For the Redwing shots, most of the wave system energy is in the waves following the first crest, and the nodal-point water depth is the most representative, especially because the theory appears to allow for the sloping bottom at surface zero when based on the data from the different turtle stations around surface zero. This is discussed at greater length in Section 3.10. For Shots Union and Yankee where the wave systems do not exhibit nodal

points and half of the wave energy is in the first crest, a measured, or estimated, average water depth over the zone of generation is most representative. The data for the assessment of wavemaking efficiency is presented in Table 3.17.

The water depths of generation in the table are those indicated above. To maintain dimensional uniformity, the ratio $\frac{h_g}{R}$ is given as a function of $\frac{Q_t}{W}$ in Figure 3.22. The crater radii used are those of Table 3.4.

With the exception of Shot Baker of Operation Crossroads, whose data falls beyond the scale of this figure, the points are closely grouped. This cluster of data gives a graphic example of one of the shortcomings of the nuclear tests to date; although the yield values have been varied over a suitable range, the depth values have varied accordingly so that the evaluation of the effect of the depth-of-generation parameter on wavemaking efficiency lacks a suitable range of data. It is impossible to draw any conclusions from the data of Figure 3.22, but if the trend is approximated by the dashed line indicated with slope 30 degrees, then

$$\frac{h_g}{R} \propto \left(\frac{Q_t}{W}\right)^{1/2} \tag{3.9}$$

$$R \propto W^{1/4} \tag{3.10}$$

or

$$Q_t^{1/2} \propto h_g W^{1/4} \tag{3.11}$$

Data to plot Equation 3.11 is available in Table 3.17 and the curve of Figure 3.22 tends to confirm the exponential proportionality of Equation 3.9.

This data shows that the total wave energy is proportional to the water depth of generation squared, and to the yield to the one-half power. As the objective is to relate a wavemaking efficiency applicable to the first crest in terms of these variables, a statement relating the first-crest energy to the total wave energy is required. The results of Section 3.16 have indicated that the partition of energy between these two is not constant but is a function of the relative magnitude and arrangement of the generated waves, i. e., the type of wave system. The data of Table 3.15 showed that approximately 50 percent of the total wave energy was in the first crest for Shots Union and Yankee, but the Redwing first crests contained a much smaller percentage. However, the turtle records for Redwing indicate that the percentage of energy in the first crest is approximately constant over these ranges of yields. The one exception is the Station 197.04 record for Navajo, and, as pointed out above, the influence of the Union-Yankee crater is believed to be the cause. In the absence of additional data, the yield range is restricted to from 375 to 4,690 kt and Q_c is assumed linearly proportional to Q_t over this range of yields, or,

$$Q_c \propto h_g^2 \, W^{1/2} \tag{3.12}$$

In view of the above discussion, this assumption is accompanied by a change of water depths of generation from the nodal-point depth to a measured or estimated average depth prior to shot time.

In Section 3.16, it was determined that $H_c \, r^{0.85}$ is a constant for any given Q_c and h_p (water depth of propagation) so

$$H_c \, r^{0.85} \propto Q_c^{\,n} \, h_p^{\,m} \tag{3.13}$$

where n and m can be constant or functional exponents. If they are assumed constant, and because the depths of propagation for these tests have been the same,

$$H_c r^{0.85} \propto Q_c^{\,n} \tag{3.14}$$

$$H_c r^{0.85} = K\left(h_g^{\,2}\ W^{1/2}\right)^n \qquad \text{from Equation 3.12} \tag{3.15}$$

The data for evaluation of K and n is given in Table 3.18 and the results are shown graphically in Figure 3.24. Now,

$$H_c r^{0.85} = 0.0234\left(h_g^{\,2}\ W^{1/2}\right)^{0.69} \tag{3.16}$$

Where: H_c = first crest height (feet) in 60 feet of water

r = refracted range (feet) from surface zero

h_g = preshot average or estimated average water depth (feet) over the area of generation defined by R

W = tnt equivalent of yield (pounds)

which is a scaling equation for the first crests from surface shots with yields of from 375 to 4,690 kt in open-lagoon waters, propagating in an average water depth of 170 feet. The height H_c is for the first crest in 60 feet of water and can be moved to other depths by Green's law, i.e., $H_{c_1}/H_{c_2} = \left(h_2/h_1\right)^{1/4}$, within the limits of 60 to 170 feet and for distances from reef lines greater than approximately 5,000 feet.

As was observed in Section 3.13, the shore-station data exhibits trends which include the reflectance, or absorptivity in the case of Site How, of nearby islands and shorelines and are not representative of the open-lagoon waves. As for other curves based upon these data, the curve of Figure 3.24 has been positioned with consideration for the induced effects of station locations, and as such is subject to individual interpretation. By way of comparison, data for Shot Tewa has been tabulated and located in this figure. Tewa was on a barge in 20 feet of water located within 300 feet of the Charlie-Dog reef, and the average water depth within a radius of 860 feet was somewhere between 10 and 30 feet. To be conservative in the following comparison, it is necessary to assume that the average water depth in this area was 50 feet. A representative value for the open-lagoon ordinate of Figure 3.24 is estimated at 7.0×10^4. The abscissa value of $(h_g)^2\ W^{1/2}$ for this ordinate indicates an average water depth of generation of 180 feet, or on a wave-size basis the data indicates that Shot Tewa looked very much like Navajo in 180 feet of water. This points out the delicateness of assigning water depths of generation under these geometries for the purpose of advance wave-height predictions. The above observations do not of course consider the reflected energy that could be directed toward the deeper lagoon waters by the reef, and as such negate the circular-crater assumption in favor of some assymetric crater and result in an increased average water depth of generation.

The results of Reference 3 tended to show that wave height as a function of range was proportional to $h_g^{0.7}\ W^{1/2}$. This was supported primarily by scaling from Shot Baker and the HE data of Reference 6 to Shot Union. As a result of the conclusions of this report, reconsideration of the results of Reference 3 lead to the following observations. The type of wave system generated in Reference 6 was very similar to that observed for Shot Union, and if identical scaled depths of propagation are assumed, the wave heights

of the two systems should be related by some exponential combination of W and h_g. Because the wave systems of Baker and Union were decidedly different, the comparative scaling of the first-crest energies with water depth and yield is questionable. The percentage of wave energy in the first crest for Baker is indicated to be greater than that of the Redwing barge tests, but it is also substantially less than that for Union (Table 3.15).

In Reference 3 a wave generation model was examined in an attempt to relate the more prominent variables determining wave size in a simple parametric form; however, the indicated variability of the generating efficiency and the energy distribution within a system, as a function of the parameters of generation, points out the inadequacy of an oversimplified model, except possibly for the scaling of identical wave systems generated and propagating in identical scaled water depths.

Equation 3.16 indicates that the first-crest height is more sensitive to the water depth of generation than previously indicated ($h_g^{1.4}$ compared to $h_g^{0.7}$) and that the wave height is less sensitive to yield ($W^{1/3}$ compared to $W^{1/2}$). It should be borne in mind, however, that this is applicable only to a very narrow band of the full spectrum of impulsively generated waves.

The difficulty lies in the fact that this discussion is concerned with two water depths: the depth of wave generation and the depth of wave propagation. For these shallow waters, relative to charge size, the depth of propagation is a determinate factor in controlling the conservation of energy, i.e., height in the first wave with increasing range, while the depth of generation is controlling primarily the energy going into the waves and the energy distribution within the system. For the nuclear tests to date, the water depth of propagation has been a single value, which has tended to minimize the dispersiveness of waves to the extent that wavelength is related to charge size. The depth of generation has been a variable, but the variations have not been of sufficient scope or in the right direction with respect to yield, so the basic problem of scaling these waves beyond the range of the data cannot be solved. In fact, the results of nuclear tests to date have permitted only a glimpse at the scope of the problem. A comprehensive series of HE tests would be required to explore the problem of depth scaling as a function of crater size and generating efficiency.

3.18 DATA FROM SHOTS ZUNI, TEWA, YUMA, HURON, AND APACHE

Wave data for these shots was much more limited in extent than for the open-lagoon barge shots. During Shot Zuni, the project efforts were plagued by instrument failures, and during Shot Tewa the rollup phase was in progress. A shore station (195.01) was kept active at the personnel pier on Site Elmer at Eniwetok Atoll to record whatever waves might come along, but the two barge shots, which from a size standpoint could have been efficient wave generators, were located inside the crater produced by Shot Mike during Operation Ivy, and the waves were comparatively small in amplitude.

The wave traces from the 60-foot water depth for these tests are included in Appendix A. With the exception of the record from Station 196.02 during Shot Zuni, all traces were recorded by shore stations, and included reflectance-induced increases in wave heights.

The data from Stations 192.01 and 196.02 (Figure A.1) indicates that the Zuni wave system in the open lagoon consisted of a first crest and a trough, after which the waves reduced rapidly in size to background. The records from Stations 191.01 and 192.01 (Figure A.1) indicate the presence of a second crest following the first wave, but this crest was not prominent in the deeper lagoon at Station 196.02. The wave action at Sites

Nan and How became confused immediately after the arrival of the first trough, but this was probably more a result of the signal-to-noise ratio than anything else. In view of the analysis of wave generation discussed earlier in this report, there are two notable features of the Zuni wave system indicated by the data. First, the energy content of the first trough is significantly greater than that of the first crest, and second, the wave action following the first trough is so small as to be almost nonexistent. Both of these features stem from the fact that the burst point was over land, very close to the lagoon shoreline. Surface zero was located on the east rim of a small water-filled crater from Operation Castle, which may have induced some asymmetry into the wave-generation process. Consequently, the wave system in the Site William direction may have differed from that in the Site Nan direction.

The first expansion formed a crater partially in the coral island, and this in combination with the shallowness of the contiguous lagoon waters allowed only a proportionally small amount of energy to go into the first crest. Because the lagoon waters could flow into the crater mainly through the restrictive breach in the crater periphery, a comparatively greater length trough, due to the rate of filling, followed the initial crest, and a larger percentage of the total energy moved out as a trough, compared to the first crest. The inflow to the crater was predominantly unidirectional instead of radially equal around the crater circumference, and this restricted the height of remount at surface zero for formation of a second crest. The energy of the initial crater minus the first-trough energy can be visualized as having been dispersed in this comparatively small remount and in the turbulence expended upon the inland periphery of the coral crater rim, and the number of waves following the first trough was drastically reduced. From the wave records, it appears that the comparative length of the first crest and trough, the relative magnitude of the second crest, and the number of waves following the first trough are indications of the source conditions of generation, and given two shots of equal size in different locations, such as on an island edge and in open water, the two locations would be identifiable by comparative observation of the wave systems from the two.

If surface zero for Shot Zuni were moved to the shallow reef area of the open lagoon so that the energy coupling to the lagoon waters would be increased, the features noted above would become more prominent as shown by the records for Shot Tewa at Stations 191.01 and 192.01 (Figure A.6). Although these records are from stations 9 to 15 miles from surface zero, and contain locally induced characteristics, the unbalance between crest and trough energy is still quite apparent. It should be noted that Tewa besides being closer to deep lagoon water had a greater yield than Zuni.

As discussed in Section 3.17, the first-crest size is affected by water depth in the zone of generation; therefore, it is futile to attempt to scale wave heights from Shots Zuni and Tewa. It can only be said that, if these shots were repeated identically, the wave heights at the same locations would be as shown in Figures A.1 and A.6. It would probably be an acceptable approximation to calculate the open-lagoon wave heights in 60 feet of water for Tewa by employing the Navajo reflectance factors for the individual stations given in Table 3.2 because of the almost identical directions of wave approach. Such an approximation would not be acceptable for the Zuni data however. In conclusion, it is noted that for the Tewa waves at Station 190.01 (Figure A.6), the reflected wave (a trough followed by crest) arrives with the identical time lag after the first crest as was noted and discussed in Section 3.7 for the Navajo wave system.

The waves recorded from Shots Yuma, Huron, and Apache in Eniwetok lagoon are included in Figure A.7. Shot Yuma was a device on a tower at Site Sally in the northeastern part of the lagoon, and the measured water wave was somewhat of an

unexpected oddity. The shot site was inspected from the air after this wave was recorded, and there was no evidence of ground cratering at the tower base, let alone at the lagoon shoreline, which was estimated to be at a distance of 150 feet. The evidence is that this wave was generated by air impulse acting upon the adjacent lagoon water.

Shots Huron and Apache were fired in the crater produced by Shot Mike. The crater restricted the wave energy that escaped to the open lagoon. The waves traveled 19 miles across the lagoon to approach Site Elmer at a refracted angle of approximately 30 degrees from the perpendicular. The records of the Huron and Apache waves (Figure A.7) show the greatest wave amplitudes to be associated with the second to third crest, which is a characteristic of the more dispersive wave systems traveling over relatively great distances. It is noted that the wave crests and troughs are not symmetrical about the mean water level for the second through fourth waves, and that this is more pronounced for the Apache waves than for Huron and must therefore be related to wave size. It is not known whether this asymmetry is associated with the open-lagoon system, or is induced by the lagoon and island topography near the station. As a result of the study of waves approaching Bikini lagoon shorelines, the latter explanation is considered the more likely. The absorptivity or reflectivity of the Eniwetok station cannot be assessed in order to estimate an open-lagoon wave height.

TABLE 3.1 SHOT PARTICIPATION

X, participated, useful data; ?, participated, partial data; 0, participated, no data.

Station Number	Bikini					Eniwetok		
	Cherokee	Zuni	Flathead	Dakota	Navajo	Tewa	Apache	Huron
190.01	X	X	X	X	X	X		
191.01	X	X	X	X	X	X		
192.01	X	X	X	X	X	X		
193.01	X	X	X	X	X			
195.01*		X		X	X	X	X	X
196.01		0	0	X	X			
196.02		X	0	X	X			
196.03			?	0				
196.04				0	0			
196.05					0			
197.01		0						
197.02		0						
197.03		0						
197.04			X	X	X			
197.05			0	0	X			
197.06			0	X	X			

* Station 195.01 was operative and yielded data for Shots Yuma, Osage, Seminole, Mohawk, Erie and Inca.

TABLE 3.2 INCREASE OF FIRST-CREST WAVE HEIGHTS IN TRAVELING FROM OPEN LAGOON TO SHORELINE

Station Number	First-Crest Height in 60 ft of Water in Open Lagoon (Figure 3.24)	Measured First-Crest Heights in 60 ft of Water at Shore Stations	Ratio of Measured First Crest to Open-Lagoon First Crest	First-Crest Height at North Nan Shoreline (Appendix B)	Ratio of First-Crest Height at Nan Shoreline to Height in 60 ft of Water in Open Lagoon
	ft	ft		ft	
Shot Navajo, tide stage = 5.9 ft					
190.01	2.9	4.5	1.5	6.8	2.4
191.01	3.8	6.9	1.8	—	—
192.01	3.5	4.8	1.4	—	—
193.01	3.7	2.9	—	—	—
			Average 1.56		
Shot Dakota, tide stage = 5.5 ft					
190.01	0.92	1.1	1.2	—	—
191.01	1.17	2.3	2.0	—	—
192.01	1.1	1.0	0.9	—	—
193.01	1.1	0.3	—	—	—
			Average 1.36		
Shot Flathead, tide stage = 5.7 ft					
190.01	0.46	0.40	0.9	1.2	2.6
191.01	0.59	0.8	1.3	—	—
192.01	0.56	0.6	1.1	—	—
193.01	0.56	0.4	—	—	—
			Average 1.1		

TABLE 3.3 FIRST-CREST TIME INTERVAL AS A FUNCTION OF RANGE

Straight-Line Range from Surface Zero	Average Celerity	Time Interval
10^3 ft	ft/sec	sec
Shot Navajo:		
12.2	76.4	33
42.5		58
73.0		84
Shot Dakota:		
12.2	71.5	36
42.5		54
73.0		69
Shot Flathead:		
12.2	73.0	33
42.5		47
73.0		60

TABLE 3.4 THEORETICAL WATER-CRATER RADIUS

Energies after $\sqrt{gh}$ travel times. Wave shape sinusoidal. Water depth at crater from nodal-point theory. Wave energies at the experimental station location. Yields are those used in calculations and do not represent final values.

Operation	Shot	Yield	Station Number	Crater Energy	Nodal-Point Water Depth	$r/W^{1/3}$	Theoretical Crater Radius
		kt		10^{11} ft-lb	ft	ft-lb$^{1/3}$	ft
Crossroads	Baker	20	27	4.0	160 *	8.63	400
Redwing	Flathead		197.04				
	Dakota		1				
			15				
	Navajo		19				
			197.05	33.0	219	6.62	827
			197.06	33.1	219	3.08	830
Castle	Union	7,000	163.02	40	145 *	3.08	1,410
	Yankee	13,500	163.02	68	220 *	3.08	1,190
	Union	7,000	163.02	17	145 *	8.90	910
	Yankee	13,500	163.02	35	220 *	7.13	870

* Union, Yankee, and Baker wave systems did not contain identifiable nodal points and associated beat phenomenon. Water depths are averaged or estimated at surface zero before shot.

† Long-period wave removed after first trough.

TABLE 3.5 THEORETICAL WATER-CRATER RADIUS

Energies after first-phase zero points. Wave shape sinusoidal. Water depth at crater from nodal-point theory. All related values not listed are the same as in Table 3.4.

Operation	Shot	Station Number	Crater Energy	Nodal-Point Water Depth	Theoretical Crater Radius
			10^{11} ft-lb	ft	ft
Crossroads	Baker	27	4.0	160 *	400
Redwing	Flathead	197.04			
	Dakota	197.04			
		197.06			
	Navajo	197.04			
		197.05			
		197.06			
Castle	Union	163.02	40.0	145 *	1,410
	Yankee	163.02	68.0	220 *	1,190
	Union	163.02	17.0	145 *	910
	Yankee	163.02	35.0	220 *	870

* Union, Yankee, and Baker wave systems did not contain identifiable nodal points and associated beat phenomenon. Water depths are averaged or estimated at surface zero before shot.

† Long-period wave removed after first trough.

TABLE 3.6 THEORETICAL WATER-CRATER RADIUS

Energies after first-phase zero points. Wave shape sinusoidal. Average water depths at the crater measured or estimated. All related values not listed are the same as in Table 3.4.

Operation	Shot	Station Number	Crater Energy	Preshot Water Depth	Theoretical Crater Radius
			10^{11} ft-lb	ft	ft
Crossroads	Baker	27	4.0	160	400
Redwing	Flathead	197.04		120	
	Dakota	197.04		140	
		197.06		140	
	Navajo	197.04		230	
		197.05		230	
		197.06		230	
Castle	Union	163.02	40.0	145	1,410
	Yankee	163.02	68.0	220	1,190
	Union	163.02	17.0	145	910
	Yankee	163.02	35.0	220	870

* Long-period wave removed after first trough.

TABLE 3.7 THEORETICAL WATER-CRATER RADIUS

Energies after first-phase zero points, integrated for first trough, and calculated as sine wave for remainder of train. Water depths at the craters measured or estimated.

Operation	Shot	Station Number	Crater Energy	Preshot Water Depth	Theoretical Crater Radius
			10^{11} ft-lb	ft	ft
Crossroads	Baker	27	4.0	160	460
Redwing	Flathead	197.04		120	
	Dakota	197.04		140	
		197.06		140	
	Navajo	197.04		230	
		197.05		230	
		197.06		230	
Castle	Union	163.02	40.0 †	145	1,410
	Yankee	163.02	68.0 †	220	1,190
	Union	163.02	17.0 †	145	910
	Yankee	163.02	35.0 †	220	670

* Long-period wave removed after first trough.
† Sine wave throughout.

TABLE 3.8 WAVE-ARRIVAL TIMES, SHOT NAVAJO

Station Number	Straight-Line Range to Surface Zero		First Disturbance	First Crest	First-Phase Zero	First Trough	Second-Phase Zero	Second Crest	First Reflected Wave Arrival Time	
									Trough	Crest
	naut mi	ft	minutes	minutes	minutes	minutes	minutes	minutes	minutes	minutes
197.06	1.08	6,566								
197.04	1.46	8,877								
197.05	2.36	14,349								
196.04	4.97	30,278								
196.02	8.32	50,585								
193.01	9.05	55,024								
191.01	9.43	57,340								
196.01	9.57	58,185								
192.01	10.22	62,138								
190.01	12.73	77,398								

TABLE 3.9 WAVE-ARRIVAL TIMES, SHOT DAKOTA

Station Number	Straight-Line Range to Surface Zero		First Disturbance	First Crest	First-Phase Zero	First Trough	Second-Phase Zero	Second Crest	First Reflected Wave Arrival Time	
									Trough	Crest
	naut mi	ft	minutes	minutes	minutes	minutes	minutes	minutes	minutes	minutes
197.06	1.24	7,560								
197.04	1.18	7,190								
196.02	8.65	52,600								
193.01	9.25	56,300								
196.01	9.92	60,300								
191.01	9.92	60,300								
192.01	10.62	64,600								
190.01	13.12	79,800								

TABLE 3.10 WAVE-ARRIVAL TIMES, SHOTS FLATHEAD AND TEWA

Station Number	Straight-Line Range to Surface Zero		First Disturbance	First Crest	First-Phase Zero	First Trough	Second-Phase Zero	Second Crest	First Reflected Wave Arrival Time	
									Trough	Crest
	naut mi	ft	minutes	minutes	minutes	minutes	minutes	minutes	minutes	minutes
Shot Flathead:										
197.04	1.18	7,190								
196.03	5.82	35,400								
193.01	9.25	56,300								
191.01	9.92	60,300								
192.01	10.62	64,600								
190.01	13.12	79,800								
Shot Tewa:										
192.01	9.23	56,100	11.25	12.80	13.20	—	14.65 *	—	—	—
191.01	10.86	66,050	13.00	14.40	15.10	—	17.50 *	—	—	—
190.01	15.3	93,200	19.70	21.00	21.35	—	23.20 *	—	—	—

* The second pass of water level through mean water level.

TABLE 3.11 COMPARISON OF FIRST-CREST ARRIVAL TIMES OVER SHOAL WATER AND REFRACTED PATHS, SHOT NAVAJO

Crater formation time neglected.

Station Number	Measured Arrival Time	Air Line Range	Refracted Range from Refraction Diagram	Arrival-Time Increment Due to Refraction (c = 74.3 ft/sec)	Arrival-Time Increment Due to Shoaling Water Along Refracted Path	Measured Arrival Time Minus Refraction and Shoaling Increments	Open-Lagoon Arrival Time from Figure 3.8	Difference	Notes
	minutes	naut mi	naut mi	minutes	minutes	minutes	minutes	percent	
197.04		1.46	Not refracted						
196.01		9.57	9.75						
193.01		9.05	9.49						Shoaling water occurs in last 2½ miles of travel

* Arrival time increment due to shoaling is difference between:
(1) Travel time of a crest from the crater lip (630 feet from zero) to Station 197.01 (7,350 feet from zero) in 500-ft increments where $c = \sqrt{gH_c \tanh kH_c}$ average and $H_c \propto 1/R$ and $\Theta_2/\Theta_1 r^{1/2}$.
(2) Travel time of a crest from the crater lip to Station 197.04 estimated from the average velocity of the first crest to Station 197.06.
t(1) = 105 sec (1.75 min)
c(2) average = 91.9 ft/sec
t(2) = 63.2 sec
} Time increment = 21.8 sec

TABLE 3.12 FIRST-CREST AND FIRST-WAVE DATA, SHOTS ZUNI, FLATHEAD, DAKOTA, NAVAJO, AND TEWA

Station	Refracted Path Range	First-Crest Height in 60 Feet of Water	First-Wave Height in 60 Feet of Water	Water Depth of Generation	First-Crest Height in Water Depth of Generation
	10^3 ft	ft	ft	ft	ft
Shot Zuni					
191.01	18.0	2.6	5.1	—	—
192.01	33.0	1.5	3.4	—	—
196.02	52.8	1.1	1.9	—	—
190.01	69.0	0.5	1.2	—	—
193.01	73.8	0.2	1.0	—	—
Shot Flathead					
197.04	7.5			120	
196.02	35.5			120	
191.01	60.6			120	
193.01	64.6			120	
192.01	64.2			120	
190.01	79.8			120	
Shot Dakota					
197.04	7.5			140	
197.06	7.5			140	
196.02	53.8			140	
191.01	60.6			140	
193.01	64.6			140	
192.01	64.2			140	
196.01	64.8			140	
190.01	79.8			140	
Shot Navajo					
197.06	6.5			230	
197.04	8.5			230	
197.05	14.4			230	
196.02	50.1			230	
191.01	57.3			230	
193.01	58.5			230	
196.01	63.3			230	
192.01	62.1			230	
190.01	77.7			230	
Shot Tewa					
192.01	57.0	3.7	7.5	20	4.9
191.01	66.0	3.4	7.7	20	4.5
190.01	93.9	1.5	2.9	20	2.0

* Total wave height estimated as twice the first-trough depth.

TABLE 3.13 MEASURED NODAL-POINT TIMES OF ARRIVAL FOR DETERMINATION OF GROUP VELOCITIES OF BARGE SHOTS

Station	Straight-Line Range	Nodal Point			
		First	Second	Third	Fourth
	10^3ft	minutes	minutes	minutes	minutes
Shot Navajo					
197.06	6.5				
197.04	8.9				
197.05	14.3				
196.02	50.6				
193.01	55.0				
191.01	57.3				
196.01	58.2				
192.01	62.1				
190.01	77.4				
Shot Dakota					
197.06	7.6				
197.04	7.2				
196.02	52.6				
193.01	56.3				
196.01	60.3				
191.01	60.3				
190.01	79.8				
Shot Flathead					
197.04	7.2				
193.01	56.3				
191.01	60.3				
192.01	64.3				

TABLE 3.14 FIRST CREST TO SECOND CREST WAVELENGTHS

Data from Section 3.11

Straight-Line Range from Surface Zero	Average Celerity	Time Interval	First Crest to Second Crest Wavelength
10^3ft	ft/sec	sec	ft
Shot Navajo			
12.2	72		
42.5			
73.0			
Shot Dakota			
12.2	71.6		
42.5			
73.0			
Shot Flathead			
12.2	70.9		
42.5			
73.0			

TABLE 3.15 WAVE-SYSTEM ENERGIES FOR OPEN-LAGOON NUCLEAR TESTS

Operation	Shot	Yield	Station	Wave-Path Range	First-Crest Energy	Energy of Waves after First Crest	Total Wave-System Energy	Percent of Total Wave Energy in the First Crest	Method of Determination	
									First Crest	Waves Following
		Mt		ft	10^{11} ft-lb	10^{11} ft-lb	10^{11} ft-lb			
Crossroads	Baker	0.020	27	3,000	1.79	4.15	5.94	30	Sine wave	Sine wave
			40	3,600	1.88	3.78	5.66	33	Sine wave	Sine wave
			21	5,000	2.01	3.21	5.22	38	Sine wave	Sine wave
			23	7,000	2.37	2.14	4.51	52	Sine wave	Sine wave
Redwing	Flathead		197.04	7,500					Graphic integration	Graphic int. - 1T Sine wave all others
			196.03	35,400					Sine wave	Sine wave
			193.01	59,000					—	—
			191.01	60,300					—	—
			192.01	64,600					—	—
			190.01	79,800					—	—
	Dakota		197.06	7,560					Graphic integration	Graphic int. - 1T Sine wave all others
			197.04	7,500					Graphic integration	Graphic int. - 1T Sine wave all others
			196.02	52,600					Sine wave	Sine wave
			193.01	59,000					—	—
			191.91	60,300					—	—
			196.01	61,400					—	—
			192.01	64,600					—	—
			190.01	79,800					—	—
	Navajo		197.06	6,566					Graphic integration	Graphic int. - 1T Sine wave all others
			197.04	8,877					Graphic integration	Graphic int. - 1T Sine wave all others
			197.05	14,349					—	Sine wave
			196.02	50,585					Sine wave	Sine wave
			193.01	57,700					—	—
			191.01	57,340					—	—
			196.01	59,280					Sine wave	Sine wave
			192.01	62,138					—	—
			190.01	77,398					Sine wave	Sine wave
Castle	Union	7	163.02	21,400	27.6	17.4	45	60	Sine wave	Sine wave
			162.03	58,575	—	—	—	—	—	—
			163.04	60,100	—	—	—	—	—	—
			163.05	75,600	15.4	6.1	21.5	72	Sine wave	Sine wave
	Yankee	13.5	163.02	21,400	58.2	—	—	—	Sine wave	—
			163.05	75,600	22.5	12.3	34.8	—	Sine wave	Sine wave

TABLE 3.16 SCALED RANGES FOR COMPARISON OF SHOT BAKER WAVE ENERGY AT 5,000-FOOT RANGE WITH WAVE ENERGY FROM SHOTS FLATHEAD AND DAKATO

Reference Figure 3.20.

Shot	Yield	Range r	Baker Scaled Range		Range, r for Energy Comparison	
			$r/W^{1/3}$	$r/W^{1/4}$	$r/W^{1/3}$	$r/W^{1/4}$
	kt	ft	ft-$lb^{1/3}$	ft-$lb^{1/4}$	ft	ft
Baker	20	5,000	14.6	63.0	5,000	5,000
Flathead						
Dakota						

TABLE 3.17 TABULATED DATA FOR ASSESSMENT OF WAVEMAKING EFFICIENCY AS A FUNCTION OF WATER DEPTH OF GENERATION

Station	Shot	Total Wave Energy Q_t	Yield W	Nodal-Point Water Depth h_g	Maximum Water-Crater Radius R	$\frac{h_g}{R}$	$\frac{Q_t}{W}$
		10^{11} ft-lb	kt	ft	ft		$10^6 \frac{\text{ft-lb}}{\text{tons}}$
27	Baker	5.94	20	160	400	0.40	29.7
197.04	Flathead						
197.06	Dakota						
197.04	Dakota						
197.06	Navajo						
197.04	Navajo						
163.02	Union	45.0	7,000	145*	910	0.16	0.64
163.02	Yankee	93.2†	13,500	220*	870	0.25	0.69

* Measured and estimated water depth.

† Q_t = Projected trough energy + measured energy of all other waves. (Tables 3.4 and 3.15.)
$Q_t = (35 + 58.2) \times 10^{11}$ ft-lb.

TABLE 3.18 TABULATED DATA FOR FIRST-CREST SCALING OPERATION REDWING BARGE SHOTS

Waves propagating in 170 feet of water. Crest height given for 60-foot water depth.

Station	Range	First-Crest H_c	Average Water Depth of Generation Measured and Estimated h_g	$H_c r^{0.5}$	$W^{1/3}(h_g)^2$
	10^3 ft	ft	ft	10^4 ft	10^8 ft^{2}lb TNT equivalent
Shot Flathead					
197.04	7.5		120		
196.03	35.5				
191.01	60.6				
193.01	64.6				
192.01	64.2				
190.01	79.8				
Shot Dakota					
197.04	7.5		140		
197.06	7.5				
196.02	53.8				
191.01	60.6				
193.01	64.6				
192.01	64.2				
196.01	64.8				
190.01	79.8				
Shot Navajo					
197.06	6.5		230		
197.04	8.5				
196.02	50.1				
191.01	57.3				
193.01	58.5				
196.01	63.3				
192.01	62.1				
190.01	77.7				
Shot Tewa 4.6 Mt					
192.01	57.0	3.7	20	12.2	0.4
191.01	66.0	3.4		12.6	
190.01	93.9	1.5		7.96	

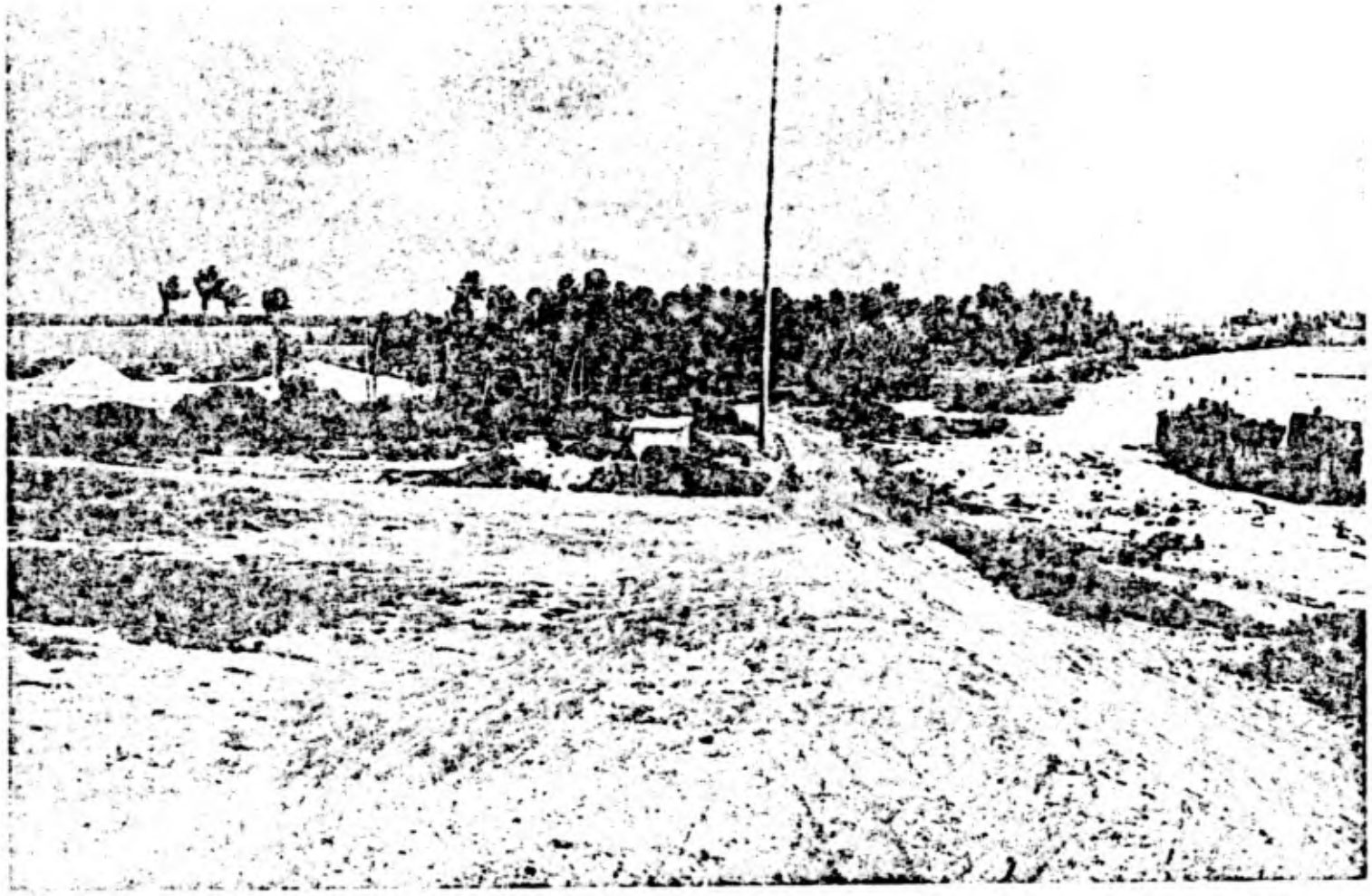

Figure 3.1 Field of view from north Nan tower showing LCU wreck.

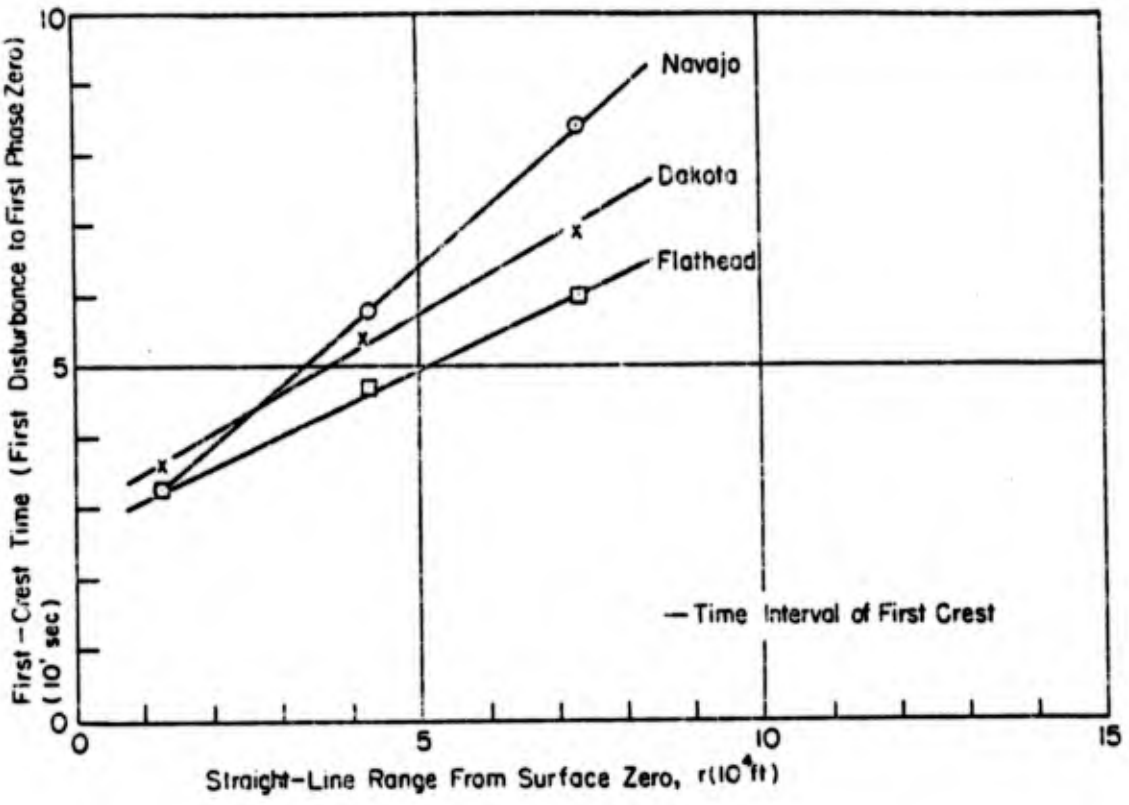

Figure 3.2 First-crest time interval.

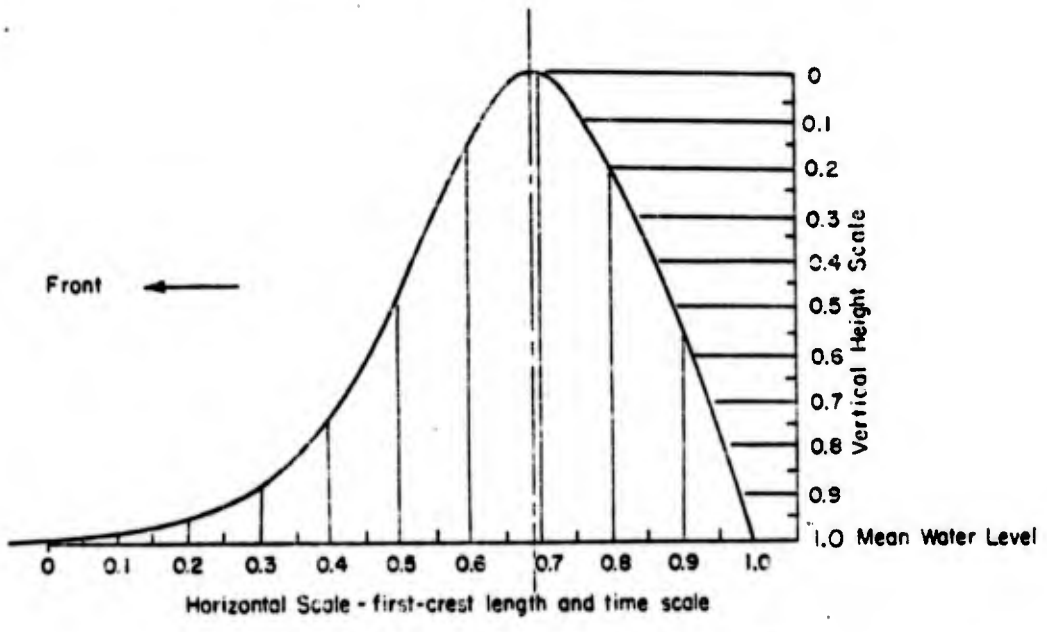

Figure 3.3 Approximate profile of first crest.

Pgs. 88 thru 95 Deleted.

1) SINE WAVE PROFILE

$$\eta = a \cos\left[\frac{2\pi}{\lambda}(X - Ct)\right]$$

$a = 0.75$

$\lambda = \frac{64}{9} = 7.11$

2) SINE WAVE PROFILE

$$\eta = \frac{a}{2}\left[1 + \cos\frac{2\pi}{\lambda}(X - Ct)\right]$$

$a = 0.75$

$\lambda = \frac{128}{27} = 4.75$

3) TROCHOIDAL WAVE

$$X = \frac{\lambda\theta}{2\pi} - \frac{a}{2}\sin\theta$$

$$\eta = \frac{a}{2}(1 + \cos\theta)$$

$a = 0.75$

$\lambda = \frac{128}{27} + \frac{\pi}{2} = 6.31$

4) SOLITARY WAVE PROFILE

$$\eta = a\,\mathrm{sech}^2\left[\sqrt{\frac{3}{4}\frac{a}{h^3}}(X - Ct)\right]$$

$a = 0.75$

$h = 1$

$"\lambda" = \frac{4}{3}\pi = 4.18$

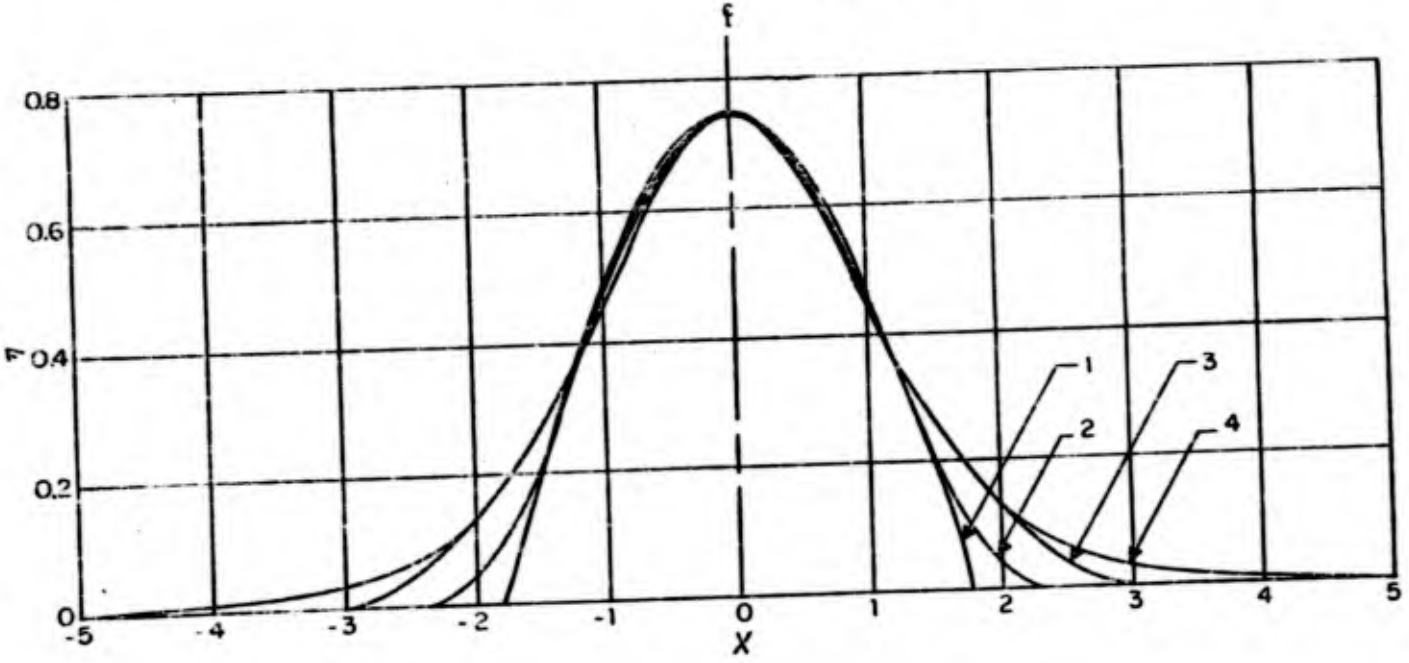

Figure 3.19 Waveforms of equal height containing equal energies.

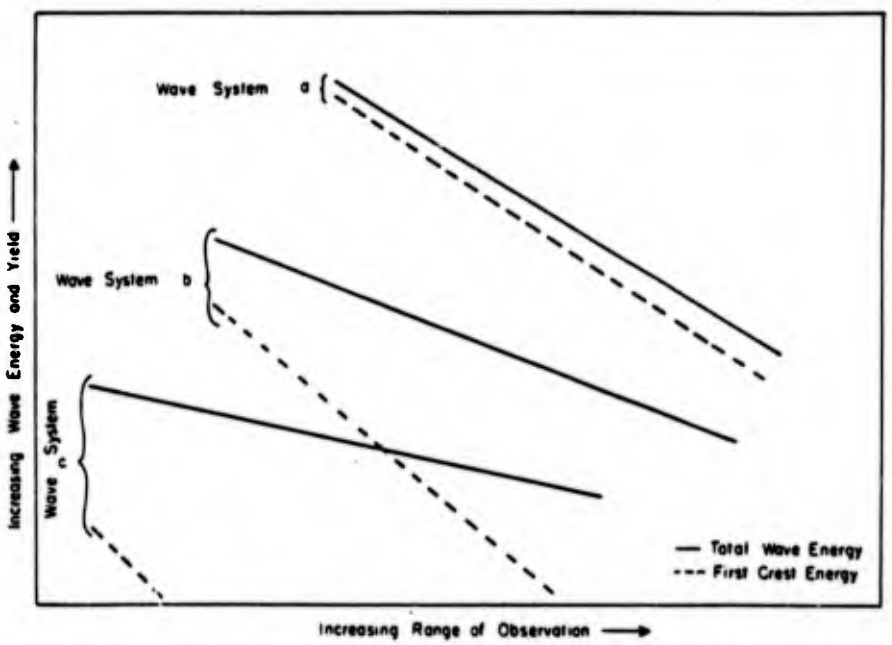

Figure 3.21 Trends of measurable first-crest and total wave energy as a function of range and yield. Constant depth, shallow water. Energy observations as a wave amplitude for increasing time at fixed range.

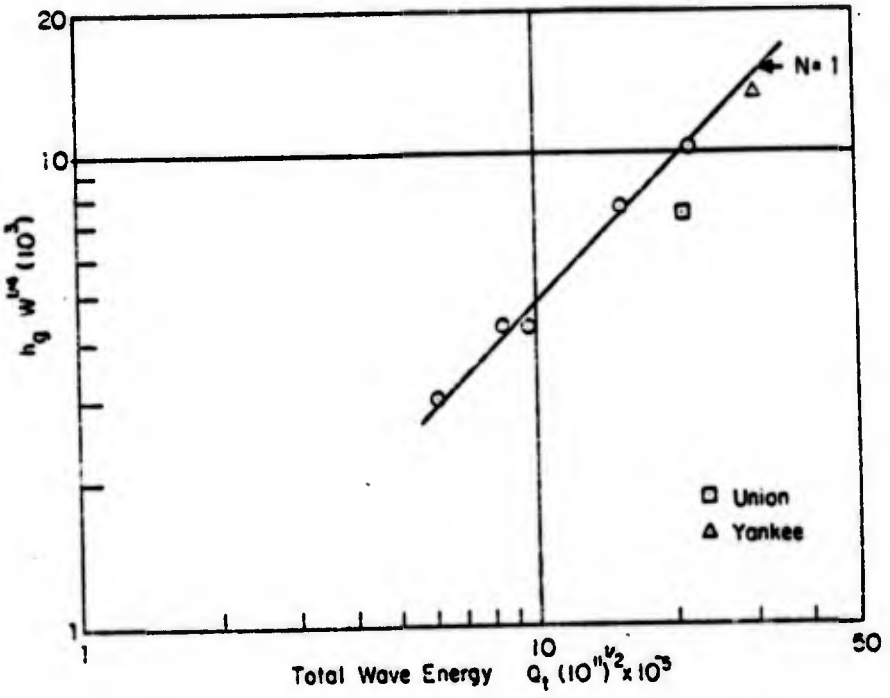

Figure 3.23 $h_g W^{1/4}$ as a function of total wave energy.

Pg. 99 Deleted.

Chapter 4

CONCLUSIONS AND RECOMMENDATIONS

4.1 CONCLUSIONS

Study of waves generated by the Redwing shots has led to methods for predicting effects of future shots within certain limitations. Of primary significance is the recognition of the separate influences upon wave height of the water depth of generation and the depth of propagation. The effect of varying depth of propagation could not be quantitatively evaluated, because it was nominally the same in all the cases considered, i.e., Bikini lagoon depth. The qualitative effects, however, are well indicated by theory and by trends in the data studied.

Study of Reference 5 and comparison with the records of impulsively generated waves has led to the conclusion that wave scaling is not a continuous function but depends upon the characteristic type of wave system generated.

Analysis from an energy standpoint of close-in wave records has given a much clearer concept of the dimensions of the generative process and has led to the isolation of the parameters of wave generation. This has not only provided the basis for derivation of a scaling law but has also indicated the need for direct measurement of these parameters in future tests.

Energy studies have also revealed the disproportionate size of the wave system from Shot Baker during Operation Crossroads, compared to those of the larger surface shots. The inescapable conclusion is that the wavemaking efficiency of Shot Baker was enhanced by its depth of submergence and cannot be classified with surface shots for purposes of water-wave analysis.

The task of analyzing and predicting inundation effects has always been rendered prodigious by the unlimited combinations of topographic features that can significantly affect the oncoming waves. Add to this the equally unlimited combinations of waves that can occur in a particular train, and the difficulty of a quantitative analysis can be well appreciated. The method presented here is applicable to a particular topographic layout and illustrates the salient factors involved in inundation of low-lying areas by longer period waves. However, inundation prediction must still remain very much a specialized art.

4.2 RECOMMENDATIONS

The present study points up the limited scope of past observations and gives a strong indication of the direction in which future work must lie. A greater range of generative conditions (yield to water depth ratios) must be explored and related to the class of wave system generated. Observation of the effect of several water depths of propagation on initially identical wave systems is also necessary.

Measurements must be made as close as possible to the center of the generative process. These must not be limited, as in the past, to water-wave records but must try

to penetrate to the water crater and measure its expansion in radius, depth, and time. Analysis of cores of the lagoon bottom on a cross section of the crater may yield valuable clues that are covered up by the wash-back from water-crater collapse. This core study could still be of value from existing craters.

Underwater shots in shallow water, such as Shot Baker, must be fitted to their proper place in the wave-producing spectrum. The existence of a critical depth of submergence as related to other parameters of generation should be resolved and evaluated.

The limitations imposed upon, and by, nuclear tests make desirable a program of intensive study, under more highly controlled geometries, using high-explosive charges. This could now be done with much greater insight into the proportions and functions to be explored than was possible in the past.

There is a need for continuous documentation of the changes which an impulsive generated wave train undergoes as it enters shoaling water and inundates a beach area. This is necessary to test the adequacy of present formulas relating wave height to water depth, and to fortify the art of inundation prediction.

APPENDIX A

WATER-SURFACE AS A FUNCTION OF TIME AND RANGE IN 60 FEET OF WATER

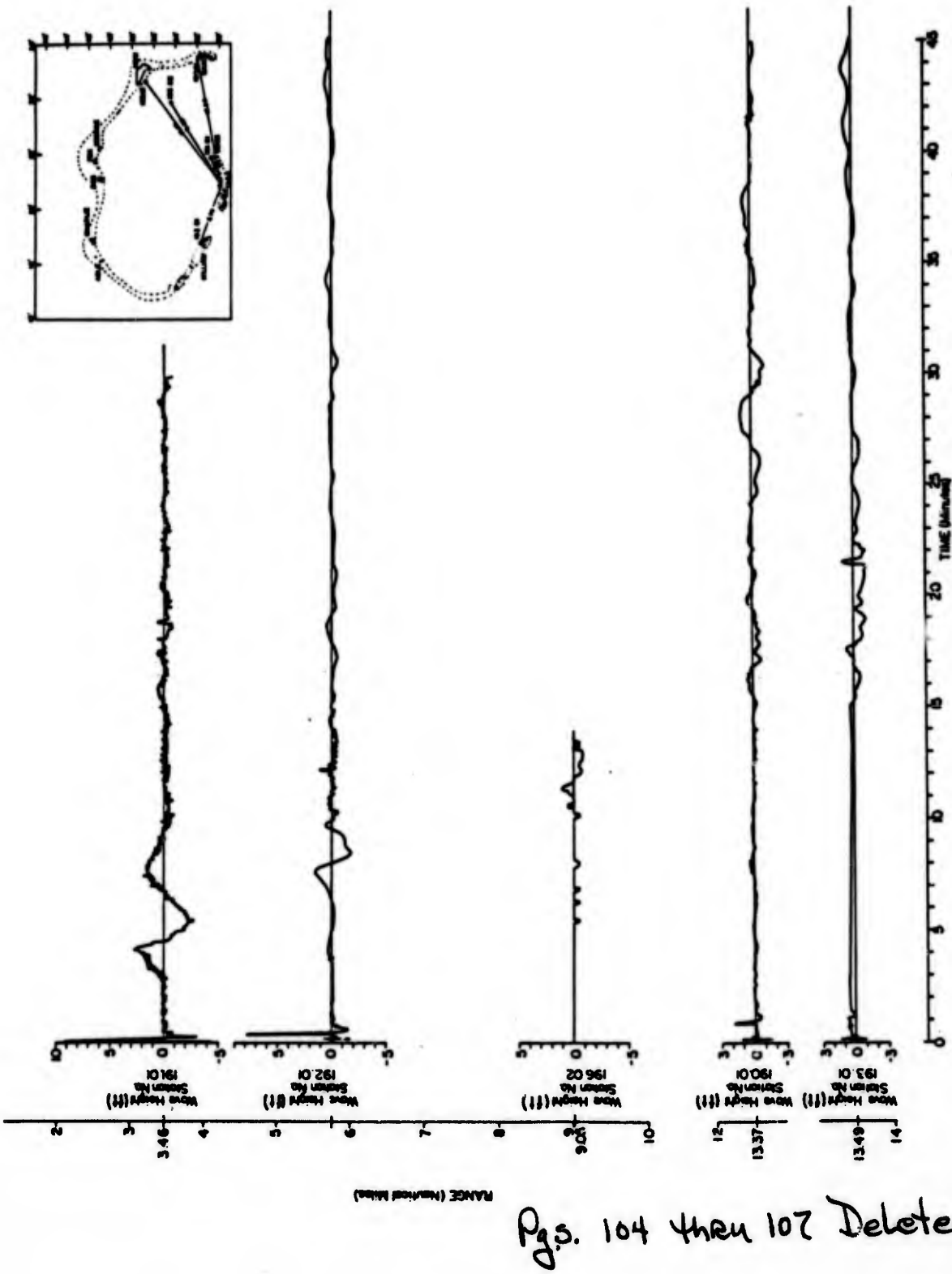

Figure A.1 Water-surface elevation, Shot Zuni.

Pgs. 104 thru 107 Deleted.

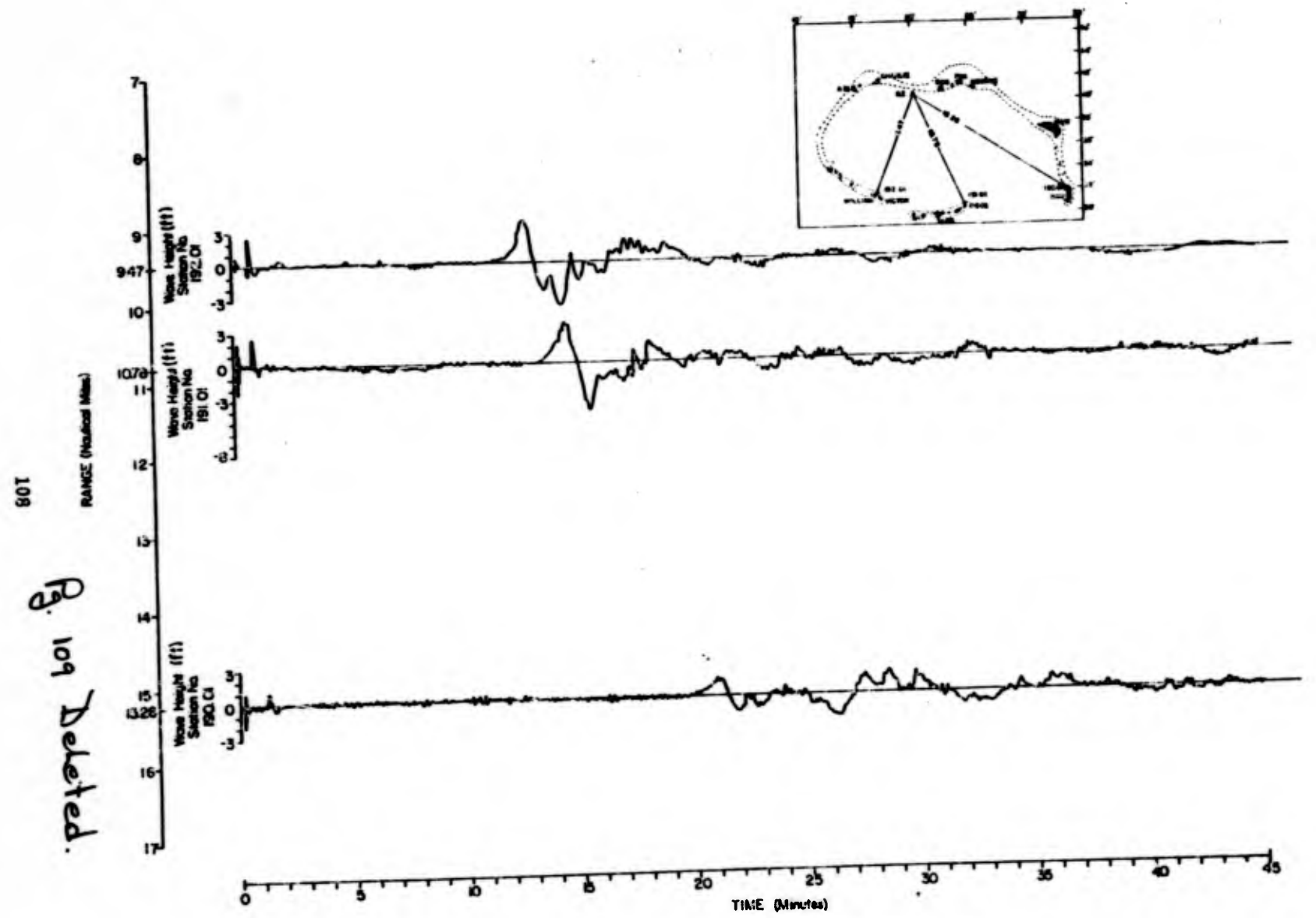

Figure A.6 Water-surface elevation, Shot Tewa.

APPENDIX B

WATER LEVEL AT SHORELINE VERSUS TIME, SITE NAN

Pgs. 111 thru 113 Deleted.

APPENDIX C

PRESSURE VERSUS TIME CURVES FROM CLOSE-RANGE STATIONS

Pgs. 115 then 118 Deleted.

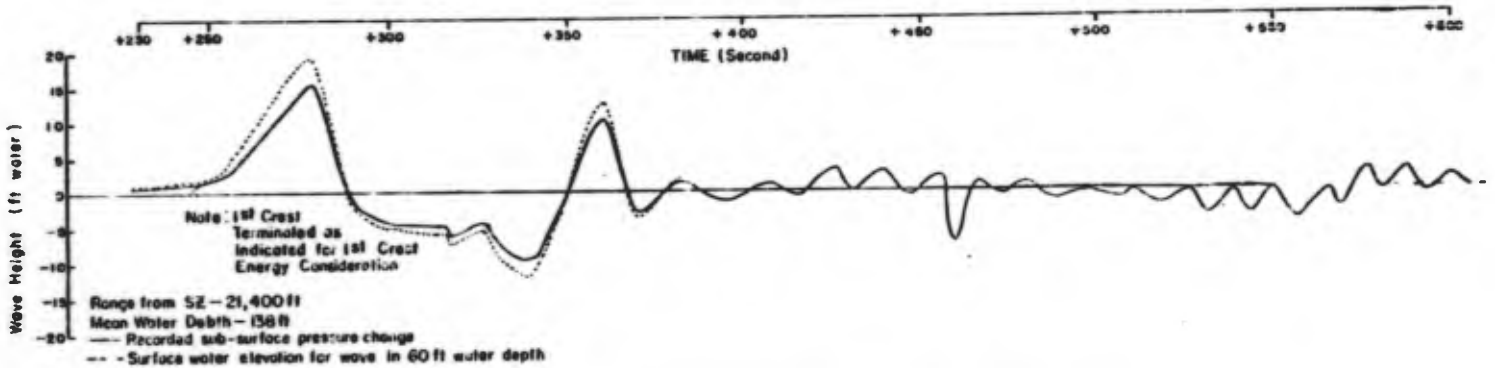

Figure C.7 Wave profile, Shot Union, Operation Castle, Station 163.02.

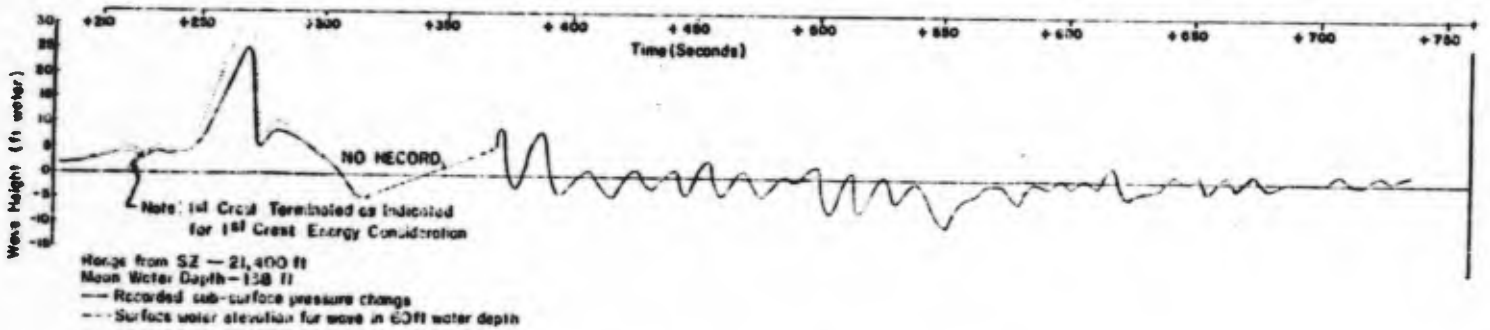

Figure C.8 Wave profile, Shot Yankee, Operation Castle, Station 165.02.

APPENDIX D

PHOTOGRAPHS OF INUNDATION EFFECTS

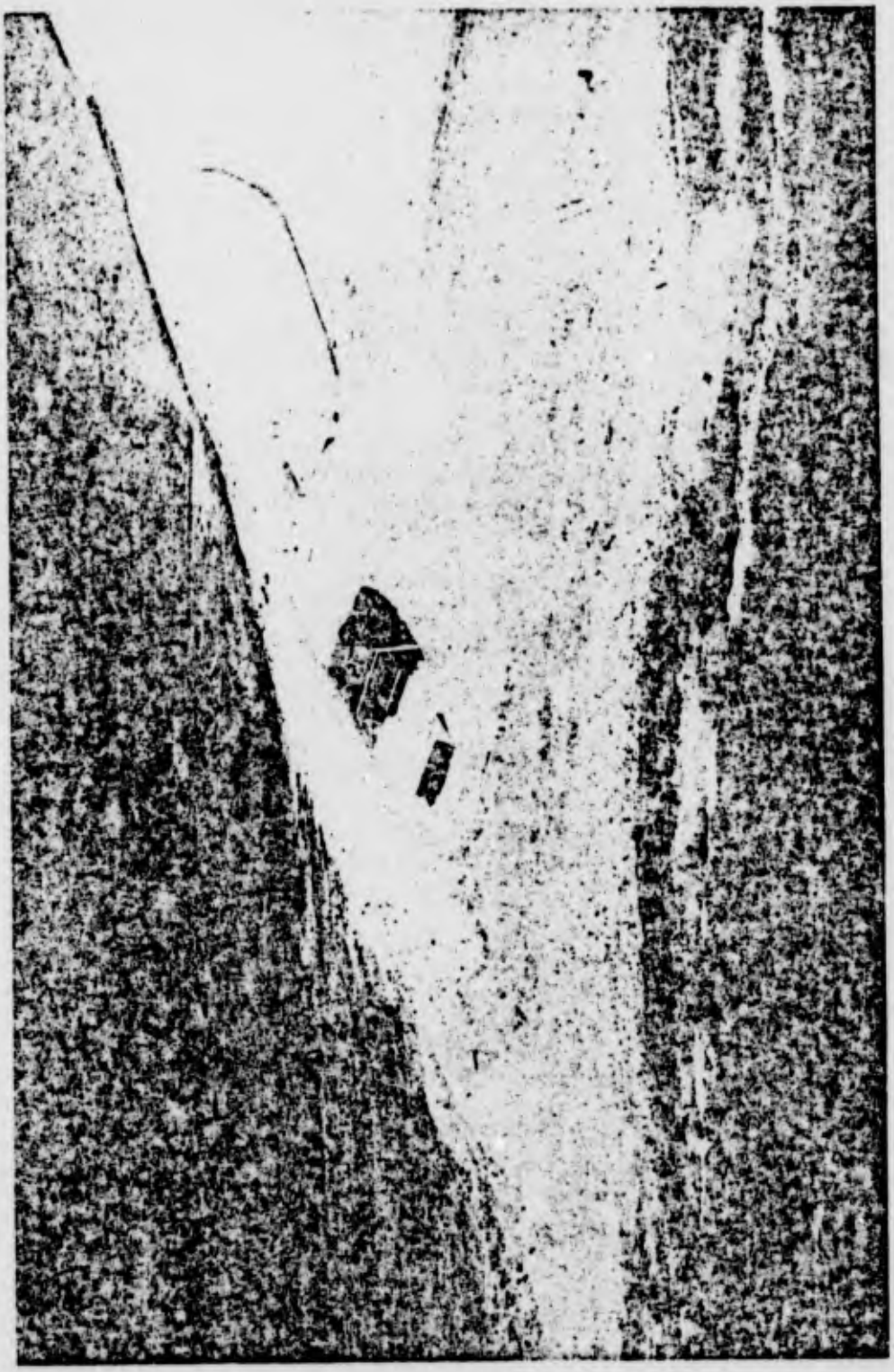

Figure D.1 Station 13?, Site Dog, pre-Shot Flathead.

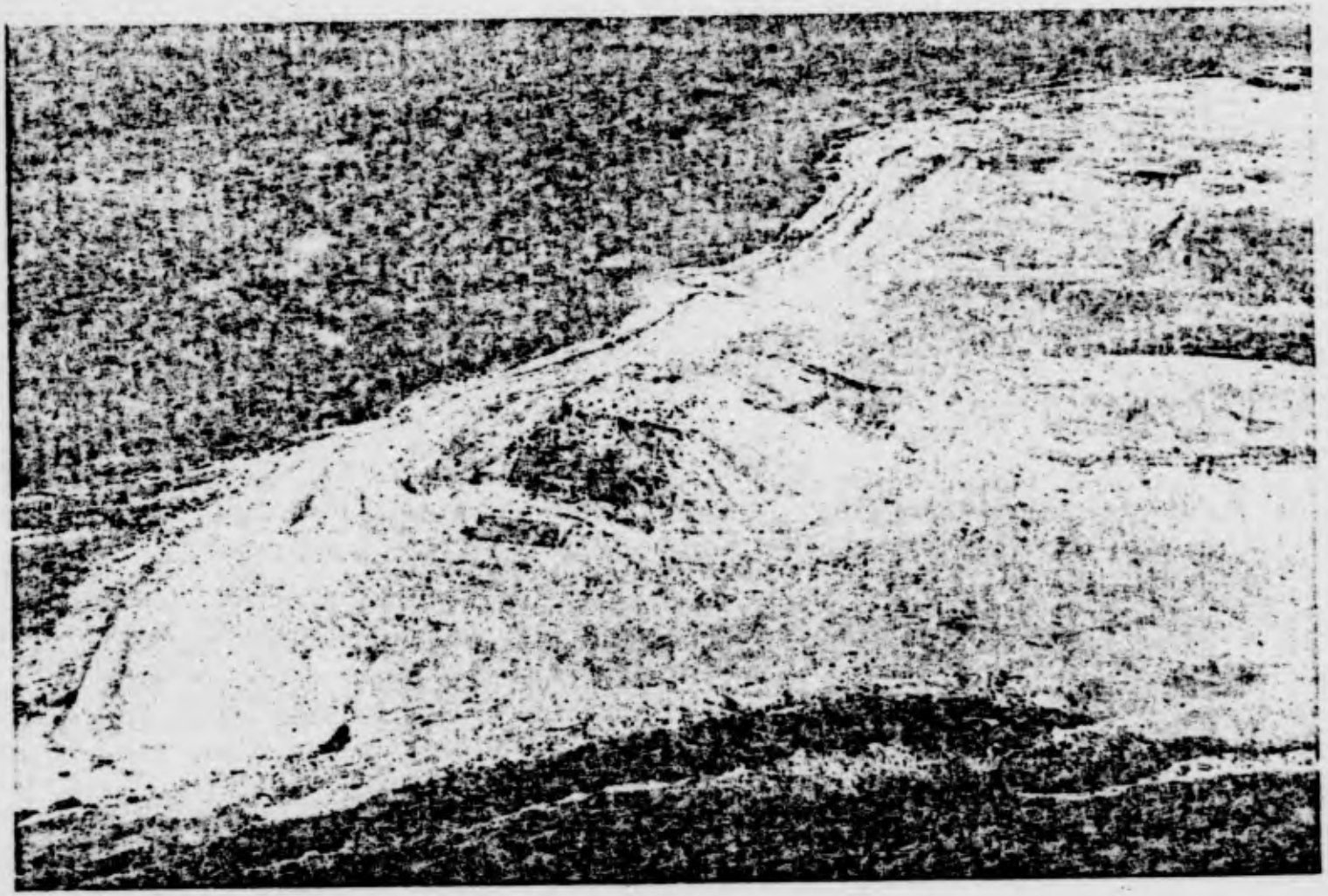

Figure D.2 Station 1320, Site Dog, post-Shot Flathead, pre-Shot Dakota.

Figure D.3 Station 1320, Site Dog, post-Shot Dakota, pre-Shot Navajo.

Figure D.4 Station 1320, Site Dog, post-Shot Navajo.

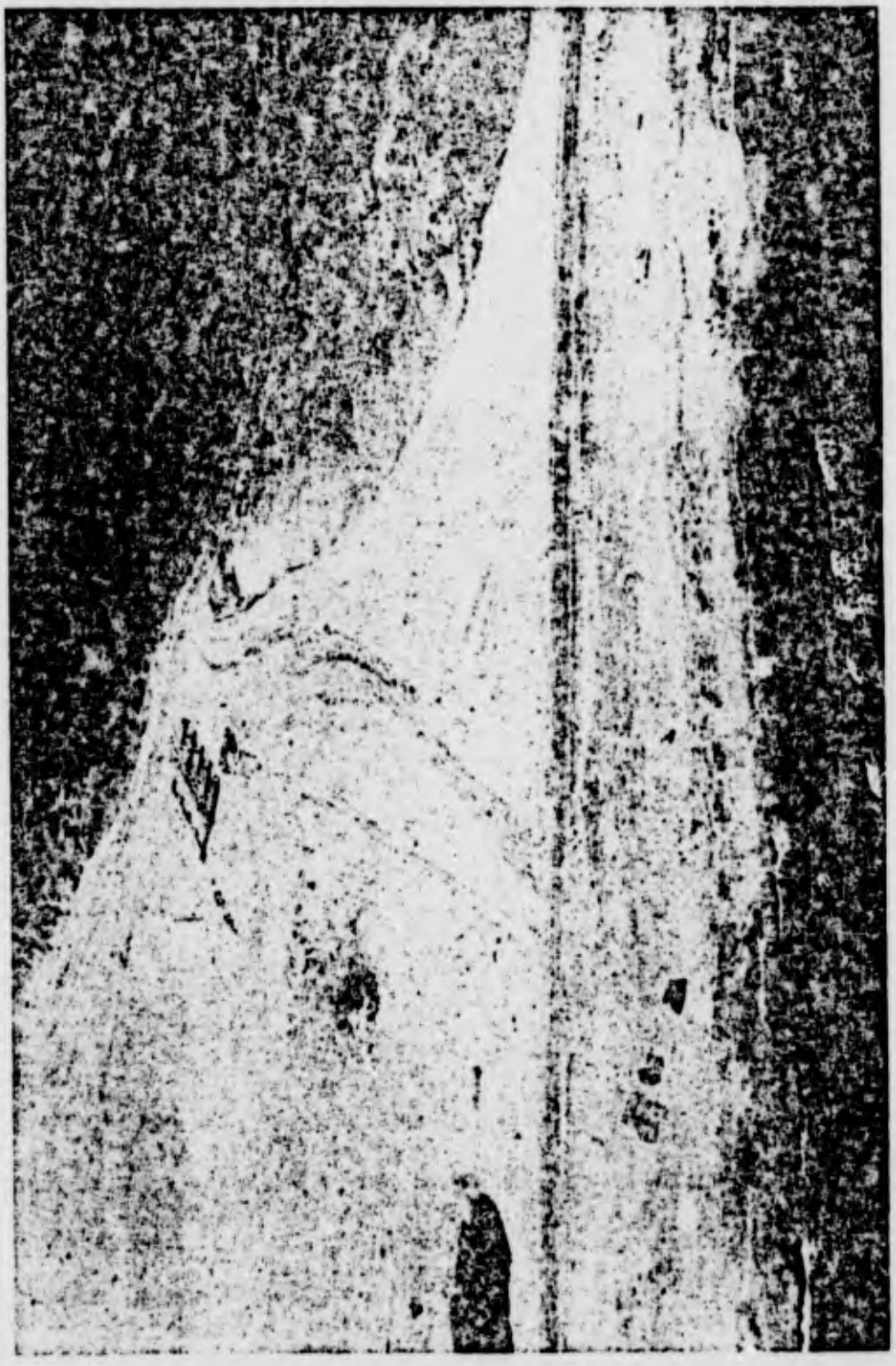

Figure D.5 Central area, Site Dog, pre-Shot Flathead.

Figure D.6 Central area, Site Dog, post-Shot Flathead, pre-Shot Dakota.

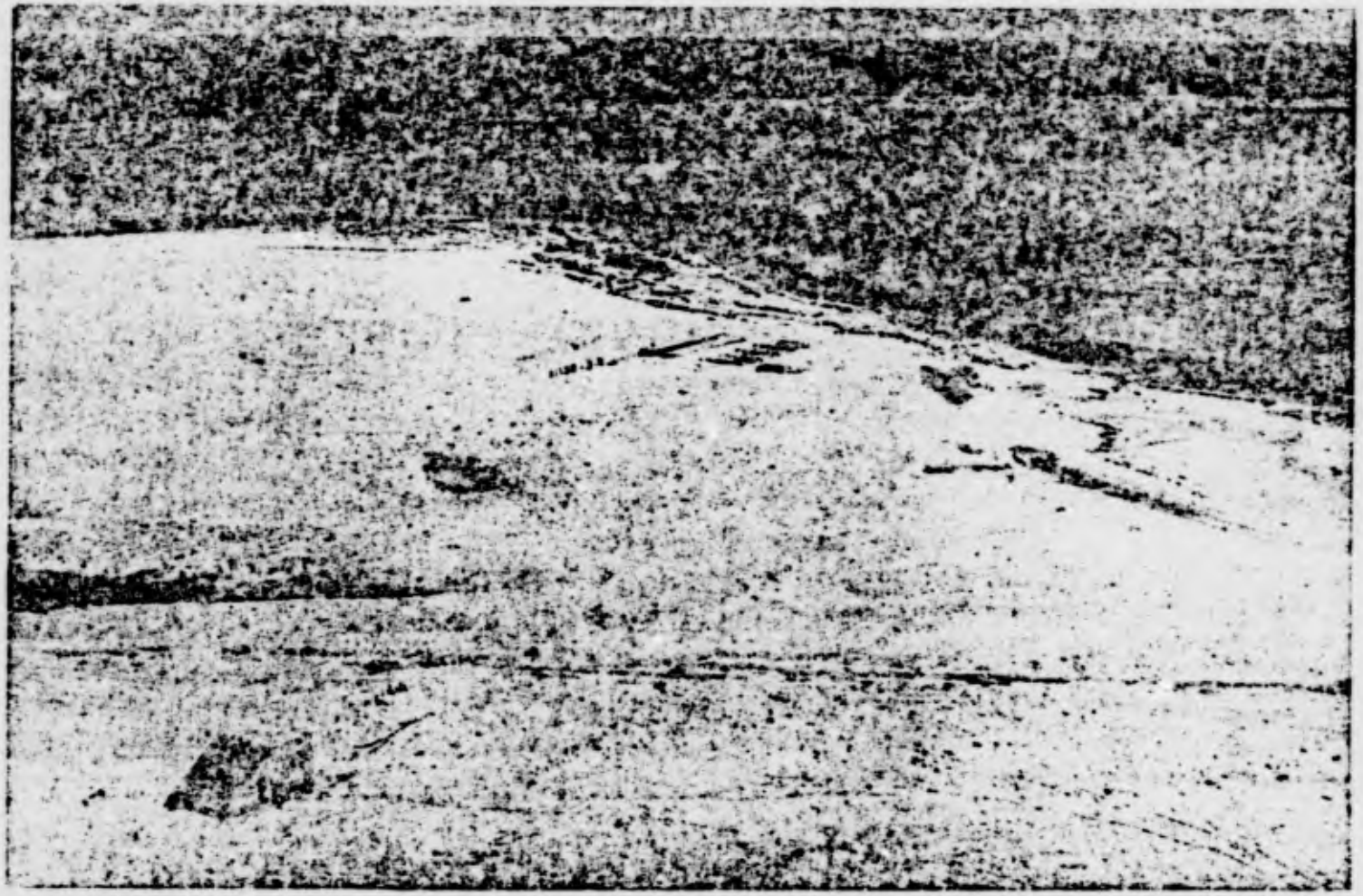

Figure D.7 Central area, Site Dog, post-Shot Dakota, pre-Shot Navajo.

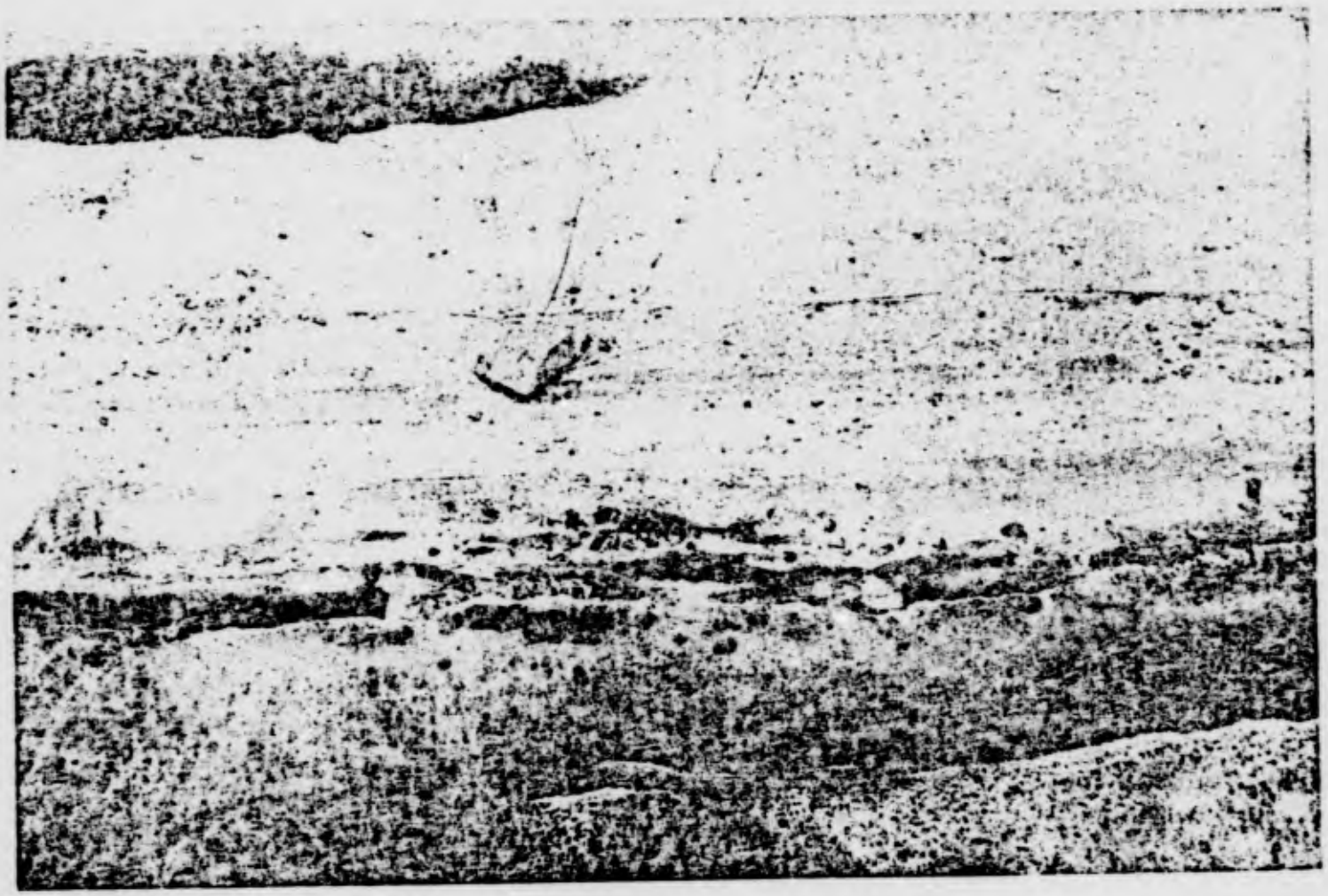

Figure D.8 Lagoon shoreline, central area, Site Dog, post-Shot Navajo.

Figure D.9 Ocean shoreline, central area, Site Dog, post-Shot Navajo.

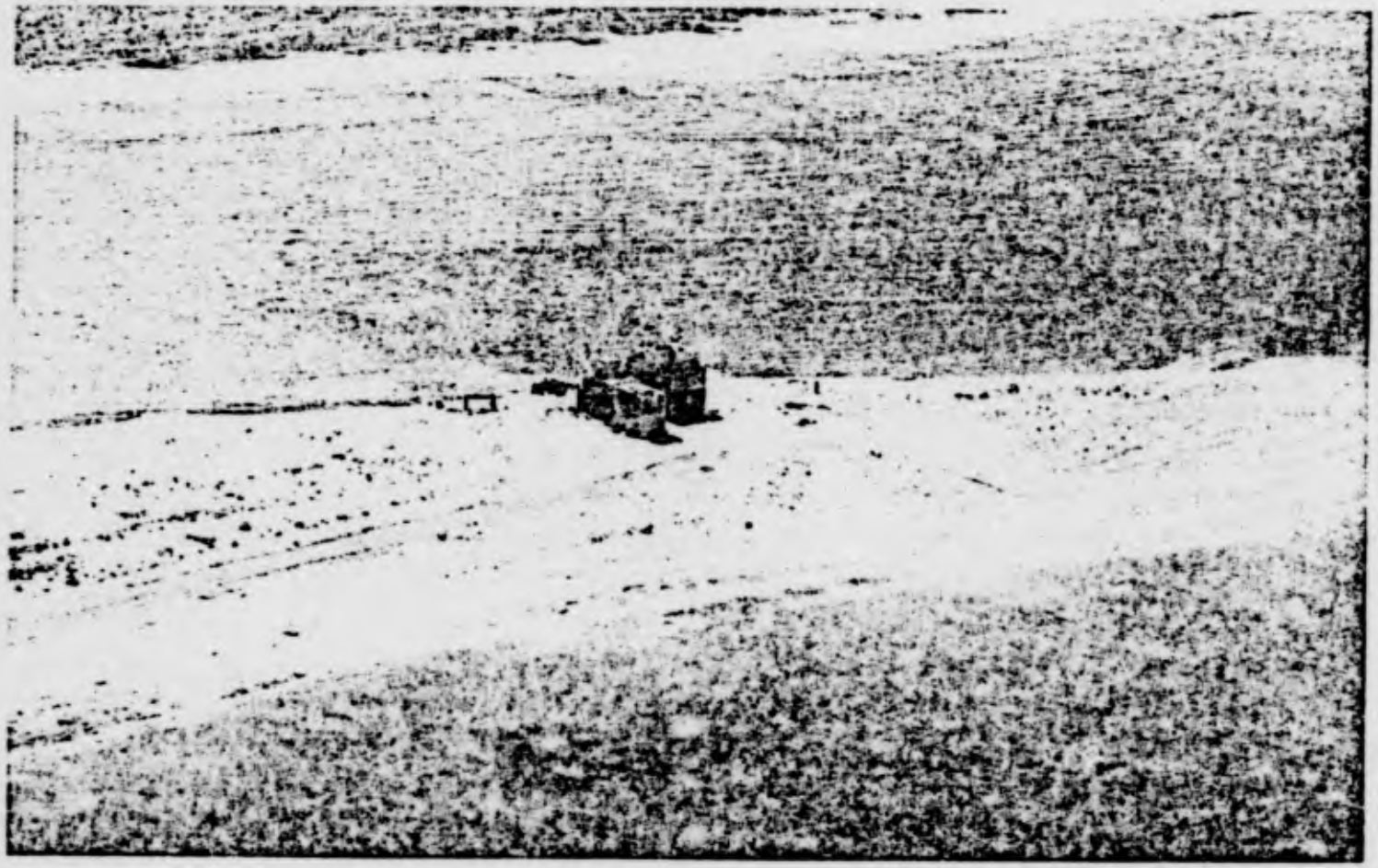

Figure D.10 Station 1830, Site George, pre-Shot Flathead.

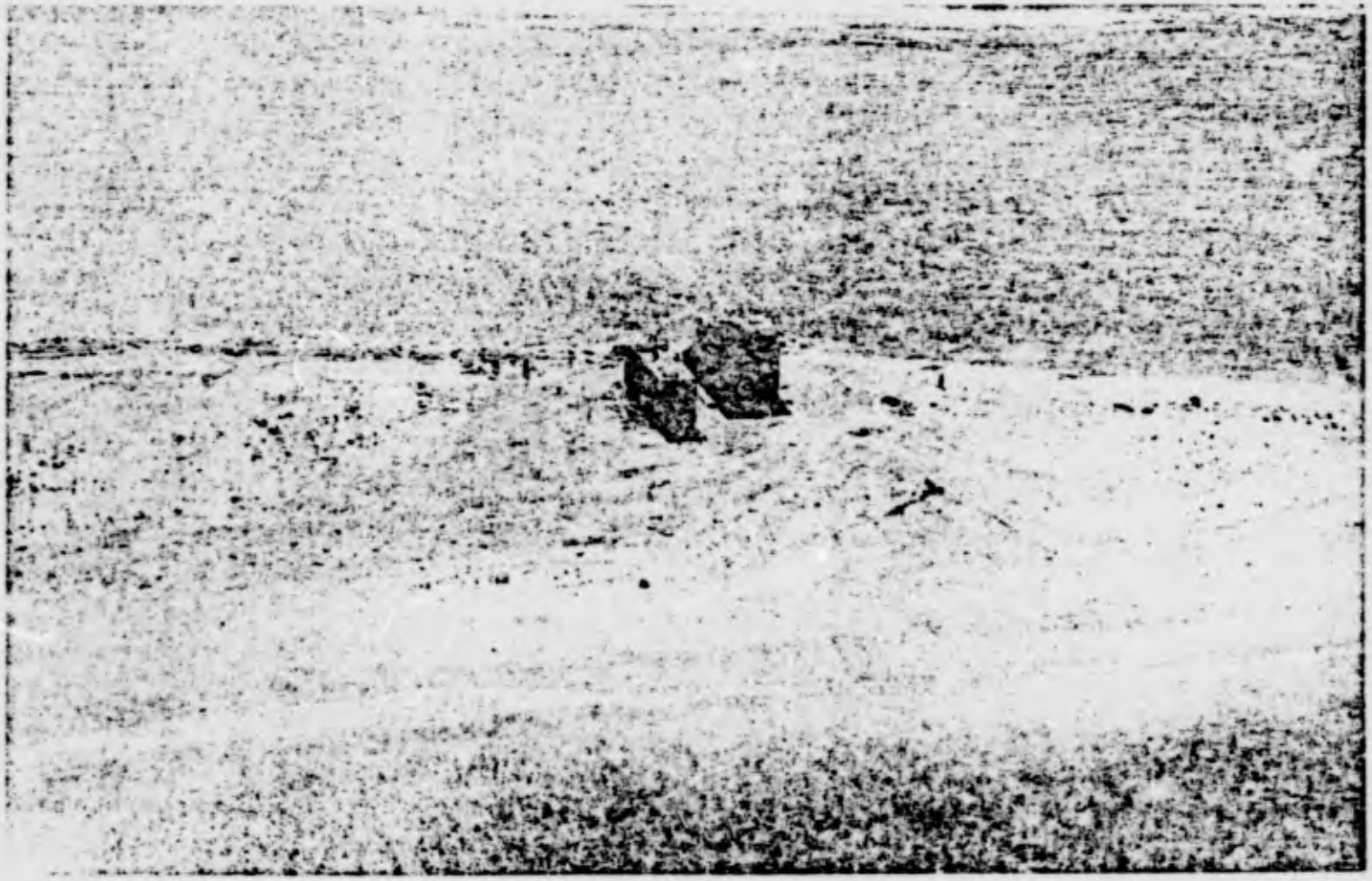

Figure D.11 Station 1830, Site George, post-Shot Flathead, pre-Shot Dakota.

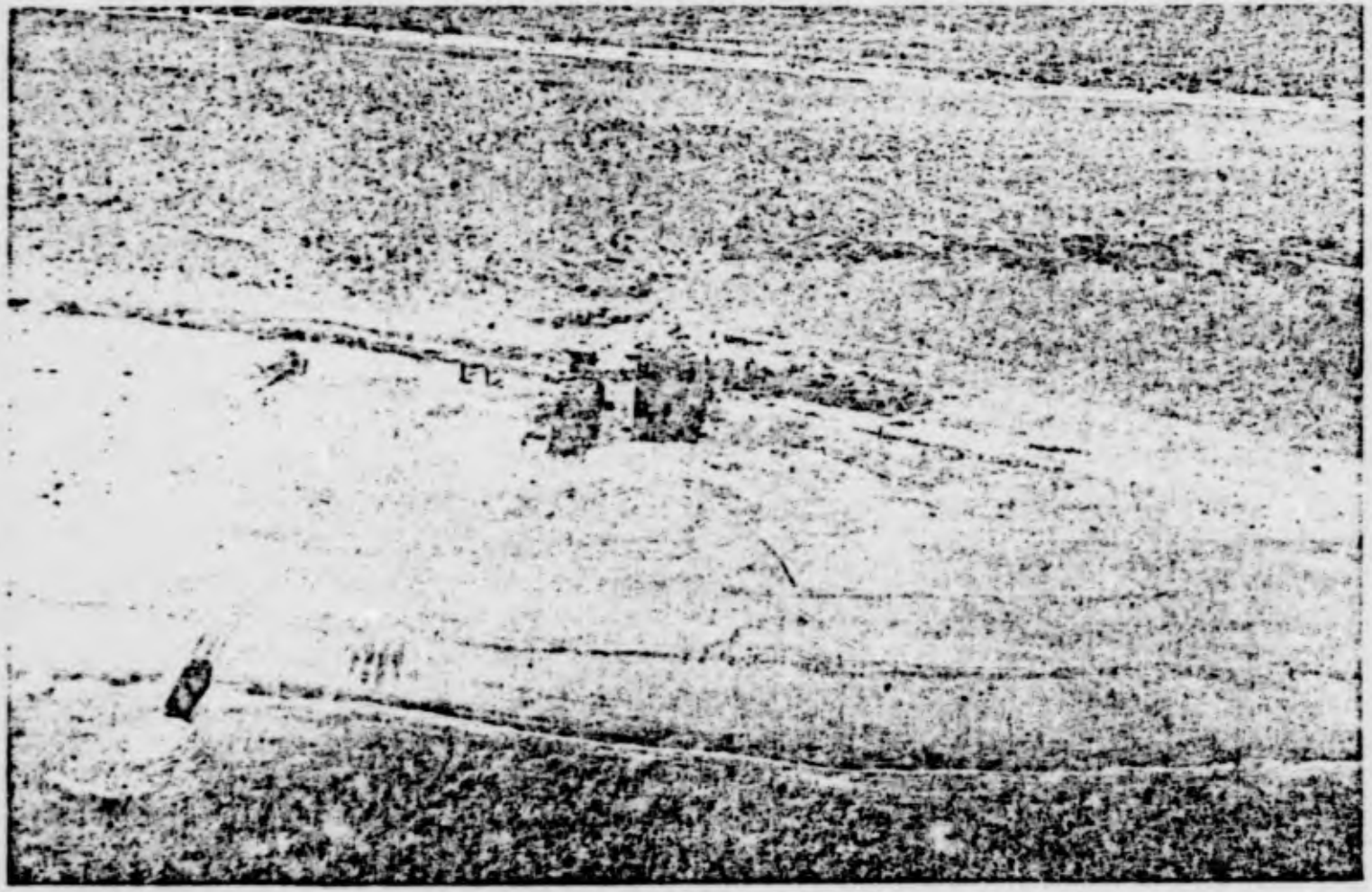

Figure D.12 Station 1830, Site George, post-Shot Dakota, pre-Shot Navajo.

Figure D.13 Station 1830, Site George, post-Shot Navajo.

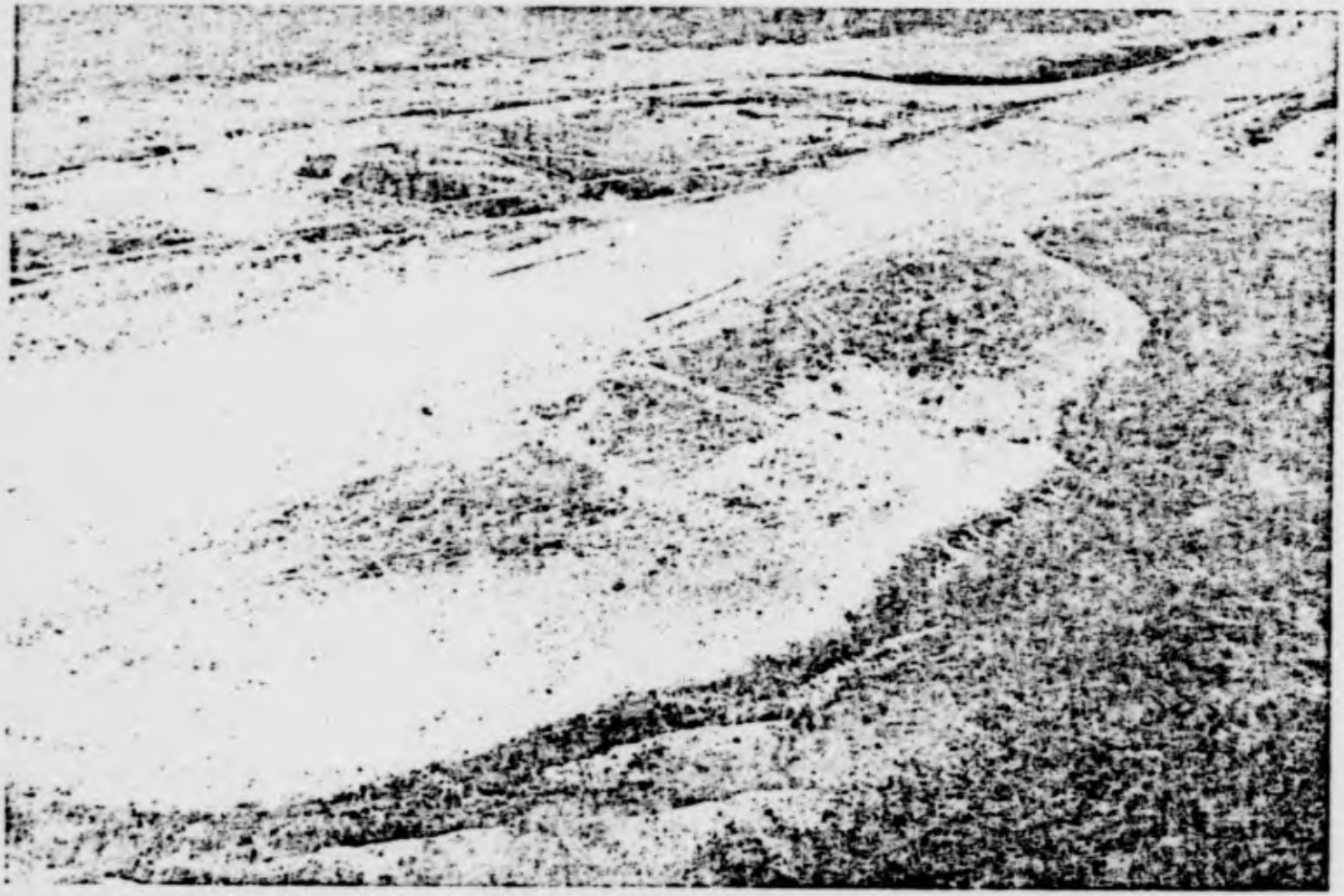

Figure D.14 Station 1515, Site Oboe, pre-Shot Flathead.

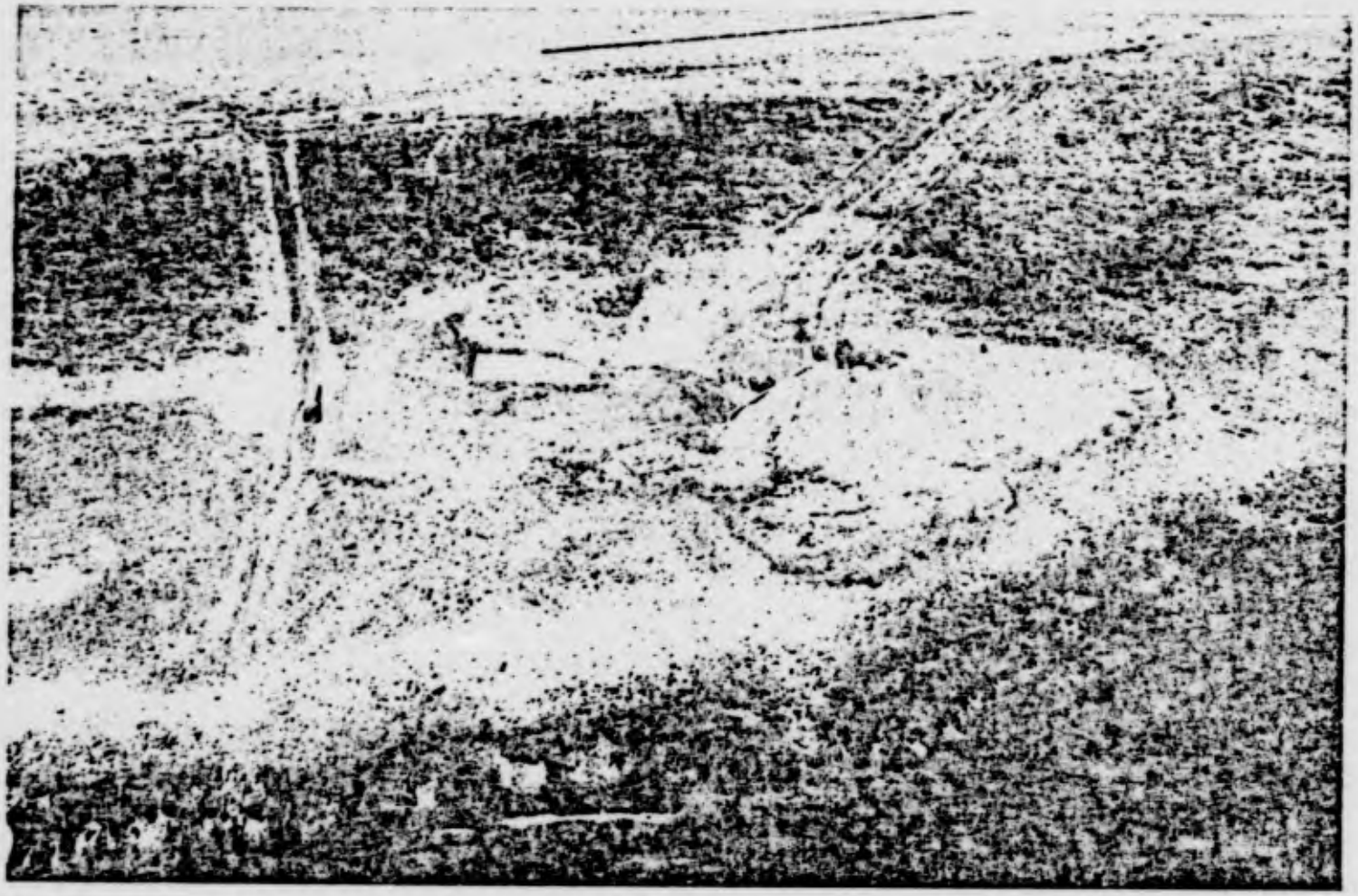

Figure D.15 Station 1515, Site Oboe, post-Shot Flathead, pre-Shot Dakota.

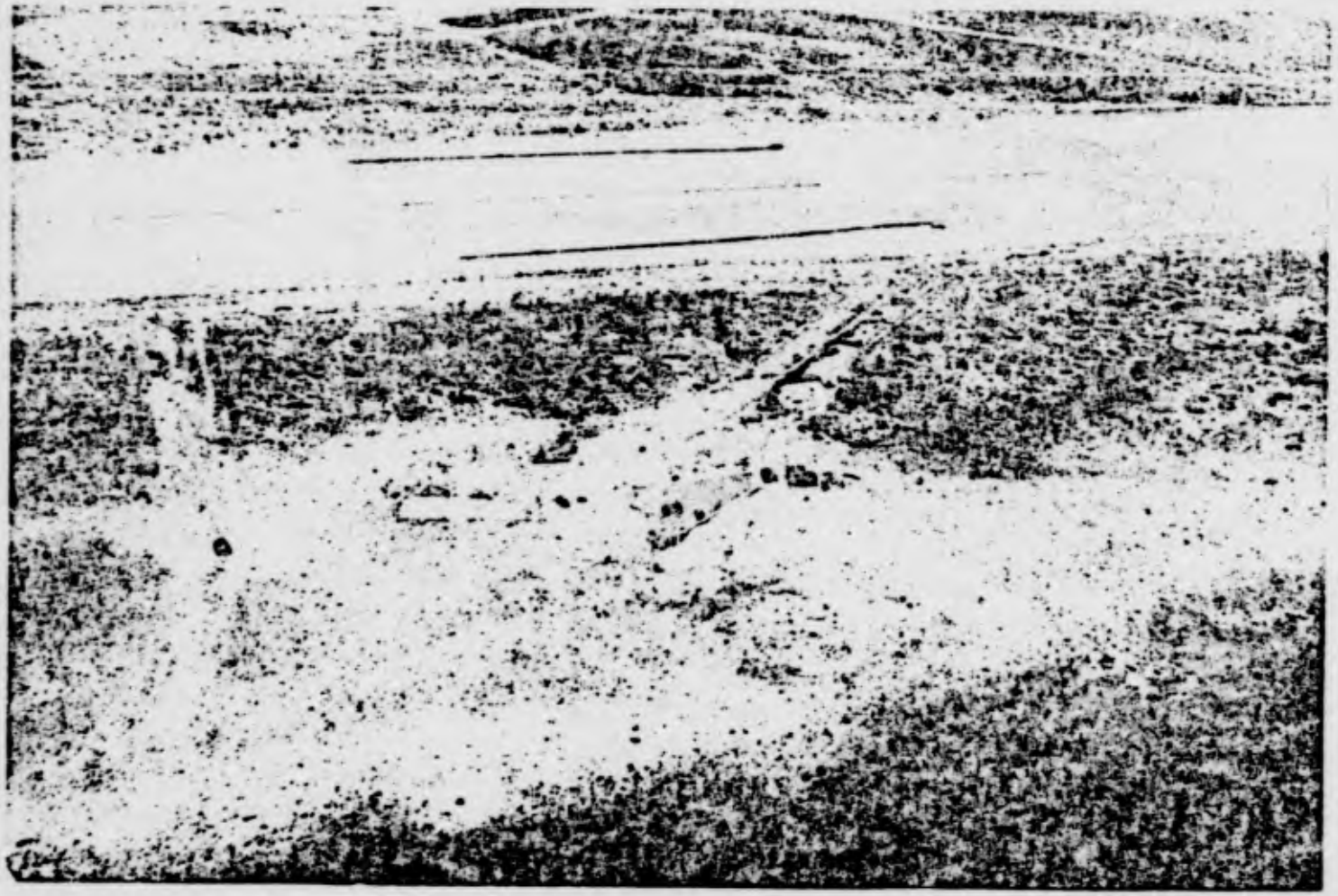

Figure D.16 Station 1515, Site Oboe, post-Shot Dakota, pre-Shot Navajo.

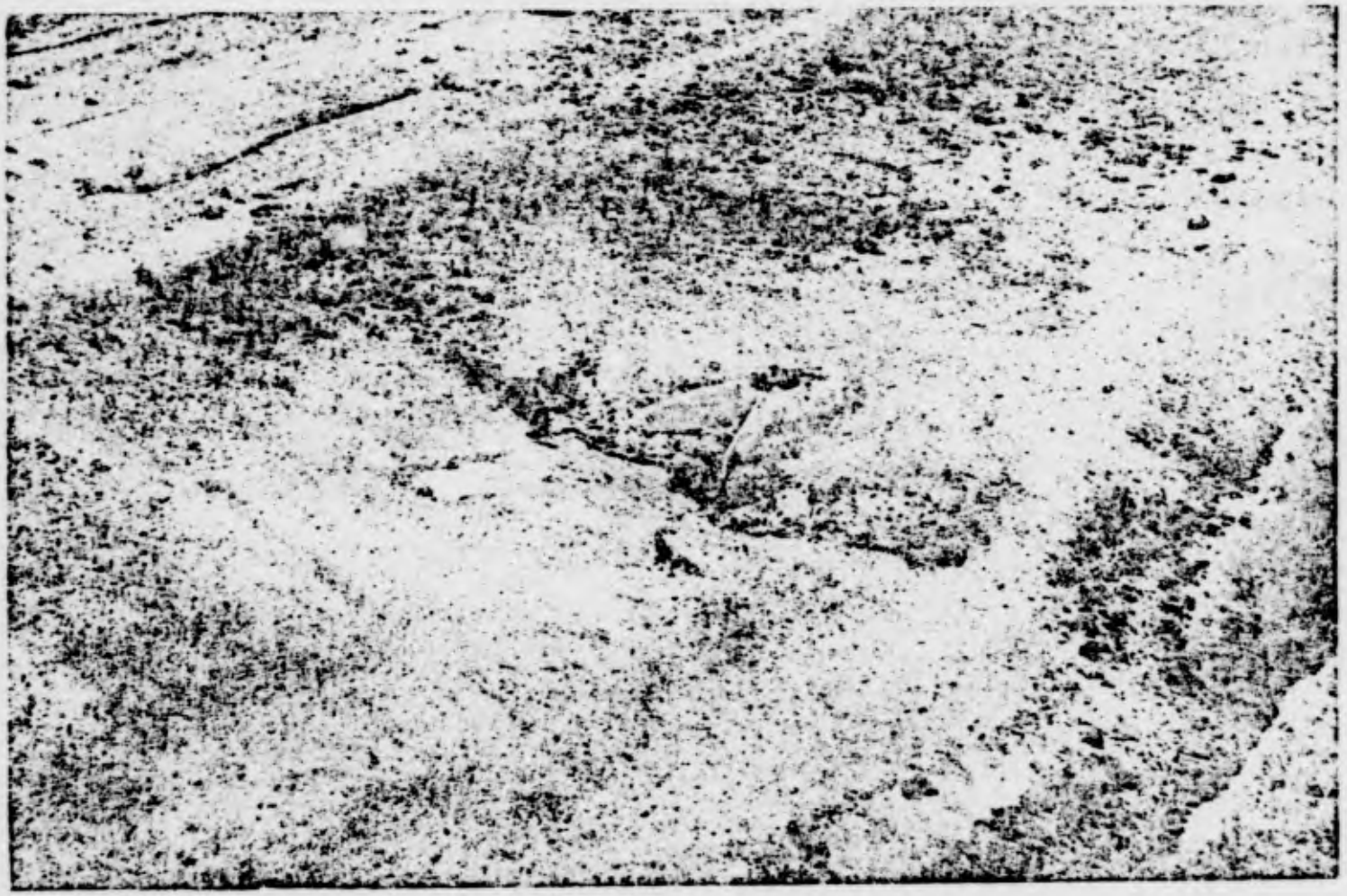

Figure D.17 Station 1515, Site Oboe, post-Shot Navajo.

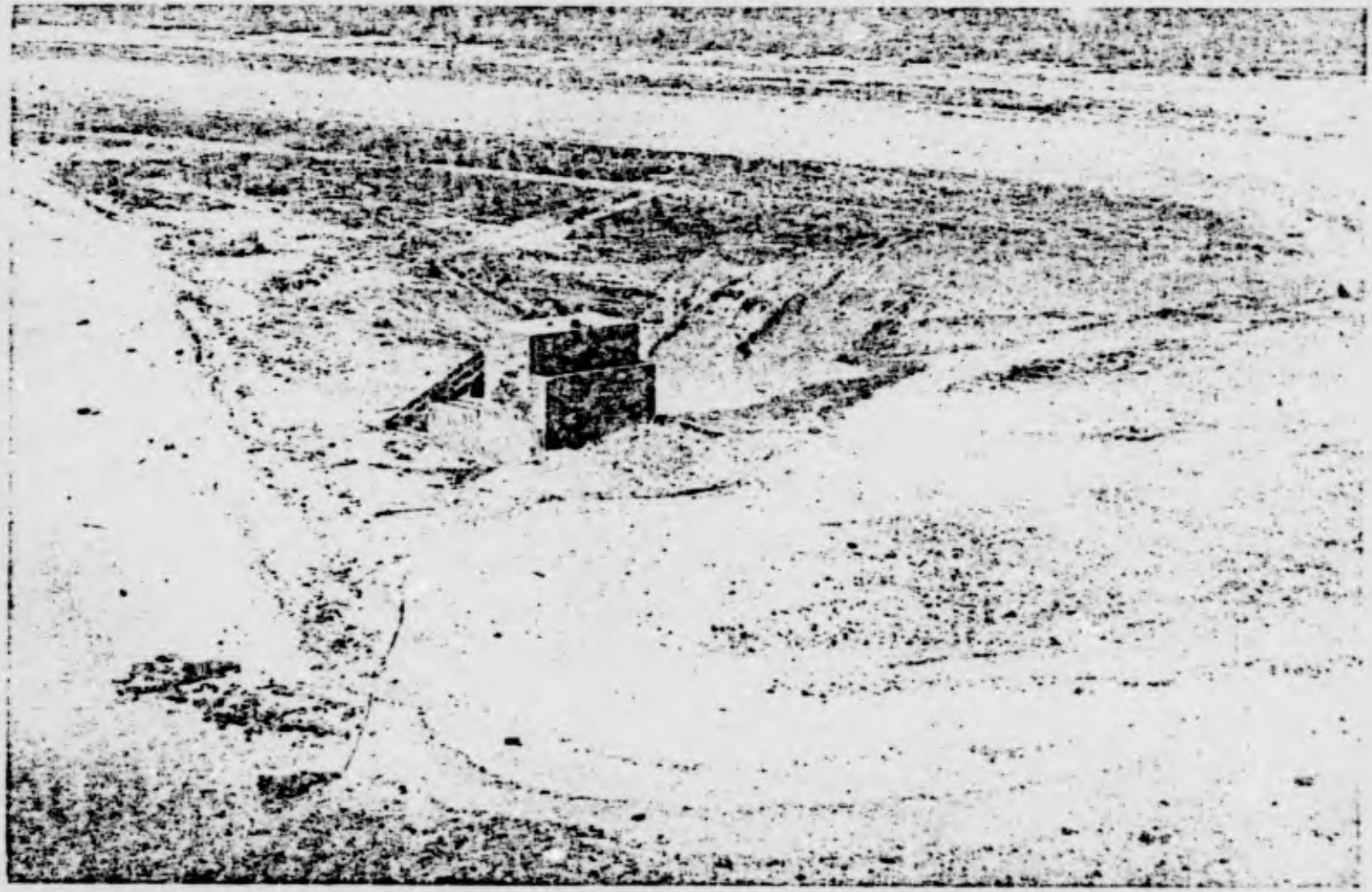

Figure D.18 Station 2300, Site Peter, pre-Shot Flathead.

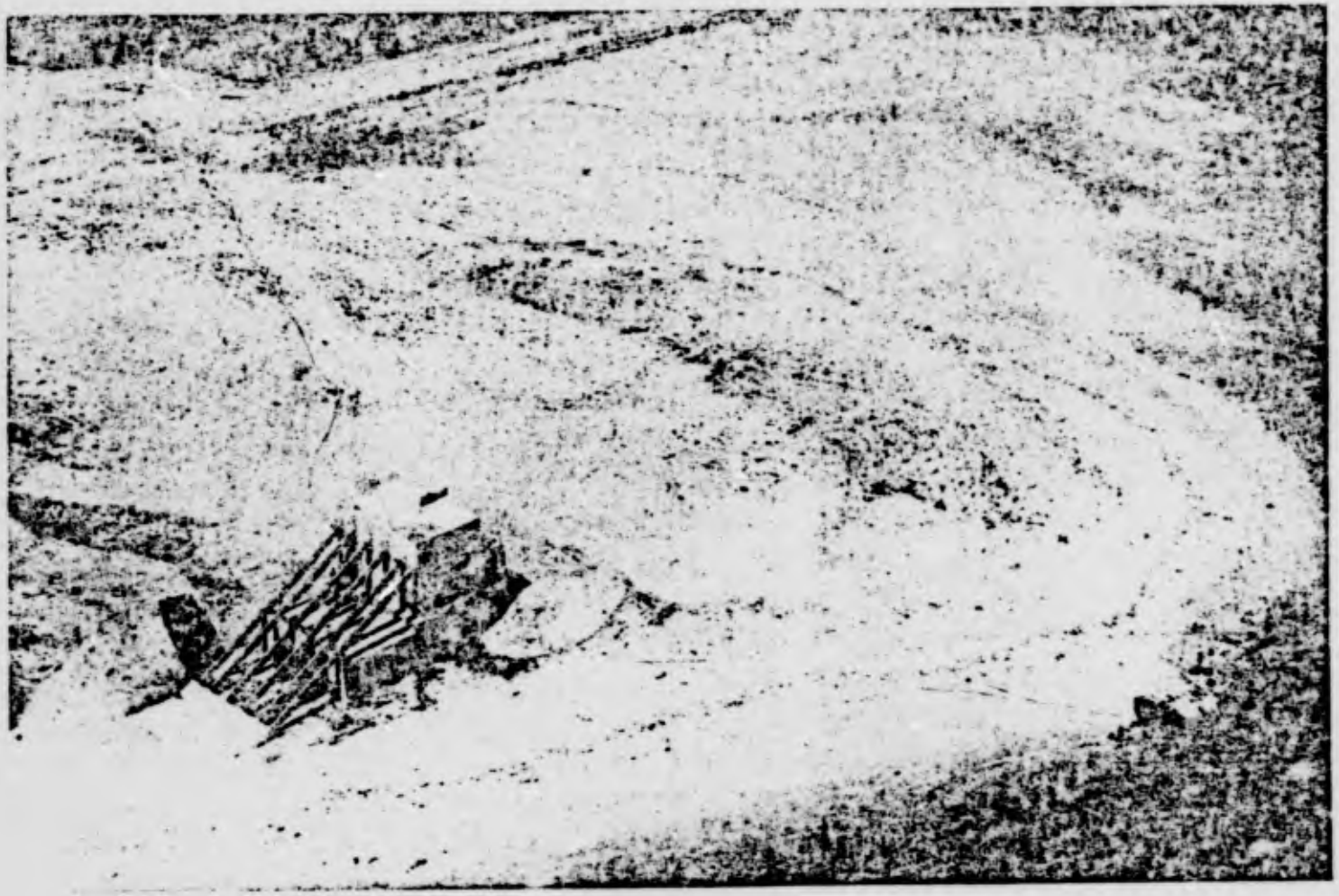

Figure D.19 Station 2300, Site Peter, post-Shot Flathead, pre-Shot Dakota.

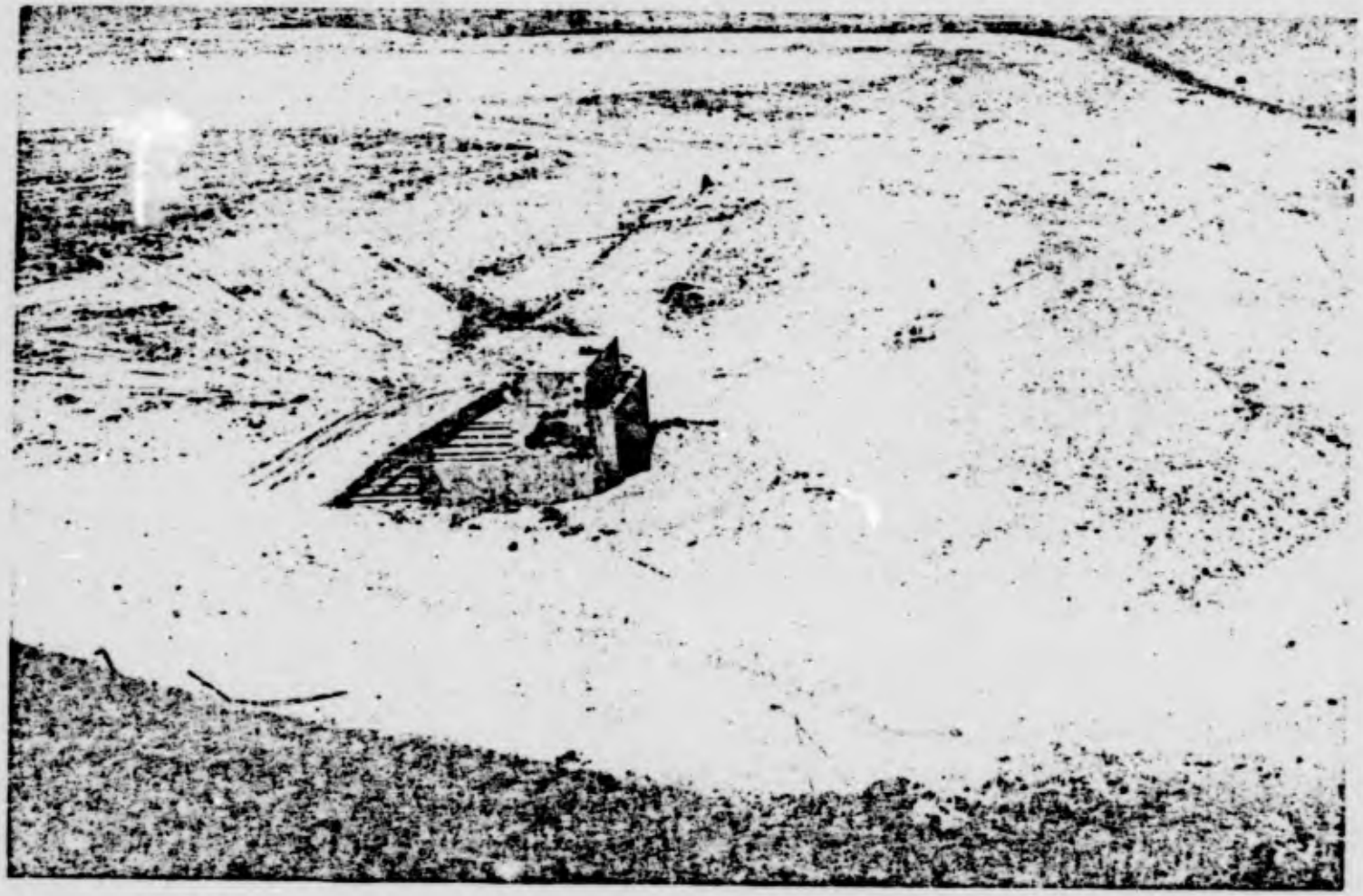

Figure D.20 Station 2300, Site Peter, post-Shot Dakota, pre-Shot Navajo.

Figure D.21 Station 2300, Site Peter, post-Shot Navajo.

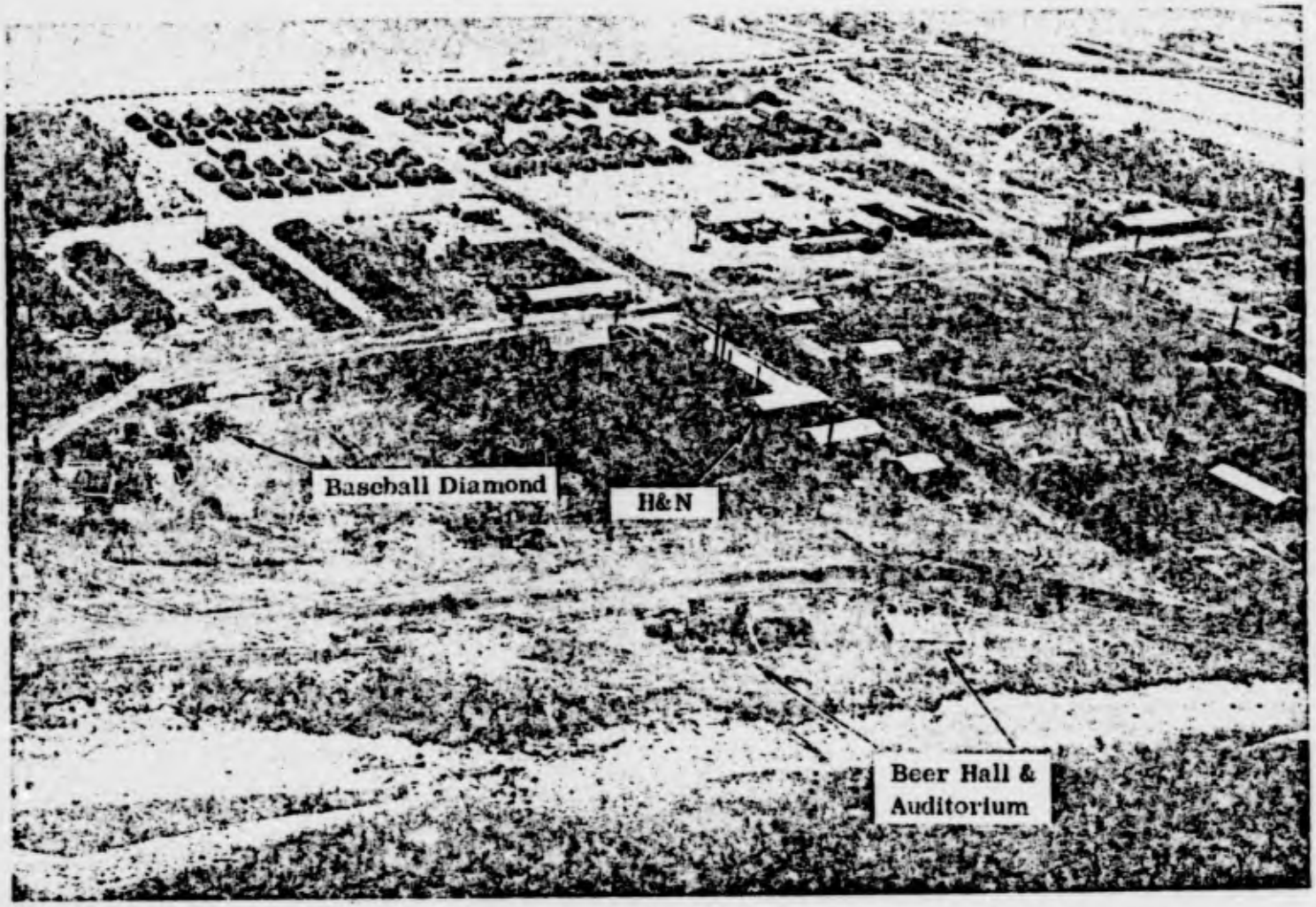

Figure D.22 Camp area, Site Nan, post-Shot Navajo.

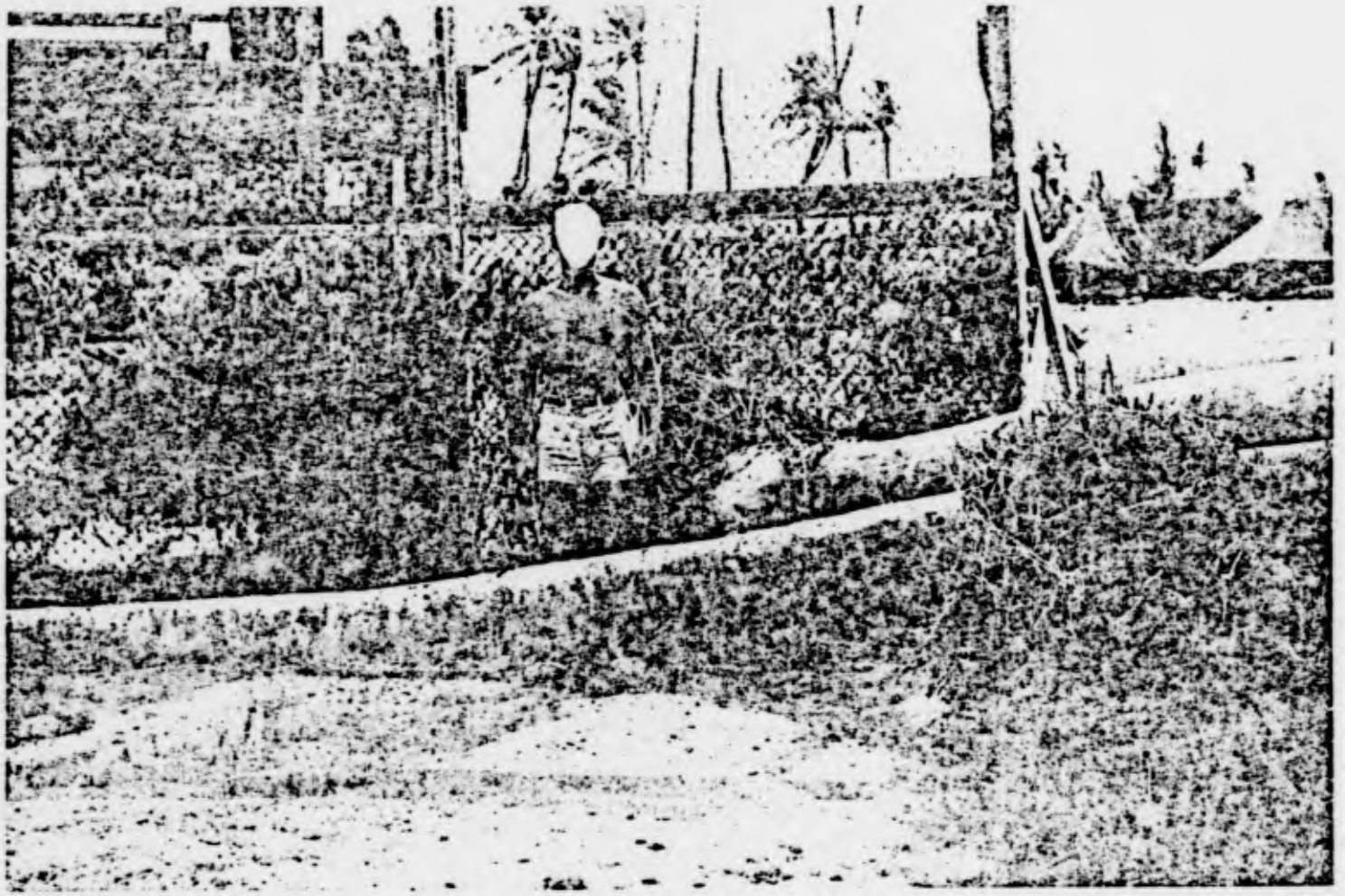

Figure D.23 Uprooted trees and waterborne grass caught in wire screen of baseball backstop, Site Nan, post-Shot Navajo.

REFERENCES

4. Herbert C. Kranzer and Joseph B. Keller; "Water Waves Produced by Explosions"; AFSWP 713, September 1955; New York University, Institute of Mathematical Sciences; Unclassified.

5. J. E. Prins; "Characteristics of Waves Generated by a Local Surface Disturbance"; Series 99, Issue 1, August 1956; University of California.

6. "Effects of Explosions in Shallow Water"; AFSWP 452, April 1955; Waterways Experiment Station, Vicksburg, Mississippi; Confidential.

7. "Gravity Water Waves Resulting from the Atomic Bomb Explosions at Bikini"; HE-116-296, Fluid Mechanics Laboratory, University of California.

9. P. H. Perroud; "The Solitary Wave Reflection Along a Straight Vertical Wall at Oblique Incidence"; Series 99, Issue 3, September 1957; Wave Research Laboratory, Institute of Engineering Research, University of California.

10. R. L. Wiegel; "Gravity Waves, Tables of Functions, Council on Wave Research"; February 1954; The Engineering Foundation, Berkeley, California.

11. H. V. Sverdrup and W. H. Munk; "Wind, Sea, and Swell: Theory of Relations for Forecasting"; Publication No. 601, March 1947; Hydrographic Office, United States Navy Department.

12. H. Lamb; "Hydrodynamics"; 6th Edition, Dover Publications, 1956, New York.

13. G. H. Keulegan; "Gradual Damping of Solitary Waves"; RP 1895, Volume 40, June 1948; Journal of Research of the National Bureau of Standards.